LEXNET
Low EMF Exposure Future Networks

D5.2 Smart low-EMF architectures: results and recommendations

Contractual delivery date: M30
Actual delivery date: M35

Document Information

Version	V5.0	**Dissemination level**	PU
Editor	Fabien Héliot (UNIS)		
Other authors	Y. Sambo (UNIS) L. Díez, L. Rodríguez de Lope, R. Agüero (UC) M. Wilson (FLE) V. Iancu, G. Popescu, E. Slusanschi (UPB) J. Penhoat, B. Radier (FT) A. De Domenico (CEA) D. Sebastião (INOV) E. De Poorter, M. Mehari (IMINDS) J. Stéphan, M. Brau, Y. Corre, Y. Lostanlen (SIR) M. Popović, J. Milinković, M. Koprivica, A. Nešković (TKS)		

Abstract	This document presents the latest development on smart network architectures and management techniques for reducing EMF exposure as well as providing recommendations for future deployment. It addresses both 3GPP and non-3GPP wireless networks and exposure originated from both user equipment and various base stations and access points. In an effort to link the work of WP2 regarding the Exposure Index (EI) definition with the novel architectures and techniques developed in this deliverable, a specific EI evaluation methodology for WP5 is also proposed. This methodology is then utilised for assessing the EMF exposure performance of real networks in a heterogeneous setting and obtaining insights on ways to reduce this exposure. In this regards, novel EMF-aware radio resource management, EMF/QoE trade-off optimisation, EMF-aware multi-hop routing, and EMF-based Wi-Fi offloading methods are proposed, analysed and evaluated through simulations and measurements. As a result of the various studies presented in this deliverable, it becomes evident that network densification can lead to a decrease in exposure and that uplink voice service should favour UMTS over GSM to bring down exposure. In addition, connection control management should consider the downlink and uplink communications jointly, whereas, coordination mechanism in conjunction with scheduling proved effective at reducing exposure through interference management. Furthermore, UDP should be favoured over TCP for video delivery over LTE networks for reducing EMF while maintaining QoE.
Key words	Low-EMF networking, Exposure Index reduction, EMF proxy metrics, network densification, small cells, EMF optimisation, EMF-aware RRM, EMF-aware routing, EMF-aware offloading, EMF/ QoE trade-off

Project Information

Grant Agreement n°	318273
Dates	1st November 2012 – 31th October 2015

Document approval

Name	Position in project	Organisation	Date	Visa
Joe Wiart	Coordinator	Orange	15/10/2015	OK

Document history

Version	Date	Modifications	Authors
V0.1	25/05/2015	First individual contributions	All
V0.11-0.14	05/06/2015	Contributions integration and editing	UNIS
V0.2	12/06/2015	Individual contributions reviewed	All
V0.21-0.27	11/07/2015	Contribution corrections	All
V0.3	26/07/2015	Integrated final version	UNIS
V0.4	23/08/2015	TSG reviewed version	TSG
V0.41-0.46	08/09/2015	Contribution corrections	All
V0.5	08/09/2015	Final version	UNIS
V1	14/09/2015	Final version validated	Alma

Executive Summary

The main aims of this document is to report on the latest development regarding smart network architectures and management techniques for reducing EMF exposure (LEXNET WP5), to provide input to project demonstration (WP6) as well as recommendations for future EMF-aware deployment. This document is not only a link between WP5 and WP6, but also between WP5 and Socio-economic analysis, EMF exposure metrics and reduction target (LEXNET WP2). Indeed, it explains in details how to use the exposure evaluation developed in WP2 for assessing the Exposure Index (EI) of the technical studies being undertaken in WP5 in a coherent and fair manner.

This EI evaluation methodology is used for assessing the EMF exposure performance of real networks in a heterogeneous setting and obtaining insights on ways to reduce this exposure. In order to provide a clear and comprehensive picture on current/future networks exposure, most studies and techniques developed in this document are considering both 3GPP and non-3GPP wireless networks and exposure originated from both user equipment and various base stations and access points.

Following the two main themes of WP5, our studies cover both topology related EMF exposure reduction and network management techniques for reducing exposure. On the one hand, EMF exposure reduction by using small cells is analysed through three topics: access network selection, autonomic networking with the new optimization goal and small cell densification. On the other hand, novel EMF-aware radio resource management, multi-hop routing, and Wi-Fi offloading methods are proposed and evaluated. The trade-off between EMF and QoE is also studied in cellular and Wi-Fi networks for both audio and video applications.

Based on the numerous results obtained in this deliverable, a set of recommendations are given. For instance, network densification can lead to a decrease in exposure by ensuring that uplink voice services are transmitted via cellular system with power control, e.g. UMTS, instead of GSM network. Moreover, connection control management should consider the downlink and uplink communications jointly to efficiently reduce both types of exposures at the same time. Interference management is also an effective approach for reducing exposure, and we recommend using coordinated mechanism in conjunction with scheduling to do so. Furthermore, it becomes evident through our studies that UDP should be favoured over TCP for video delivery over LTE networks such that EMF can be reduced while maintaining QoE.

List of Acronyms

Acronym	Meaning
2G	2nd generation
3G	3rd generation
3GPP	3rd Generation Partnership Project
4G	4th generation
ACK	Acknowledgment
AM	Acknowledge Mode
ANDSF	Access Network Discovery and Selection Function
AP	Access Point
BS	Base Station
BSC	Base Station Controller
CDF	Cumulative Distribution Function
CDMA	Code Division Multiple Access
CRE	Cell Range Extension
CS	Circuit switched
CSI	Channel State Information
D2D	Device to Device
DAS	Distributed Antenna System
DASH	Dynamic Adaptive Streaming over HTTP
DF	Duty Factor
DL	Downlink
EE	Energy Efficiency
EI	Exposure Index
eICIC	enhanced ICIC
EMF	Electro-magnetic field
eNB	eNodeB
eNodeB	4G base station
EPC	Evolved Packet Core
FFR	Fractional Frequency Reuse
FTP	File Transfer Protocol
GSM	Global System for Mobile Communications
HetNet	Heterogeneous Network
HTTP	Hypertext Transfer Protocol
ICIC	Inter-Cell Interference Coordination
ICNIRP	International Commission on Non-Ionising Radiation Protection
ICT	Information and Communication Technologies
IEEE	Institute of Electrical and Electronics Engineers
IETF	Internet Engineering Task Force
IP	Internet Protocol
ISD	Inter-Site Distance
LTE	Long Term Evolution
MOS	Mean Opinion Score

MOSBO	Multi-Objective Surrogate Based Optimisation
MPD	Media Presentation Description
OFDMA	Orthogonal Frequency Division Multiple Access
OPF	Optimal Pareto Front
OSI	Open System Interconnection
P2P	Peer-to-Peer
PDF	Probability Density Function
PSNR	Peak Signal to Noise Ratio
PSS	Packet Switched Streaming
QoE	Quality of Experience
QoS	Quality of Service
RAT	Radio-Access Technology
RBRP	Reward Based Routing Protocol
RF	Radio-Frequency
RLC	Radio Link Control
RNC	Radio Network Controller
RRM	Radio resource management
RSCP	Received Signal Code Power
RSRP	Reference Signal Received Power
RTM	Reference Traffic Model
Rx	Receiver
SAR	Specific Absorption Rate
SE	Spectral Efficiency
SINR	Signal-to-Interference-plus-Noise Ratio
StdDev	Standard Deviation
SUMO	SUrrogate MOdeling
TCP	Transmission Control Protocol
TS	Time Slot
Tx	Transmitter
UDP	User Datagram Protocol
UE	User Equipment
UL	Uplink
UMTS	Universal Mobile Telecommunications System
VoIP	Voice over Internet Protocol
Wi-Fi	Wireless Fidelity
WLAN	Wireless Local Area Network
WP	Work Package

1 INTRODUCTION

One of the main objectives of the LEXNET project, and the key goal of WP5, is to investigate and design network architectures and management techniques for reducing human exposure to ElectroMagnetic Field (EMF) without compromising the Quality of Service (QoS) / Quality of Experience (QoE) perceived by the end-users. In this regards, the first deliverable of WP5,[LEXNET D5.1], introduced general strategies and further elaborated on novel architectures and techniques for reducing EMF exposure, from topology and management issues to algorithms dedicated to different layers of the Open System Interconnection (OSI) model. In addition, preliminary evaluations of these novel techniques have been performed mainly based on proxy metrics, e.g. Specific Absorption Rate (SAR), Transmit (Tx) / Receive (Rx) power, duration of connection.

Another major goal of the LEXNET project is to provide a novel methodology for measuring the EMF exposure. This task has been performed in WP2 and a new metric known as Exposure Index (EI) has been defined in deliverable D2.4 [LEXNET D2.4]. This metric combines the exposure originated by base stations (BSs) or Access Points (APs) (downlink/passive exposure) with that from User Equipment (UE) (uplink/active exposure). It also considers the daily average dose (measured as specific absorption rate in time) received by population in an area. Due to its nature, the EI cannot be directly applied to real-time management techniques (which mainly focuses on short-term dynamic adjustment of the network), and, hence, this has motivated our use of proxy metrics (directly related to the EI) for designing novel EMF-aware techniques and providing a preliminary assessment of their potential in deliverable D5.1 [LEXNET D5.1].

This deliverable aims at providing a definitive picture on the performance of the proposed schemes of D5.1 as well as recommendations on EMF-aware network management. Those techniques presented in D5.1, which have been extended and finalised, as well as more recently developed techniques, are not only assessed in terms of proxy metrics, but are also evaluated via the EI assessment framework provided by WP2. In this regard, Section 2 describes the exposure evaluation process that has been designed in WP2 and indicates how to adapt it towards the technical studies being undertaken in WP5, namely for management and configuration of the underlying networks. Given that EI calculation is dependent on various parameters, it is crucial to identify the important WP5 related parameters affecting the EI (e.g. location and number of access points, transmit power, handover, protocols, etc.) and choosing the proper scenarios for evaluating it. The EI evaluation methodology for WP5 technologies in Section 2 follows three steps (applicability of life segmentation data, traffic model, and relation between EI and WP5 technologies) that correspond to the EI generalised scenario of WP2.

As a use case for the EI evaluation methodology, exposure assessment of real networks has been undertaken in Section 3. In this regard, performance of Heterogeneous Networks (HetNets), e.g. GSM/UTMS/LTE with Wi-Fi systems, when considering different scenarios, varying usage, mobility, number of users, etc. have been assessed via simulations in order to better comprehend the impact of exposure on different systems configurations and users' behaviours. The simulation results in a

HetNet scenario have been complemented with real-network measurements assessing the impact of services, technologies and radio conditions on the exposure of legacy systems. Both uplink and downlink exposure is considered for exploring the benefit of offloading from a macrocell to underlaid smaller cells.

Section 4 provides novel EMF-aware radio resource management (RRM) techniques for uplink and/or downlink as well as long or short time scale. Indeed, the cell association framework for HetNets, which was initially presented in D5.1 [LEXNET D5.1], is extended here and used to analyse the optimum cell association in terms of EMF exposure and users' QoS when –downlink (DL) and uplink (UL) are jointly considered in a HetNet setup. Regarding short term RRM, two novel EMF-aware scheduling schemes are proposed; a scheduling/power allocation scheme for minimising the EMF exposure of each individual user subject to a QoS target, i.e., transmitting a target number of bits, in the uplink of cellular systems; and, a low-complexity coordinated scheduling algorithm for reducing the passive EMF exposure in the downlink of HetNet systems.

EMF exposure reduction and user QoS/QoE are two optimisation criteria that are inherently conflicting, and as such, they cannot be optimised at the same time, but only through a trade-off. The trade-off between EMF exposure reduction and user QoS/QoE is studied in Section 5 for both cellular and Wi-Fi systems; more precisely, an algorithm that selects the transport protocol according to radio network information is proposed for streaming video while achieving a trade-off between EMF exposure reduction and QoE. Moreover, the simulation framework initially presented in D5.1 [LEXNET D5.1] for studying the EMF vs. audio quality trade-off has been here extended for more complex scenarios and by including more realistic audio metric as well as real time exposure measurement capability in the framework.

Routing over wireless multi-hop topologies was also identified in D5.1 as a promising enabler for reducing the EMF exposure, where the Reward-Based Routing Protocol (RBRP) was proposed. In Section **Erreur ! Source du renvoi introuvable.**, this algorithm has been enhanced by including power management for mesh deployments, such that it can be used for reducing EMF exposure in multi-hop networks. Additionally, a theoretical framework for assessing routing-level EMF exposure has been proposed; it will allow a better characterisation of the routing alternatives performance from an EMF exposure perspective.

In Section 7, the impact of Wi-Fi offloading on EMF exposure is analysed, where three complementary simulation tools, i.e., Access Network Discovery Selection Function (ANDSF) simulation, dynamic system-level simulations, and coverage-based predictions, running on a common dense urban scenario are utilised. The main idea is to complement the results of one tool with the others in order to analyse the same problem from different perspectives and abstraction levels.

In fine, Section 8 concludes this deliverable with the summary of achievements / results and recommendations that have been drawn from them.

2 A COMMON WP5 EXPOSURE EVALUATION METHODOLOGY

This section gives an update on the exposure evaluation process adapted towards the technical studies being undertaken in WP5, namely for management and configuration of the underlying networks.

The EI definition has now been consolidated in WP2 activities [LEXNET D2.6], [Varsier 2015]. **Figure 1** below provides an overview of the components that contribute towards the EI defined in WP2.

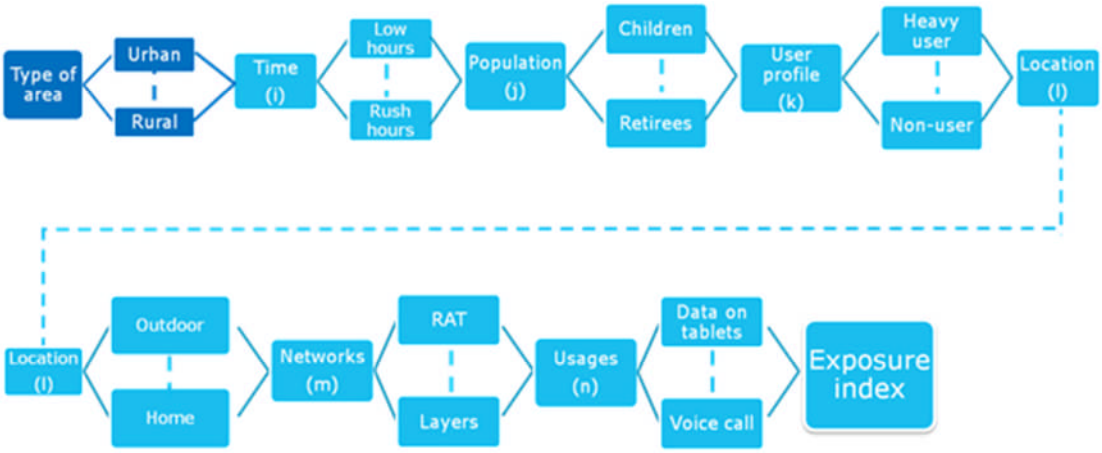

Figure 1: Exposure index formulation components

Fundamentally WP5 has focused on the design of networks for minimisation of the EI within an area without impacting the coverage and capacity requirements for that network. In addition, it has proposed a number of techniques to carry out the subsequent management of a deployed network, in particular the connectivity of end-user devices and reconfiguration procedures.

Calculation of the EI requires a broad set of inputs which altogether provide an unmanageable set of combinations from the network angle. From this perspective, it is essential to identify the implications on the WP5 studies and to pragmatically target certain scenarios for which the EI can be evaluated.

The overall target for WP5 technologies is to reduce the EI within an area by controlling network parameters such as the accumulated transmit powers of the BSs and mobile devices over a period of time without impacting the end-user experience (coverage, capacity, QoS).

In addition, the project has defined the generalised test case scenario for EI evaluation, covering the course of a 24 hour period. The methodology for the evaluation of the WP5 technologies is based on these underpinning activities within WP2. The test case provides a set of statistical and measurement based values for the components that constitute the EI formulation. From a networking perspective many of the developed technologies tend to focus on specific use cases that expand the assumption of the generalised scenario developed in WP2. The aim of the

methodology developed in WP5 is to identify which EI component parts are impacted by each technology and how the technologies may complement or compete with each other in the reduction of the overall EI.

Figure 2 provides a summary of the different categories of EI components, i.e. time of the day, population, user profile, environment, Radio Access Technology (RAT), cell type, posture, usage type, that are quantified [LEXNET D2.6] as part of the overall EI generalised scenario.

Time	Population	User Profile	Environment	RAT	Cell Type	Posture	Usage
Day	Children	Heavy	Home	2G	Macro	Standing	Voice, mobile
Night	Young people	Medium	Office	3G	Micro	Sitting	Data, mobile
	Adults	Light	Outdoor	4G	Pico		Data, Tablet
	Seniors	Non user	Moving	Wi-Fi	Femto		Data, Laptop

Figure 2: Categorisation for the General EI Scenario

The EI evaluation methodology for WP5 technologies is presented in three stages, which correspond to the EI generalised scenario developed in WP2:

- The first one considers the applicability of the life segmentation data from the general scenario towards the different WP5 technologies.
- The second stage is focused on the traffic models defined in the generalised scenario and how these can be applied in the validation of WP5 technologies.
- The final stage is to identify the relationship between the WP5 technologies with the EI, since they generally impact one or more of the EI components. In addition in this last stage, the contribution of each WP5 technology towards the different time periods of the 24 hour scenario is identified.

Note that sub-scenarios are defined for potentially competing technologies.

2.1 Stage1: WP5 Network Technologies Applicability

In order to evaluate the contribution to EI reduction from the different networking techniques investigated in WP5, the first stage is to identify which networking technologies are appropriate for each phase e.g. Indoor, home during the EI evaluation period (nominally 24 hours). For some of the techniques, specific configuration of the underlying networks relevant for that technique is captured. This will to some extent depend on the specific approach to validation, either using measurements or by simulation.

Steps 1.1 to 1.4 focus on the definition of the network configurations and to what extent the overall life segmentation data impacts the WP5 technologies.

The population categorisation from the life segmentation data will be used as statistical input to the overall EI calculation of WP5 technologies.

2.1.1 Step 1.1: Impact of Life Segmentation Data

Within the LEXNET project, the EI reference scenario has been developed to cover the EI calculation over a 24 hour period. From a networking perspective and in order to evaluate the overall EI, assumptions on the availability of RATs during the different phases encountered during the 24 hour period is essential. This enables the contribution to the overall EI calculation for each of the WP5 techniques that may address a subset of RATs. **Table 1** provides an overview of the Life Segmentation inputs [LEXNET D2.4] to the generalised scenario.

Table 1: Life Segmentation Inputs for EI Evaluation

Population category	Day (8 AM-6 PM)			Night (6 PM- 8AM)		
	Indoor (office-school-home)	Outdoor	Transportation (bus, car, subway etc…)	Indoor (home)	Outdoor	Transportation (bus, car, subway etc…)
Adults	8h15 (82.5%)	1h10 (11.5%)	35 min (6%)	13h05 (93.5%)	20 min (2.5%)	35 min (4%)
Young people/students	8h20 (83%)	1h10 (11.5%)	30 min (5.5%)	13h10 (94%)	20 min (2.5%)	30 min (3.5%)
Children	8h15 (82.5%)	1h30 (15 %)	15 min (2.5%)	13h45 (98.5%)	0 min (0 %)	15 min (1.5%)
Seniors	7h35 (70%)	2h10 (27.5%)	15 min (2.5%)	13h05 (93.5%)	40 min (5%)	15 min (1.5%)

Taking a network perspective, it is essential to qualify the assumptions on the availability of networks throughout the different phases of the period under analysis. This enables calculation of the downlink exposure during each phase of the day as well as the network options for connectivity and data transfer for the user devices. Specific techniques (e.g. Wi-Fi offload) can only be applied in the phases where appropriate networks are available. **Table 2** provides an initial assumption on the network availability during different phases of the 24 hour period.

The underlying assumptions made for this network reference scenario are: that during the day while the user in the area of work (dense urban) that there are a range of networks available including Wi-Fi and LTE hotspots and Wi-Fi both indoor and outdoor. In the evening the user is in a suburban area with LTE, 2G and 3G coverage as well as indoor Wi-Fi. While travelling only 2G and 3G are assumed to be available.

Table 2: Assumed availability (see above paragraph) of networks during phases of 24 hour scenario

RAT	Day (8 AM-6 PM)			Night (6 PM- 8AM)		
	Indoor (Work)	Outdoor	Transportation	Indoor (Home)	Outdoor	Transportation
LTE (Hotspot)	✓	✓		✓	✓	
UMTS	✓	✓	✓	✓	✓	✓
GSM	✓	✓	✓	✓	✓	✓
Wi-Fi	✓	✓		✓		

2.1.2 Step 1.2: Identification of Applicable WP5 Techniques

The next step is to identify which of the technologies developed in WP5 is applicable to a particular network deployment. This should take into account the technical applicability for each technique to be used in a specific RAT, in conjunction with the actual studies undertaken within the project that may evaluate the technology for a subset of the applicable RATs. Table 3 indicates how the different technologies investigated in WP5 relate to the different RATs that are available during some part of the 24 hour scenario. In some cases a certain technology may be more widely applied, but the validation within the project has focused on a specific RAT.

Table 3: Applicability of WP5 technologies to available RATs

WP Solution Title	Ref	LTE	UMTS	GSM	Wi-Fi	Additional Guidance
EI Aware Routing	Section 6	✓			✓	Evaluation focused on Wi-Fi but with a technology agnostic approach. Could be applied to Device to Device (D2D) communication in LTE.
Enhanced User Association	Section 4.1	✓	✓	✓		Study focus LTE but can be applied to other RATs
Wi-Fi Offloading	Section **Erreur ! Source du renvoi introuvable.**	✓			✓	Focus on LTE but traffic distribution available for other RATs
Enhanced Inter-Cell Interference Coordination (eICIC)	D5.1	✓				Complementary with Cell individual offset. It can be used when eICIC

						not available.
Cell Individual Offset	D5.1	✓	✓	✓		Study focus LTE but can be applied to other RATs
Joint RRM for EMF Minimisation	Section 4.2.2	✓	✓	✓		Downlink
EMF-QoS Tradeoff cellular	Section 5.1	✓	✓	✓		Access technology agnostic, but configuration for each technology is needed.
EMF-QoS Tradeoff Wi-Fi	Section 5.2				✓	Dense HetNets
EMF Aware Scheduling	Section 4.2.1	✓	✓	✓	✓	Uplink

Note: the greyed out ticks indicate that a solution may be applicable to other radio technologies but these were not studing with the current LEXNET project.

2.1.3 Step 1.3: Identification of Network Assumptions

From a WP5 perspective, however, the applicability of techniques developed may need to be categorised in finer detail. Potentially, techniques may be applicable to certain network deployments such as particular frequency bands and network layers, e.g. macro, pico. The overall scenario being generic, these networks specifics will be formulated as assumptions on the available networks with the 24 hour scenario.

In particular, Table 4 describes the applicability of each WP technique in particular for a specific network deployment or topology, such as an overlay network in a dense urban area. In addition, if the technologies apply to a specific network configuration, e.g. frequency band, this should also be specified. This type of detailed network configuration is necessary for validating some of the technologies.

Table 4: Applicability of WP5 technologies to different network configurations

Technical Study	Network Topology	Other Network Assumptions
EI Aware Routing	Indoor/Dense Network	Mesh Topology [*]
Enhanced User Association	Dense Urban	
WiFi Offloading	Indoor/Dense Network	Overlay Network
eICIC	Outdoor, Hetnet	Validation requires more detailed configuration parameters and network topologies such as Tx powers, propagation details etc.
Cell Individual	Outdoot. Hetnet	Validation requires more detailed

Offset		configuration parameters and network topologies such as Tx powers, propagation details etc.
Joint RRM for EMF Minimisation	Outdoor, Cellular generally	Validation required assumptions on frequency bands, services being used. However the results are quite broad and applicable to other network solutions.
EMF-QoS Tradeoff cellular	Cellular Network	Evaluated over cellular networks; nevertheless, the methodology is access technology agnostic, but implementation would depend on the specific technology (cross layer)
EMF-QoS Tradeoff Wi-Fi	HetNet	
EMF Aware Scheduling	Dense Urban	

[*] Mesh Technology implies a different connectivity model at the network edge with potential for routing of local traffic; Device to Device (D2D) is a potential future use case.

2.1.4 Step 1.4: Identify Technology Solutions Applicability

The final sub-step is to map the different WP5 technologies onto the overall 24 hour scenario identified in WP2 (see **Table 5**).

Table 5: Applicability of WP Technologies to different times throughout the 24 hour period

Technology	Day (8 AM-6 PM)			Night (6 PM- 8AM)		
	Indoor (Work)	Outdoor	Transit	Indoor (Home)	Outdoor	Transit
EI Aware Routing	✓ [**]	✓		✓ [**]	✓	
Enhanced User Association	✓	✓			✓	
Wi-Fi Offloading	✓	✓		✓		
eICIC	✓	✓				
Cell Individual Offset	✓	✓				
Joint RRM for EMF Minimisation	✓	✓	✓		✓	✓
EMF-QoS Tradeoff cellular	✓	✓	✓	✓	✓	✓
EMF-QoS Tradeoff Wi-Fi	✓	✓		✓		
EMF Aware Scheduling	✓ [**]	✓	✓	✓ [**]	✓	✓

[**] When not connected through Wi-Fi.

2.2 Stage 2: Assumptions on ICT Data Usage

The LEXNET reference scenario defines a set of traffic models based on various environments that provide the baseline for evaluating the numerous WP5 technologies and their impact on the overall EI calculation.

The previous stage has already identified the RATs and network morphologies relevant to each of the WP5 technologies. This stage focuses on the relationship of the individual WP5 solution and whether extensions are necessary to the reference traffic model to validate a specific technology.

2.2.1 Step 2.1: Network Usage Assumptions for WP5 techniques

Some networking technologies may target certain types of data (video, voice). The implication is that only a subset of the overall traffic will benefit from the EI reduction for these technologies. **Table 6** identifies the cases in which WP5 technologies target specific service types such as data, video, voice. In some cases the technology may be more generally applied but validation has focused on a specific service or services.

Table 6: Application of WP5 Technologies to Service Types

WP Solution Title	Usage	Comments
EI Aware Routing	All Services	
Enhanced User Association	All Services	
WiFi Offloading	Data Only	
eICIC	Data for validation but more generally applicable	
Cell Individual Offset	Data for validation but more generally applicable	
Joint RRM for EMF Minimisation	All Services	
EMF-QoS Tradeoff cellular	Data Only	Focus on video delivery Downlink
EMF-QoS Tradeoff Wi-Fi	Data Only	Focus on audio delivey
EMF Aware Scheduling	All Services	Uplink

2.2.2 Step 2.2: Identify Extensions to Existing Reference Traffic Models

The WP2 reference scenario segments the overall traffic based on measurements and data derived from external sources and providing segmentation of traffic in a variety of ways, categorised into heavy, medium and light usage based on:

- RAT
- Device Type
- User Category
- Service/Application Type
- Network Morphology
- Time of Day

From a WP5 perspective the challenge is to identify how each of the technologies under investigation maps onto these different characteristics and derive the appropriate traffic models to validate the specific technologies. Table 7 identifies any extensions or assumptions to the reference traffic model (RTM) to enable validation of the WP5 technologies.

Table 7: Applicability of WP2 Reference Model for validation of WP5 Technologies

WP Solution Title	Reference Usage Model
EI Aware Routing	Current RTM Applicable
Enhanced User Association	Current RTM Applicable
WiFi Offloading	Refinement for data with different latencies and additional segmentation of EI period (wake up time, busy hours, video hours at home & night). Impact the load assumptions on each RAT.
eICIC	Current RTM is applicable but studies based on different data traffic ratios (future scenario)
Cell Individual Offset	Current RTM is applicable but studies based on different data traffic ratios (future scenario)
Joint RRM for EMF Minimisation	Extensions for specific network aspects
EMF-QoS Tradeoff cellular	Extensions to properly model video services
EMF-QoS Tradeoff Wi-Fi	Extensions for specific network aspects
EMF Aware Scheduling	Current Reference Traffic Model (RTM) Applicable

2.3 Stage 3: Identification of Complementary and Competing Technologies

In this stage the aim is to identify the different sub-scenarios (Time of Day, RAT, Network Topology, Service Type, etc) and the WP5 technologies that would be applicable.

2.3.1 Step 3.1: Network Technology Impact on EI

From the networking perspective the main impacts that can be controlled to reduce the EI are:

- The location of BSs: Either through network planning and deployment or switching base stations on and off.
- The Tx power of base stations, e.g. exploiting self-organising network frameworks.
- The duration that mobile devices are attached to particular RAT or BS through techniques such as offloading, network selection and handover, which impact the Tx power of the end user device.
- The way that data is exchanged between a mobile device and the network such as the mode of operation, delayed transfer.

Table 8 identifies the EI component that is targeted by each of the WP5 technologies. This partially assists in the identification of competing technologies although further evaluation of the WP5 technologies is required to determine the extent to which the technologies can be used in combination.

Table 8: EI Components targeted by WP5 technology

WP Solution Title	Target EI Component
EI Aware Coordinated Scheduling	DL Tx Power
EI Aware Routing	UL&DL Tx Power
Enhanced User Association	UL Tx Power
WiFi Offloading	Load on macro network
eICIC	UL Tx Power + UL & DL duration (Increased throughput)
Cell Individual Offset	UL Tx Power + UL & DL duration (Increased throughput)
Joint RRM for EMF Minimisation	UL Tx Power + duration / DL Tx power
EMF-QoS Tradeoff cellular	DL Tx Power + duration
EMF-QoS Tradeoff Wi-Fi	UL&DL Tx Power
EMF Aware Scheduling	UL Tx Power

2.3.2 Step 3.2: Identification of Sub-scenarios

For each of the WP5 technologies under evaluation, its applicability to each period throughout the 24 hour scenario, including the impact over the available RATs will build a number of sub-scenarios. This will aid in determining the complementary and competing technologies at various times throughout the EI calculation period.

Table 9: WP5 Complementary technologies and Competing Technologies (forming sub-scenarios)

EI Scenario Segment	RAT	Technologies	Sub scenarios (For different network configurations)
Indoor (home)	WiFi Cell	• WiFi Offload	
	GSM/UMTS		
Outdoor (Night)	GSM/UMTS	• Joint RRM	
	LTE	• Joint RRM	
Transport	GSM/UMTS	• Joint RRM	
Indoor (work)	WiFi Network	• WiFi Offload • EI Aware Routing (Mesh)	
	LTE	• EMF Aware Coordinated Scheduling • EMF Aware Scheduling • Joint RRM • Enhanced User Association • eICIC • Cell Individual Offset • EMF-QoS Tradeoff1	• EMF Aware Coordinated Scheduling • EMF Aware Scheduling • Joint RRM • Enhanced User Association
			• eICIC • Cell Individual Offset • Joint RRM • Enhanced User Association
	GSM/UMTS	• EMF Aware Coordinated Scheduling • EMF Aware Scheduling • Joint RRM	
Outdoor (day)	WiFi Network	• WiFi Offload	
	LTE	• EMF Aware Coordinated Scheduling • EMF Aware Scheduling • Joint RRM • Enhanced User Association	• EMF Aware Coordinated Scheduling • EMF Aware Scheduling • Joint RRM • Enhanced User Association

		• eICIC • Cell Individual Offset • EMF-QoS Tradeoff1	• eICIC • Cell Individual Offset • Joint RRM • Enhanced User Association
	GSM/UMTS	• EMF Aware Coordinated Scheduling • EMF Aware Scheduling • Joint RRM	

3 EXPOSURE EVALUATION IN REAL NETWORKS: SIMULATION AND MEASUREMENTS

In the following, exposure assessment of real networks is undertaken. First in Section 3.1, exposure assessment in heterogeneous networks accounting for up- and downlinks is done through simulations. This section looks at exposure in heterogeneous networks (cellular + Wi-Fi) from a different set of scenarios/assumptions, so that these results can be used as additional parameters for network management. Using these exposure values, the EI was calculated for the considered scenario which enabled to have a better understanding of the overall exposure in heterogeneous networks. Then in Section 3.2, the simulations results are complemented with real-network measurements. These measurements help to assess the impact on exposure of the used services, technologies and radio conditions in both uplink and downlink.

3.1 Exposure Assessment in Heterogeneous Networks Accounting for Up- and Downlinks

Existing metrics to evaluate EMF exposure are well adapted to check the compliance with limits, but not at all to evaluate a global exposure of a population. Previous studies on this matter usually only look into a specific system, or to a specific mechanism that allows one to reduce exposure [Pedersen 2013], [Plets 2013]. Other studies analyse heterogeneous networks, but usually looking at the effect of adding small cells [Stephan 2014], or by using different allocation or routing strategies [ElAbdellaouy 2014].

One of the objectives of LEXNET was to define a new metric to evaluate the exposure of a population induced by a given wireless telecommunication network. The so-called Exposure Index (EI) [Varsier 2015] metric captures simultaneously the contributions of personal devices (as the mobile phone) and of the infrastructures of networks (as base station antennas) to the global exposure of users. By using this approach, initial simulations were made to estimate global exposure on multi-RAT heterogeneous networks (GSM, UTMS, LTE and Wi-Fi systems), considering different scenarios, varying usage, mobility, number of users, etc. Afterwards, the EI was estimated for the considered systems and given scenarios. This enabled to have a better understanding of the overall exposure in heterogeneous networks, allowing one to know the exposure impact of the different considered systems, and for different users' behaviours.

3.1.1 Exposure Index Model

As it has been seen in Chapter 2, the model proposed to evaluate the EI of users in a given area with several communication systems is based on the work carried out in the LEXNET project [LEXNET D2.4], [LEXNET D2.1] and [LEXNET D5.1]. The model divides the EI into downlink and uplink components:

$$EI = EI^{DL} + EI^{UL} \text{ [W/kg]}, \quad (1)$$

where:

- EI^{DL} is the total downlink EI for all communication systems,
- EI^{UL} is the total uplink EI, coming from the devices in the proximity of the user, and unlike the downlink, the EI of the uplink depends solely on the active connections of the user.

The downlink EI exists independently of whether the user has an active connection, or even carries a communication system, i.e., it merely exists due to the presence of base stations. The total downlink EI is the sum of the EI components for each system, each one depending on the distance of the user to the base station of a system, the duration of the stay of the user inside the scenario, the transmission power, etc., as it has been defined in [LEXNET D2.4]. In the EI, power control is not considered for the downlink. The frequencies and power/antenna gain values for the various simulated communication systems are given in **Table 10**. The normalised SAR for the downlink is given in **Table 11**.

Table 10: Frequency, maximum transmission power and antenna gain for the simulated systems

	f_s [MHz]	P_{tx} [W]	G_{tx} [dBi]
GSM	1 800	40	0
UMTS	1 940	40	14
LTE	2 600	40	14
WLAN	2 400	0.1	0

The total downlink EI, for a total of S systems, is then given by:

$$EI^{DL}(t) = \sum_{s=1}^{S} EI_{s_n}^{DL}(r_s, t, f_s), \quad (2)$$

where:

- $EI_{s_n}^{DL}(\dots)$ is the downlink EI for system *n.*

Unlike the downlink, the EI of the uplink depends solely on the active connections of the user with system s. The distance to the communication device is taken into account by the normalised SAR value. The uplink EI for a given system, EI_s^{UL}, is depending on the transmission power, the activity factor and the uplink normalised SAR values for the considered systems.

Table 11: Normalised SAR for the different communication systems [LEXNET D2.4]

	Normalised SAR [kg^{-1}]	
	Downlink	**Uplink**
GSM (1800 MHz)	0.0043	0.0053
UMTS (1940 MHz)	0.0043	0.0053
LTE (2600 MHz)	0.0039	0.0053
WLAN (2400 MHz)	0.0053	

3.1.2 Simulations and Scenarios

The scenarios were simulated using Riverbed Modeler [Riverbed], and show a macro cell approach [LEXNET D2.3], with a 200m side square area, where there are GSM, UMTS and LTE base-stations collocated at the centre of the cell as depicted in **Figure 3**. The GSM base station is omnidirectional, whereas, the UMTS and LTE ones are tri-sectorised with 14 dBi antennas. The cell also contains a number of WLAN APs, randomly positioned within the cell. Users are also randomly positioned within the cell.

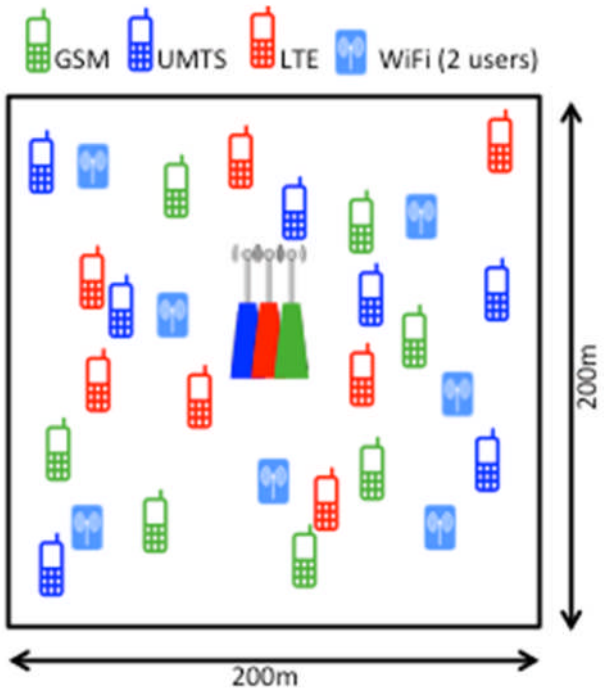

Figure 3: Simulated scenario

The considered reference scenario is composed of the four considered systems, with 7 users per cellular system/technology, and 7 APs with 2 users each. As for the service, GSM users are using voice, while the rest of the users from the other systems are using data (Peer-to-Peer – P2P, to be more exact). It was decided to focus on the worst-case approach when designing and configuring the scenario: although the area under study is small, it is considered to be a macro-cell (thus, larger BS transmission power), the used propagation model is free space loss only. LTE is considered as not having power control on the uplink, and UMTS is considered as without HSPA.

Based on the reference scenario defined above, several variations were defined to analyse specific scenarios:

- User's movement (pedestrian speed, without leaving the area under study);
- Different types of traffic (File Transfer protocol – FTP, P2P with heavier load, video conferencing) for all users except GSM ones who are always just doing voice;

- Clustering of the cellular users with different distances to the base stations (10, 50, 100, 200, and 500 m; the last one already falling outside the considered square for the reference scenario);
- Increase the number of users of the cellular systems (to the double, triple, and quadruple of the reference situation).

The LEXNET EI-model was implemented in Octave software [Octave 2015], by using reference values from the aforementioned simulations, and the Normalised SAR values already presented.

3.1.3 Simulation Results

3.1.3.1 Received Powers Values (Uplink and Downlink)

Given that the EI is highly dependent on the transmission and reception powers, see equation (1) of [LEXNET D2.4], we first obtained these values. The presented results in the following tables are the power values for both the downlink (average downlink received power for all transmissions received) and uplink (average transmission power for all radio transmissions) for each of the users, in each of the systems. The results from all the users of a given system are averaged so that one can compare the "average exposure" between systems in both directions. In **Table 12**, results from the reference scenario are presented, including the Standard Deviation (StdDev).

Table 12: Reference scenario power values for all systems in both uplink and downlink

	Power			
	Downlink		Uplink	
	Mean [dBm]	StdDev [dB]	Mean [dBm]	StdDev [dB]
GSM	-25.4	<0.01	9.3	<0.01
UMTS	-96.2	0.54	-48.4	0.59
LTE	-37.3	0.87	12.9	2.18
WLAN	-54.9	5.22	-40.1	23.35

As can be seen in **Table 12**, UMTS has much lower power values (hence, lower exposure) when compared to other cellular systems. This is easily explained as UMTS uses a very good power control mechanism, and there is a reduced number of users/load in the considered reference scenario. For LTE and GSM the values are several orders of magnitude higher, but nevertheless, the power values are quite low, due to the relative small scenario, thus all users being at a relatively short distance from the base stations. As for WLAN, power values are quite low in both uplink and downlink. As for the cellular systems, the standard deviation is quite low as expected: there is no movement on the reference scenario, and thus, the transmitted power variation is also quite low. The standard deviation of WLAN is quite high, which can be explained by the reduced number of sensors probes used in the simulations for WLAN users, thus leading to higher variability between results.

There was also a variation on the type of service being considered, and it was seen that independently of the type of service used, downlink and uplink average powers did not show any appreciable variation, as it can be seen in **Figure 4**. This indicates

that the type of service does not yield a great influence on the considered power values.

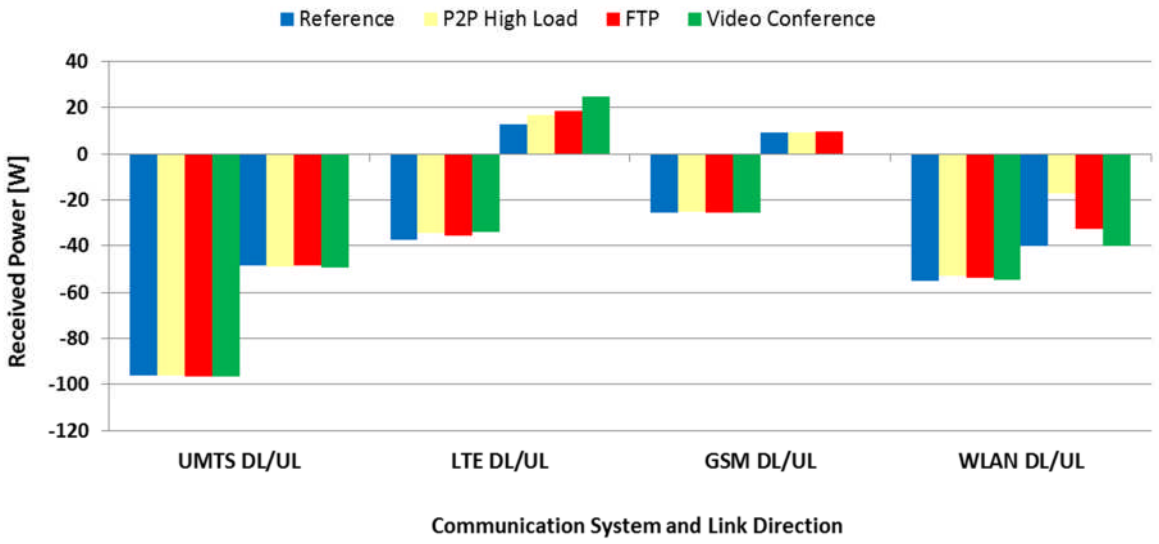

Figure 4: Comparison of the received signal powers for different services

The next step was to look at the impact of clustering, and of the distance from the users to the base station, the results being presented in **Figure 5**. Simulations were performed with users clustered at distances of 10, 50, 100, 200 and 500m from the base stations. There are no big changes in the results, but one can see the effects of power control (or lack thereof such as LTE uplink) on the received and transmitted power of the various systems under consideration. The considered scenario is small, and so power control can almost compensate the effect of the distance (as in UMTS downlink).

In **Figure 6**, the results are shown for the received powers when the number of users (or the load) increases. This was done with increase by a factor of 2, 3 and 4 on the number of users, when compared to the reference scenario.

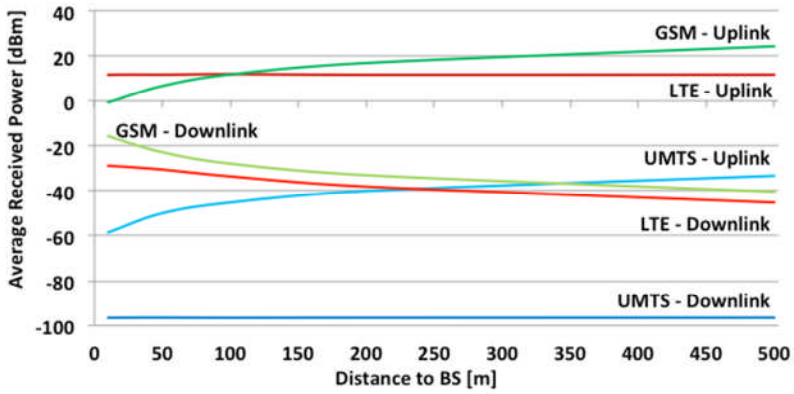

Figure 5: Comparison of the received signal powers at the users' location of the systems for different distances to the BS

UMTS power values, as expected, are very dependent on the load, but even so, it continues to be the system with the lower exposure values. As for the other systems, the variation is negligible among the different scenarios.

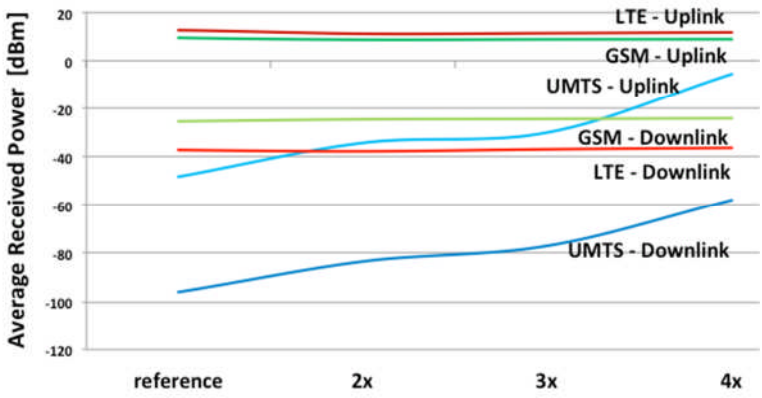

Figure 6: Received signal powers at the users' location for user densities

3.1.3.2 SAR Distribution Simulations

In this section the SAR is simulated for the downlink and uplink of each simulated systems, for the same considered scenario. For UMTS, LTE and GSM, a keep-out or exclusion zone of 10m around the base-station is considered. The closest distance to the communication device of any system is 10 cm. Both uplink and downlink of WLAN are considered with a 10 cm keep-out zone. The effect of the keep-out zones around the base-stations can be recognised by flattened peaks of the SAR around the base-station, i.e., at coordinates (0,0). SAR is used in this section to better reflect the differences between UL and DL, and has a basis for the EI calculation. The results for GSM, UMTS, LTE and Wi-Fi are shown in **Figure 7**, **Figure 8**, **Figure 9** and **Figure 10**, respectively. The results for all systems combined are shown in **Figure 11**.

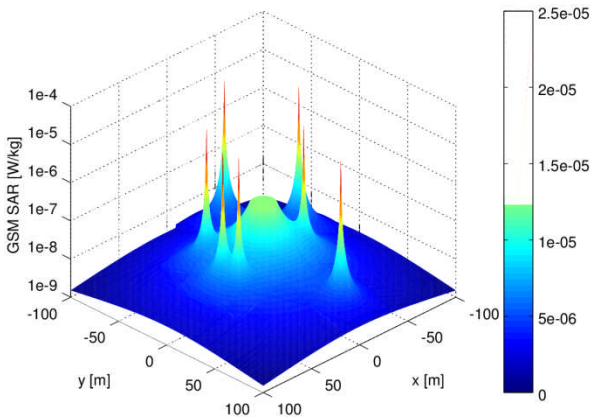

Figure 7: Combined downlink and uplink SAR Distribution in a single cell for GSM

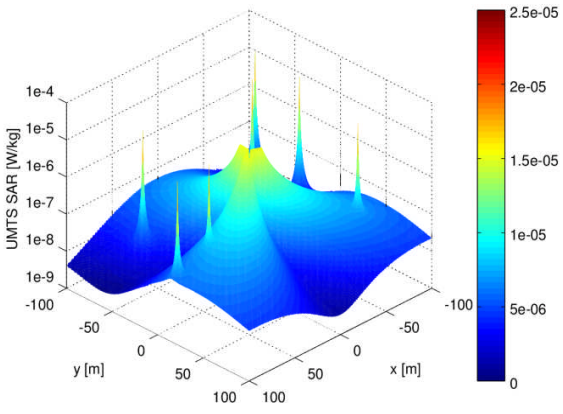

Figure 8: Combined downlink and uplink SAR Distribution in a single cell for UMTS

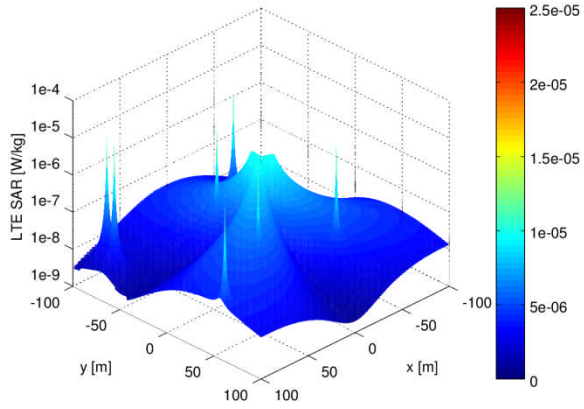

Figure 9: Combined downlink and uplink SAR Distribution in a single cell for LTE

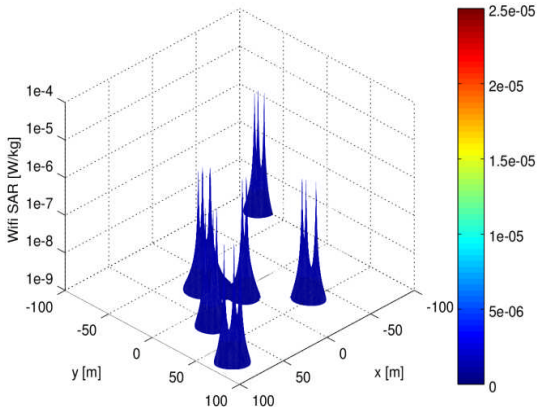

Figure 10: Combined downlink and uplink SAR Distribution in a single cell for Wi-Fi

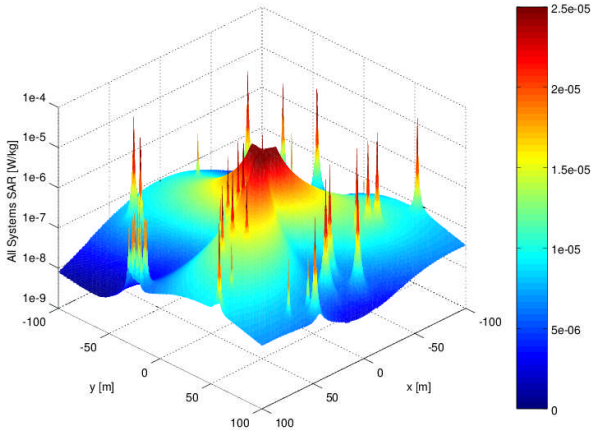

Figure 11: Combined UMTS, LTE, GSM and WLAN SAR Distribution in a single cell

Each Wi-Fi AP has 2 active users in its vicinity as it has been considered on the system level simulations, and this is easily recognisable in **Figure 10c**, as there are some clusters of three peaks closely together.

In all simulations, the results were well below the limit of 2W/kg (head) and the maximum average of 0.08W/kg (complete body) as defined by the International Commission on Non-Ionising Radiation Protection (ICNIRP) recommendations [3GPP TR 36.872] , with UMTS being clearly the system with lower transmissions powers.

3.1.3.3 Exposure Index Simulations

The total cumulative SAR for a single user without mobile is simulated and averaged over 1000 runs for a cell with four communication systems. SAR is estimated in order to calculate the EI for the considered scenario. The cumulative effect from both downlink (from the base stations/access points) and uplink (from the users) is considered. Three different traffic levels are simulated, i.e., low, medium and high. The low traffic level is the same level as the standard scenario, i.e., 7 active users for UMTS, 7 active users for LTE, 7 active users for GSM and 7 APs with 2 active users

each. In the medium and high traffic scenarios, the number of active users is increased to 14 and 28, respectively, for each of the cellular systems.
The user follows a random-walk with a constant speed of 4 m/s. The user is bounced back from the outer areas of the cell and keeps on moving during the entire simulation. The user position is evaluated every second for a period of 1 hour. The results for these simulations are given in **Table 13**. Due to the fast-decay of the transmitted powers with distance; the increase in active users does not have a significant impact in the observed EI.

Table 13: Exposure index simulations for different user densities and a user without mobile terminal

	Exposure Index [mW/kg]		
	Mean	Max	StdDev
Low (7 active users)	0.76	5.17	0.83
Medium (14 active users)	0.81	5.44	0.84
High (28 active users)	0.76	5.35	0.76

The results from **Table 13** do not include the radiation from the users' own mobile terminal. Assuming a sufficient number of active users in the cell, such that the radiation of the users' mobiles is independent of the exposure from all other radiators, the component of the radiation perceived from the own terminal can simply be added to the already obtained values, **Table 14**. The calculations were done considering perfect power control for all systems and using a noise margin for the receiver of -120dBm and a receiver margin of 30dB. Both LTE and UMTS use directional base station antennas with a maximum gain of 14dB and no antenna gains at the mobile.

Table 14: Exposure index of the different systems from the own terminal

	Exposure Index [mW/kg]		
	Mean	Max	StdDev
GSM	29.12	62.47	11.16
UMTS	7.77	35.90	6.08
LTE	13.56	64.48	10.92

The results in **Table 14** are the average value, maximum and standard deviation for 1 000 random walk patterns. Since these values are purely dependent of the users' mobile, the number of active users in the cell does not have any influence, which is expected for a single cell scenario.

UMTS due to its very advanced power control shows the lowest EI, followed by LTE and then GSM. Wi-Fi was not considered, as it is not reasonable to expect Wi-Fi coverage over the entire cell-range, which would lead to underestimated results.

In **Table 15**, the total Exposure Index (downlink and uplink) is given for the different systems, as well as the relative components for each of the directions.

Table 15: Absolute and relative exposure index of different systems

	Exposure Index		
	Total [mJ/kg/h]	Downlink [%]	Uplink [%]
GSM	29.88	2.5	97.5
UMTS	8.53	8.9	91.1
LTE	13.56	5.3	94.7

As expected, the radiating power from ones' own mobile terminal is responsible, in average, for over 90% of the EI total value.

3.1.4 Concluding remarks

The goal of the LEXNET project is to take into account the public concern on possible health effects of electromagnetic fields and to improve the acceptability of existing and future wireless systems through low exposure systems without compromising the user's perceived quality. Under this flag, this section investigated the EI for the down- and uplinks, as experienced by users in a single cell.

Simulations, which have been performed by using the Riverbed modeler, were undertaken for different mobility patterns, services, users and user clustering. The base scenario (no mobility, 7 users for each system in a 200mx200m area) shows that UMTS has a much lower exposure value, compared to the other systems. Increasing the number of users shows the largest impact in UMTS, as it is based on Code Division Multiple Access (CDMA) technology. The type of service does not have a large impact on the results, as in all cases the system has a decent traffic load.

The EI simulations provide SAR distributions for each system in the down- and uplinks, and a combined SAR distribution for all systems. From these figures one can extract that the peaks for the SAR follow the user distribution. SAR is needed in order to estimate the EI values.

Simulations showed that power control has a major impact on the cumulative SAR a person is exposed to, or to estimated EI value. More interestingly, simulations have also shown that the uplink from the users' terminals is responsible for over 90% of the overall EI, when users are making a call or using a data connection. Of course, this depends on the time frame over which the EI is evaluated, as DL is always present and UL in only when the user is making a connection. Also, the user has little control over the downlink contribution, as it depends on all the users in the cell. Future communications systems need to optimise the uplink power and power control mechanisms, as it is the main component of the exposure of users (even considering downlink is continuous and uplink is not). More dense networks can lead to a decrease in the EI, as the user is closer to the base station, needing less power to transmit.

3.2 Exposure assessment in live 3GPP and WLAN networks

Guidelines for future EMF-aware network deployments should be based on solid simulation studies and real-network measurements, in order to be able to establish which RAT to use and under which conditions. As already noted in deliverable D5.1 [LEXNET D5.1], the choice of the right RAT from an EMF exposure point of view depends on many factors, such as current traffic load, radio conditions, mobility, current application, available networks, UE capability. Different types of access technologies, or layers, are desirable for different radio and load conditions [LEXNET D5.1].

For a given topology, the layout of users per network layer should be decided, while for EMF-critical zones the change of topology must be considered. This presents a challenging question, whether the EMF reduction, as a reason for deploying new technologies, may prevail over commercial aspects in some areas (e.g. low traffic/income, GSM-only). Hopefully, ever-growing capacity needs will lead to deployment of newer, low-EMF technologies even in such areas.

Although the research attention is drawn to HetNets and LTE, the legacy networks, i.e., 2G and 3G, will still induce a significant share of the overall exposure in the years to come. This section first explores the impact of services used, over different technologies and in different radio conditions. Both uplink and downlink exposure is considered. In order to explore the validity of the offloading from a macrocell to underlaid smaller cells, measurements were performed in live (active) 2G/3G and Wi-Fi cells, in indoor environment. As the offload in current 2G/3G networks cannot be performed in an automated manner, the test cases include turning smaller cells on and off, and performing measurements under different signal levels.

EMF exposure assessment requires combining data, mostly statistical, from many different sources (operational support system, but also customer analytics system, probes on network interfaces, etc.), and processing huge amounts of data. Proper mapping of measurement data from network reports with usage data raises a significant challenge. Future guidelines could include modifications to user equipment, in order to gather and send relevant information to the network server, simplifying the process.

3.2.1 Duty Factor measurement results

The Duty Factor (DF) or the activity factor shows the actual activity of transmitters, i.e., the appearance of the signal on the radio interface. This factor is very important for EMF exposure calculations, specifically for time-averaging of uplink transmitting power. The time-averaging is necessary since the samples obtained in the UE measurement reports (generated by network tools) or in drive-test measurements are taken only when the transmitter is actually transmitting. In order to determine the average UE power that is required for EI calculations, the average UE power when the transmitter is actually transmitting should be combined with the DF.

The DF depends on the application (service) and the radio interface used. It represents the ratio between activity periods (T_{act}) and total time of transmission on the radio interface (T_{tot}):

$$DF = \frac{T_{act}}{T_{tot}} \times 100\% \quad (3)$$

For the purpose of this study, DF measurements for UE transmission were performed for mobile terminals and WLAN clients. Further, the measurements were conducted in three representative radio conditions, i.e., good, medium and bad, as described in the **Table 16Erreur ! Source du renvoi introuvable.**. These values were determined using operational networks statistics, as values for users near the base station, users in the middle area of the cell and users at the edge of the cell.

Table 16: Definition of good/medium/bad radio conditions

Radio conditions	Good	Medium	Bad
UMTS Received Signal Code Power (RSCP) [dBm]	-76	-94	-102
GSM DL Rx Lev [dBm]	-70	-88	-95
WLAN S/N [dB]	44	27	17.5

DF measurements were performed for the most commonly used services. For voice services the transcript of conversation was made, and then repeated in every test case. VoIP and Video call tests were performed with Skype application; camera turned off in only VoIP tests, and turned on in video call tests. Web surfing was performed on web site http://www.b92.net, with predefined sequence of web pages for opening and pauses between them. For automatisation of web browsing, Selenium IDE 2.7.0 extension for Mozilla Firefox web browser in WLAN test cases and NEMO drive test tool in UMTS/GSM test cases, were used. Online radio was chosen as a model for audio live streaming and http://www.naxi.rs/live web page was used. Video buffered streaming test cases were performed by using the video *"Novak Djokovic tells David Latterman how he started playing tennis",* with resolution of 640x360p, framerate 30 fps and duration of 3min and 49s. During the each test of 15min duration same video was repeated, so the buffering of video was done several times. A Television (video live) streaming test case was also performed using host "*Live Station*", where the chosen channel was *„Al Jazeera English"*[1], because of its relatively uniform content, thus providing minimal influence of content to measurement results in different tests. File was configured such file size that allowed download/upload without interruption during each test of 10 minutes duration.

DF measurements were performed using Rohde & Schwarz (R&S) ESPI Test Receiver controlled by R&S ROMES software. A frequency-selective measurement system was measuring signal level with a measuring antenna placed in the close proximity to the UE (<10 cm), which enabled the extraction of the signal originating from that UE only. The sampling time was 100µs.

[1] *http://www.livestation.com/en/aljazeera-english*

For the case of a mobile phone, DF measurements were conducted for GSM, digital cellular service and UMTS technology using SonyXperia V mobile phone. Results are presented in **Table 17**, **Table 18** and **Table 19**, respectively. For the case of WLAN client DF measurements, AP Cisco 1240 and Cisco Aironet 802.11a/b/g Wireless Adapter were used. Measurements were conducted for 802.11g and 802.11a WLAN standards; results are presented in **Table 20**.

Table 17: DF of GSM mobile phone for the most commonly used services

DF (%)	Radio conditions		
	Good	Medium	Bad
Web	6.00	5.98	9.88
Voice (noisy env*)	12.41	11.63	12.42
Voice (normal env)	5.0	6.7	6.7
Video Streaming	6.75	8.15	10.48
Skype VoIP	21.21	23.58	22.07
Skype Video	22.11	22.04	17.44
TV	No service	No service	No service
File Upload	23.68	19.86	24.09
File Download	6.99	9.29	12.06
Audio Streaming	5.30	6.49	10.11

* Due to large quantities of acoustical noise surrounding the speaker

Table 18: DF of GSM 1800 mobile phone for the most commonly used services

DF (%)	Radio conditions		
	Good	Medium	Bad
Web	5.59	5.70	6.11
Voice	11.91	12.02	12.37
Video Streaming	5.76	6.44	7.35
Skype VoIP	22.39	22.18	17.06
Skype Video	21.68	22.96	22.96
TV	No service	No service	No service
File Upload	22.53	23.53	19.14
File Download	6.66	6.60	7.53
Audio Streaming	4.58	4.71	6.12

Table 19: DF of UMTS mobile phone for the most commonly used services

DF (%)	Radio conditions		
	Good	Medium	Bad
Web	49.17	50.74	31.49
Voice	97.90	94.41	99.40
Video Streaming	48.69	54.02	45.22
Skype VoIP	45.92	46.33	71.12

Skype Video	55.76	59.26	62.58
TV	72.24	74.41	48.82
File Upload	99.18	95.26	40.50
File Download	83.77	48.81	37.54
Audio Streaming	30.89	54.09	66.58

Table 20: DF of WLAN client for 802.11g and 802.11a network for the most commonly used services

DF (%)	802.11g Radio conditions			802.11a Radio conditions		
	Good	Medium	Bad	Good	Medium	Bad
Web	0.89	0.68	0.91	0.26	0.51	0.52
Skype VoIP	2.22	3.02	4.55	1.39	1.52	1.83
Skype Video	8.77	13.41	20.32	5.2	6.43	7.63
Audio Streaming	0.4	0.53	0.56	0.21	0.26	0.25
Video Streaming	1.9	1.96	3.51	1.06	1.64	1.31
File Download	8.1	8.27	10.17	5.04	7.07	6.72
File Upload	56.81	71.26	73.66	36.6	54.64	57.69
TV	2.23	3.1	3.46	1.27	1.88	1.76

The variety of the above results, from almost 100% for file upload in good radio conditions of the UMTS to 0.21% for audio streaming over Wi-Fi with a good SNR, implies that the duty factor plays a crucial role in the evaluation of the EI. UE Tx power samples recorded over 3GPP networks when the transmitter is actually transmitting do not mean much without the effect of pauses in transmission taken into account. Further, it is evident that the DF depends heavily on the application used, the technology used, and radio conditions, while it may as well depend on network load conditions.

Considering the behaviour of the DF regarding the radio conditions it can be concluded that DF has higher value for worse radio conditions. That is expected, because in the worse radio conditions more robust radio techniques are used. These radio techniques have a less throughput and need more time to transmit same data volume. Exceptions to previous conclusion could be seen in UMTS web browsing, file upload and download. Actually, in those cases DF has lower values for worse radio conditions. It should be noted that, in order to measure DF while the service is active, duration of each test was the same, with continuous service during the test, thus leading in transmission of different traffic volumes for different radio conditions. Comparing the radio technologies, it can be concluded that UMTS has the highest DF values for all considered applications, with exception of FTP upload in bad radio conditions where WLAN prevails. This is a consequence of the fact that in UMTS transmitter often transmits continuously in contrast to a GSM transmitter which transmits in time slots or to WLAN transmitter which transmits on per packet basis. GSM has higher values of DF for applications comparing to WLAN, except for FTP upload. Regarding the analysed applications, it can be concluded that more

demanding applications in uplink, lead to higher values of DF. The highest values of DF are obtained for FTP upload, as expected. Again, exception could be seen in case of UMTS in bad radio condition, where highest DF values are obtained for real time applications.

However, distinguishing different services and correlating them with recorded power levels is not possible at the moment in a real cellular network, thus combining the power levels with DF values may be done only on average values basis. For establishing this correlation, the network would need new intelligence, real-time correlation of radio parameters (L3 messages in the radio part) with applications used (e.g. from probes in the core). Agents deployed in mobile phones could also help establish this correlation.

3.2.2 Voice service analysis with respect to UL EMF exposure

Voice service can be realised in different ways: circuit-switched (CS) service over GSM and UMTS or packet-switched (for example, Skype) service over UMTS and WLAN. The measurements presented in this section tend to answer the question which kind of voice service impacts the EMF exposure the most.

The analysis needs to take into account many factors:

- Technology (multiple access schemes, circuit/packet-switched, coding, power control…)
- Propagation (radio) conditions
- User's environment
- Transmitter activity factor (duty cycle)
- Transmitter's power while emitting

Measurements were performed using mobile terminals or WLAN clients. Tested voice services were CS GSM, CS UMTS, Skype over UMTS, and Skype over WLAN. Measurements were taken for three representative radio conditions, i.e. good, medium and bad, as described in **Table 16**.

The transmitter activity (duty factor) of mobile terminals and WLAN clients was measured using R&S ESPI Test Receiver. The transmitter power of the mobile devices (UE Tx power) was read using NEMO Drive test tool. At this point, it should be noted that WLAN clients are working with constant power.

3.2.2.1 Duty factor

Duty factor measurements were performed for various services under different radio conditions, and the processed results for voice services are shown in
Table 21. For GSM voice, acoustical noisy environment results in almost theoretical occupancy of dedicated time slots (as described in D5.1 [LEXNET D5.1], the technology itself implies usage of 1 out of 8 time slots in the uplink for voice service, which corresponds to 12.5% duty factor). For a normal conversation, with pauses in speaker activity, the duty factor is smaller (due to discontinuous transmission functionality of the system).

Table 21: Duty factor for different voice services under different radio conditions

DF [%]	Radio conditions		
	Good	Medium	Bad
GSM900 Voice (noisy env.)	12.4	11.6	12.4
GSM900 Voice (normal env.)	5.0	6.7	6.7
GSM900 Skype VoIP	21.2	23.6	22.1
GSM1800 Voice (noisy env.)	11.9	12.0	12.4
GSM1800 Skype VoIP	22.4	22.2	17.6
UMTS Voice	97.9	94.4	99.4
UMTS Skype VoIP	45.9	46.3	71.1
WLAN 802.11g Skype VoIP	2.2	3.0	4.6

3.2.2.2 Transmitter's power

Measurements of the UE Tx power for regular voice CS service over GSM and UMTS were performed for good, medium and bad radio conditions. The results are shown in Figure 12: UE Tx power for regular CS voice service over GSM and UMTS**Figure 12**, where the Probability Density Function (PDF) of measured UE Tx power samples is displayed, and the average values are summarised in **Table 22**.

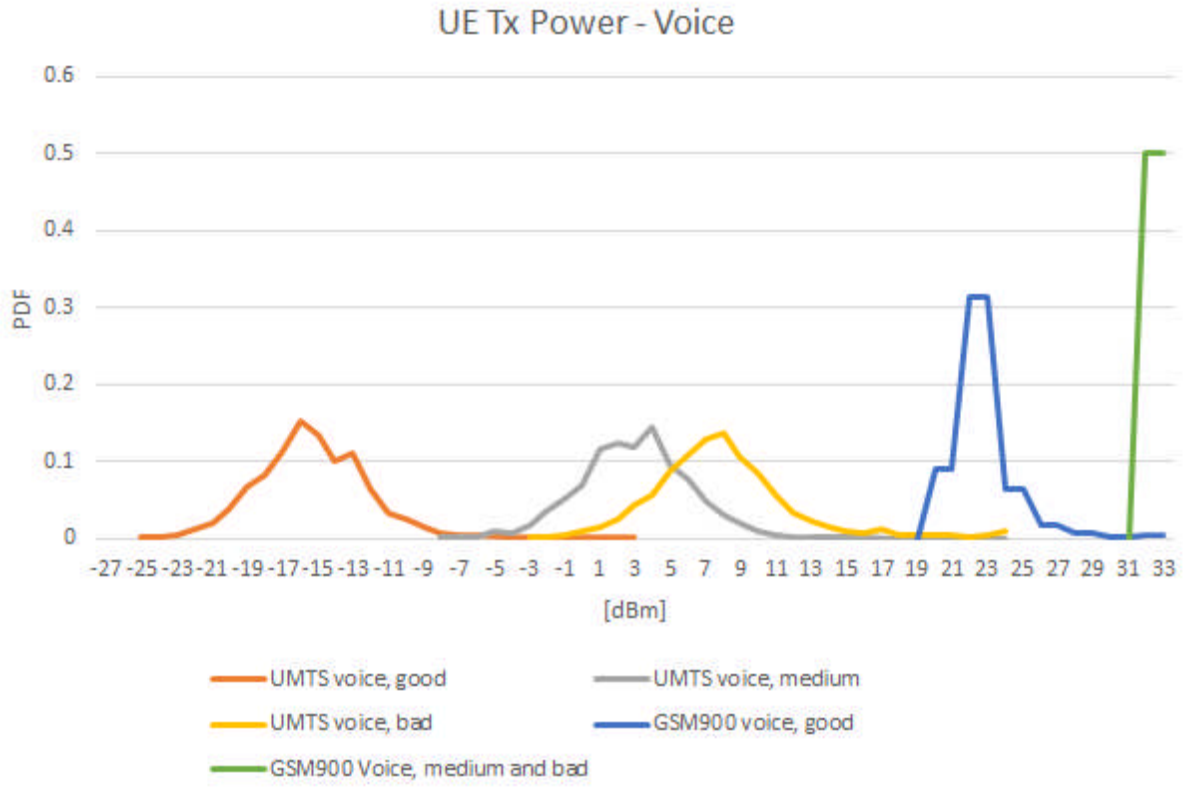

Figure 12: UE Tx power for regular CS voice service over GSM and UMTS

Figure 12 shows that UMTS voice service in good radio conditions yields the lowest UE Tx power levels, as expected. Worsening of the radio conditions leads to higher power levels, but still lower in comparison with recorded GSM levels. One should note that the presented results are based on raw recorded samples, i.e. no pauses in transmitter activity are included. It is interesting to note that GSM voice service even in medium radio conditions yields maximum UE Tx power levels.

Table 22: Average UE Tx power and average Rx signal level for GSM and UMTS voice service

	UMTS good	UMTS medium	UMTS bad	GSM900 good	GSM900 medium	GSM900 bad
Average UE Tx Power [dBm] *	-15.34	3.09	7.98	22.77	32.50	32.50
***Average DL Signal Level* [dBm]**	-74.35	-94.41	-101.38	-68.81	-88.00	-95.00

* Transmitter's power while emitting

Measurement results of the UE Tx power for UMTS Skype VoIP service are shown in Figure 13, and the average values are summarised in Table 23.

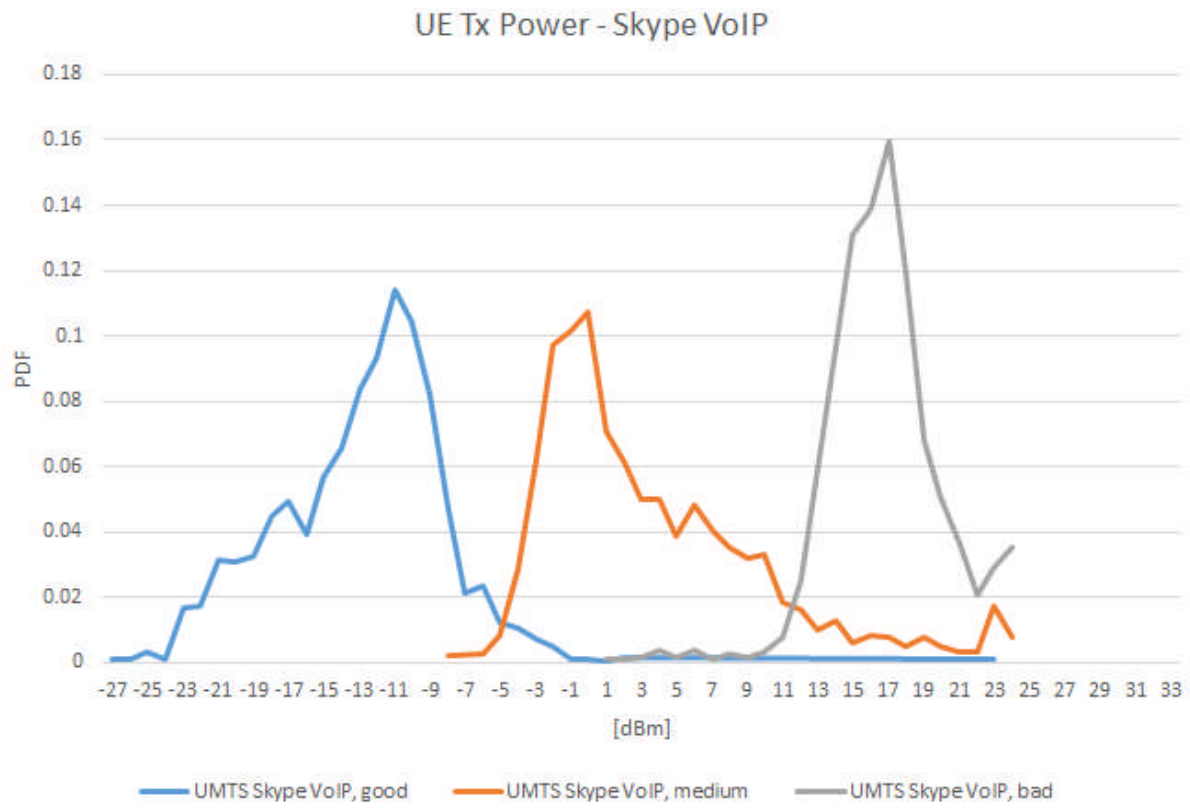

Figure 13: UE Tx power for UMTS Skype VoIP service

Again, good radio conditions yield the lowest UE Tx power levels. Looking at the average values, the obtained values for UMTS Skype service in good radio conditions are better (smaller) than for regular CS voice service over UMTS. For

medium radio conditions, these two values are comparable, while in bad radio conditions Skype yields higher values than regular CS voice service. This behaviour should be further explored. Namely, the explanation may lie in the following. In good radio conditions, regular CS voice service is granted higher power levels than data service, due to its real-time nature i.e. sensitivity to delay. Data service, on the other hand, may afford packet losses and retransmissions (which are obviously rare in good radio conditions). As the radio conditions worsen, the loss of packages and the needed retransmissions for VoIP service grow, thus total throughput requirements grow, and the terminal at the end emits with higher power levels than for regular CS voice service under same radio conditions.

Table 23: Average UE Tx power and Average Rx signal level for UMTS Skype VoIP service

	UMTS Skype good	UMTS Skype medium	UMTS Skype bad
Average UE Tx Power [dBm]*	-12.88	3.67	16.74
***Average DL Signal Level* [dBm]**	-76.62	-93.80	-102.02

* Transmitter's power while emitting

Measurement results of the UE Tx power levels for Skype VoIP service over WLAN 802.11g are illustrated in **Figure 14**. WLAN clients transmit with constant power, due to the absence of power control, i.e., 100 mW (20 dBm), which is a rather high value. Comparing with values shown in **Table 22** and **Table 23**, higher average (per samples) values are obtained only for GSM CS voice service. Nevertheless, the average value in time needs to count for the duty factor, and this may bring a rather different picture of the actual exposure.

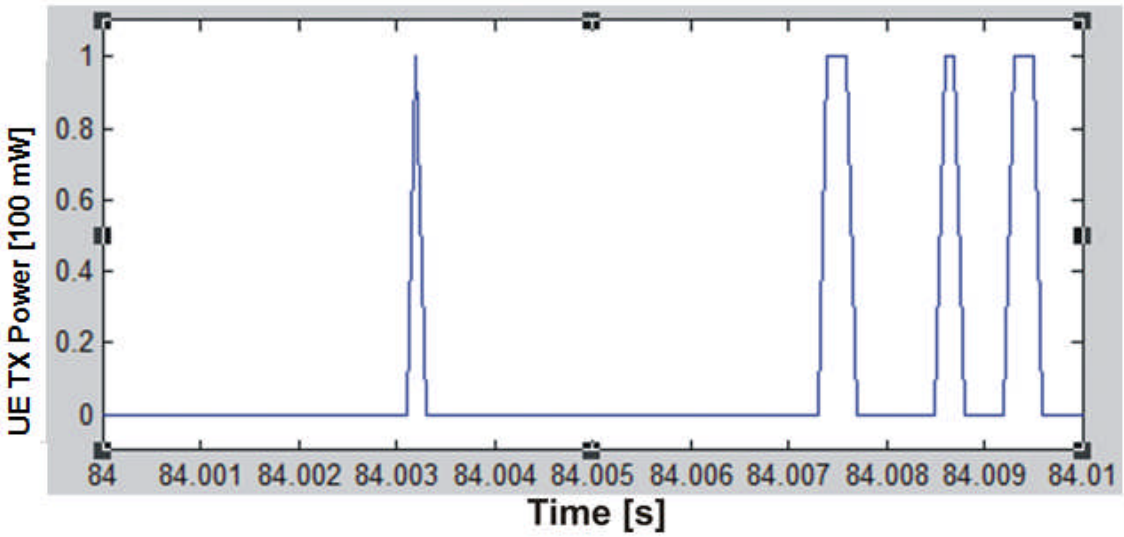

Figure 14: Output power of the WLAN client transmitter

3.2.2.3 Comparison of different Voice service types with respect to EMF exposure

In order to compare the contribution of uplink exposure for voice service to the overall EI, a *δEI* is defined, as a part of EI originating from the transmitted power of the terminal device, and normalised with respect to time duration of exposure.

Starting from the EI equation [LEXNET D2.6], the *δEI* is calculated for:

- one person,
- a considered technology,
- used service (voice),
- the same posture (standing),
- two population categories (adult and child),
- an indoor environment.

In addition, it is normalised for the same user profile and the time duration of usage. Thus, *δEI* is a comparative value for varying services and radio conditions.
The comparison results for good, medium and bad radio conditions are given in tables **Table 24**, **Table 25**, and **Table 26**, respectively. In these tables, GSM and UMTS Tx power levels are obtained by measurements (see **Table 22** and **Table 23**). The only exception is for GSM in bad propagation conditions where the maximum value of 33dBm is assumed. Also, for GSM Tx power, normal and noisy environments are considered in the same manner. On the other side, WLAN transmitters always operate with constant power (20dBm). Duty factor values are taken from
Table 21. Finally, the voice service normalised SAR values for child and adult (standing position) are taken from [LEXNET D2.6]. Based on these data, values of *δEI* are obtained as a product of normalised wbSAR, Tx power and duty factor.

Table 24: Comparison of different voice service types for good radio conditions

Good radio conditions	GSM (noisy)	GSM (normal)	UMTS	UMTS Skype VoIP	WLAN Skype VoIP
Tx power [dBm]	22.77	22.77	-15.34	-12.88	20
Duty factor [%]	12.4	5	97.9	45.9	2.2
Normalised wbSAR (child)	0.029	0.029	0.011	0.011	0.014
Normalised wbSAR (adult)	0.012	0.012	0.0052	0.0052	0.0047
***δEI* (child)*10^6 [W/kg]**	680.49	274.39	0.31	0.26	30.80
***δEI* (adult)*10^6 [W/kg]**	281.58	113.54	0.15	0.12	10.34

Table 25: Comparison of different voice service types for medium radio conditions

Medium radio conditions	GSM (noisy)	GSM (normal)	UMTS	UMTS Skype VoIP	WLAN Skype VoIP
Tx power [dBm]	32.5	32.5	3.09	3.67	20
Duty factor [%]	11.6	6.7	94.4	46.3	3

Normalised wbSAR (child)	0.029	0.029	0.011	0.011	0.014
Normalised wbSAR (adult)	0.012	0.012	0.0052	0.0052	0.0047
***δEI* (child)*10^6 [W/kg]**	5982.13	3455.20	21.15	11.86	42.00
***δEI* (adult)*10^6 [W/kg]**	2475.36	1429.74	10.00	5.61	14.10

Table 26: Comparison of different voice service types for bad radio conditions

Bad radio conditions	GSM (noisy)	GSM (normal)	UMTS	UMTS Skype VoIP	WLAN Skype VoIP
Tx power [dBm]	32.5	32.5	7.98	16.74	20
Duty factor [%]	12.4	6.7	99.4	71.1	4.6
Normalised wbSAR (child)	0.029	0.029	0.011	0.011	0.014
Normalised wbSAR (adult)	0.012	0.012	0.0052	0.0052	0.0047
***δEI* (child)*10^6 [W/kg]**	6394.69	3455.20	68.67	369.20	64.40
***δEI* (adult)*10^6 [W/kg]**	2646.08	1429.74	32.46	174.53	21.62

Table 27 summarises values of δEI x 10^6 for different voice service types and radio propagation conditions for adults. A similar summary can be also created for children.

Table 27: Comparison of δEI x 10^6 for different voice services and radio conditions, for adults

Radio conditions	GSM (noisy)	GSM (normal)	UMTS	UMTS Skype VoIP	WLAN Skype VoIP
GOOD	281.58	113.54	0.15	0.12	10.34
MEDIUM	2475.36	1429.74	10.00	5.61	14.10
BAD	2646.08	1429.74	32.46	174.53	21.62

Generally, the lowest exposure is achieved by using UMTS technology. When using Skype service over UMTS, the exposure is lower than when using regular CS voice service under good and medium radio conditions. On the contrary, in bad radio conditions, using regular UMTS voice CS service is much better than using Skype over UMTS (from **Table 27**, over 5 times less exposure is obtained for UMTS vs. UMTS Skype VoIP in bad radio conditions).

GSM is by far the worst technology to use for voice service. In all radio conditions, the exposure is several orders of magnitude higher than for UMTS.

Using WLAN technology yields small variations in exposure for different radio conditions, since there is no power control. Whether the conditions are good or bad, the exposure is almost the same. It only slowly grows with worsening radio

conditions, probably due to the needed retransmissions. Compared to GSM, it's better to use UMTS technology in good radio conditions (over 70 times less exposure), while the preference is somewhat prevailing for WLAN in bad radio conditions (however the quality of the connection is disputable in such cases).

The results unambiguously show that UMTS is the preferred technology among the ones considered, and that providing a good signal for the population reduces the exposure. This means that a higher density of base stations in the network would yield lower exposure of users to the RF radiation of the terminal devices. Although this analysis is devoted to comparison of UL exposure, it should not be forgoten that the higher density of base stations can lead to an increase of DL exposure.

3.2.3 The analysis of various 3G services with respect to UL EMF exposure

The measurement results for UE Tx power for several services under different radio conditions are presented in this section. The measurements were performed for the following services: voice, Skype voice, Skype video, Audio stream, Web browsing, FTP download, FTP upload, TV stream, and Video stream. The same traffic model is used as described in Section 3.2.1.

The PDF of measured UE Tx power samples (transmitter's power while emitting) for various UMTS services in good radio conditions is shown in Figure 15. FTP upload results in distinguishably highest power samples, followed by FTP download and Skype video.

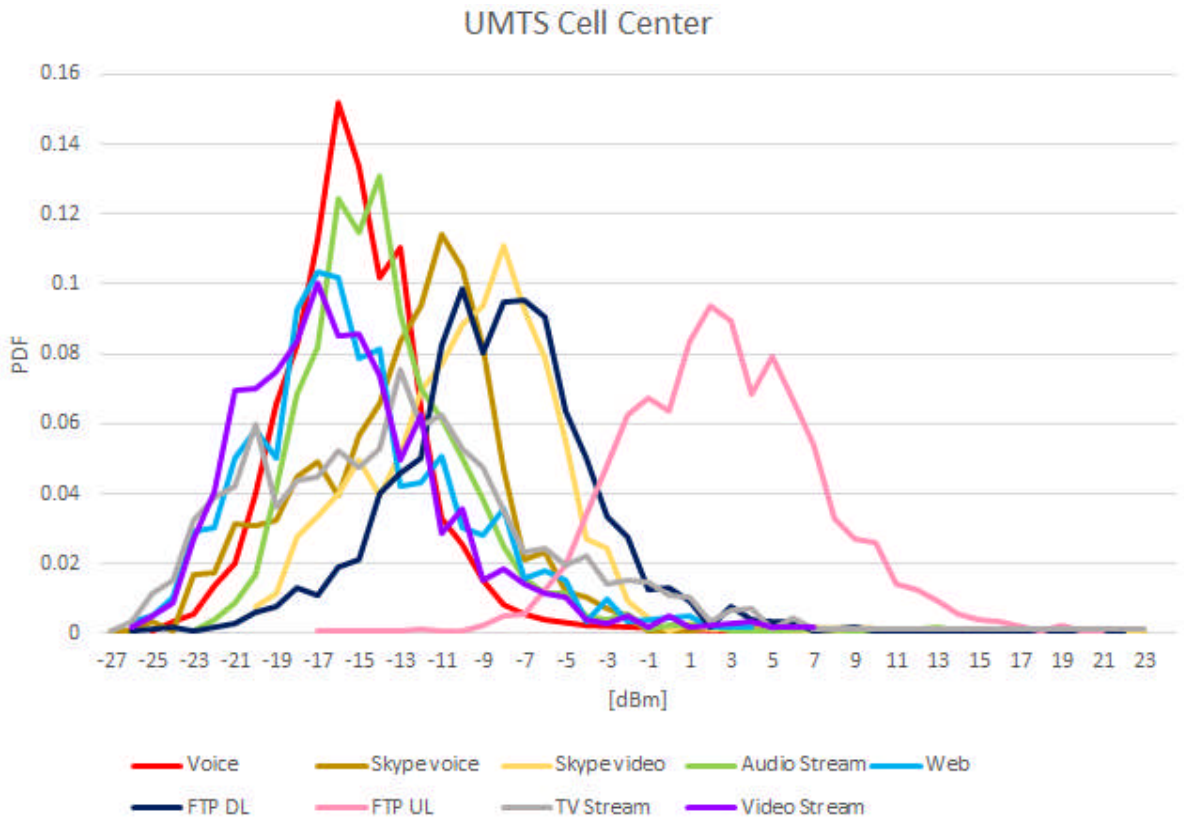

Figure 15: UE Tx power in UMTS for various services in good radio conditions

The results for medium radio conditions are shown in **Figure 16**, revealing a movement of average power levels for all services towards the higher values. FTP upload reaches maximum powers, again followed by Skype video and FTP downloads.

The results for bad radio conditions are shown in **Figure 17**. The recorded power levels for all services are squeezed more to the left, i.e., to the higher values, and besides the FTP upload which is again the least desirable service from the EMF exposure point of view, Skype video may be distinguished, with Skype voice approaching. Power levels for other services are rather smeared, and the least exposure may be expected from Web browsing and regular voice.

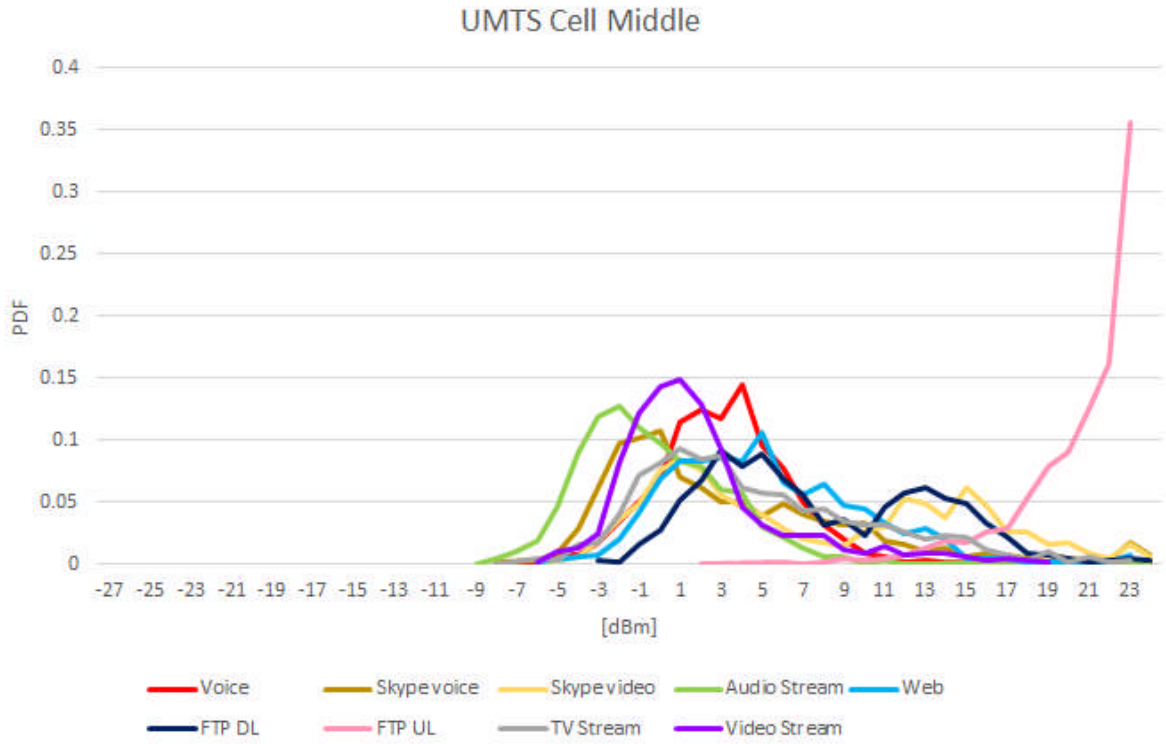

Figure 16: UE Tx power in UMTS for various services in medium radio conditions

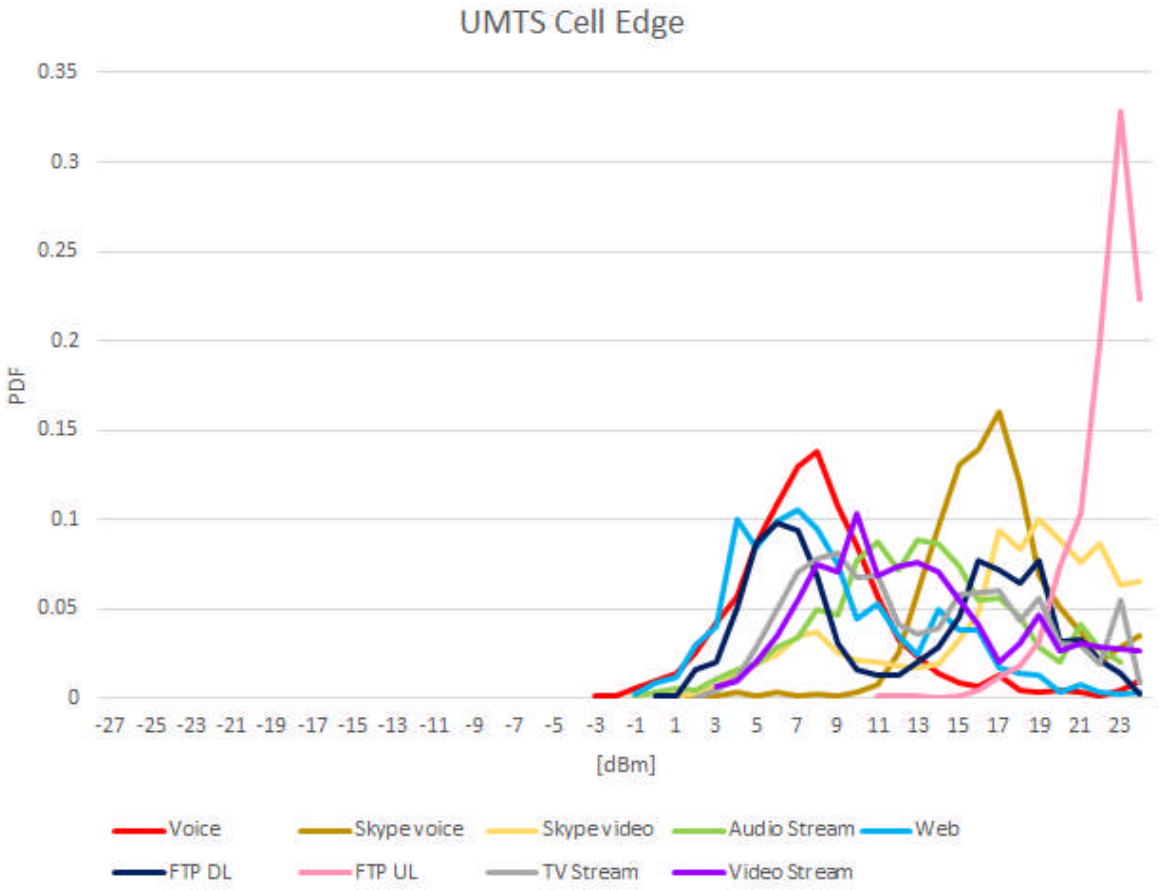

Figure 17: UE Tx power in UMTS for various services in bad radio conditions

Table 28 summarises average values of UE Tx power for various UMTS services in different radio conditions.

Table 28: Average Tx power of UMTS mobile phone for the most commonly used services

Average UE TX Power [dBm]*	Radio conditions		
	Good	Medium	Bad
Web	-15.14	5.25	8.67
Voice	-15.34	3.09	7.98
Video Streaming	-15.62	2.06	13.01
Skype VoIP	-12.88	3.67	16.74
Skype Video	-9.90	7.62	16.80
TV	-13.01	4.80	13.15
File Upload	2.64	20.57	22.23
File Download	-8.38	7.87	11.90
Audio Streaming	-13.52	-0.13	13.04

* Transmitter's power while emitting

The duty factor was also measured for all considered services and radio conditions, and the results are summarised in Table 19.

Again, combining measured power samples with duty factor values, for a person, posture, given user profile and technology, will give the *δEI,* i.e., the uplink part of the EI for a given service in given radio conditions. While the uplink exposure may be dominant in medium and bad radio conditions, for part of the users in good radio conditions, positioned in the cell centre (close to the base station), the downlink part of exposure might play a significant role, especially on a daily basis. Namely, for people who live and work near the BS, DL exposure should also be considered.

3.2.4 The impact of cell size: GSM CS voice

This section describes the measurements performed in order to compare the overall (uplink and downlink) exposure for the case of classical macrocell coverage and the case of deploying an additional microcell layer for covering a relatively small area.

The measurements were performed in two locations:

- Site ETF: Besides the classical macro site (served by macro base stations), two micro base stations are deployed for providing indoor coverage,
- Site LOLA: Besides the classical macro site, a base station with distributed antenna system is deployed for providing micro indoor coverage

Here, the difference between the single antenna (close to the micro base station) and distributed antenna system (DAS) should be emphasised. Base station with DAS deploys a number of spatially distributed antennas connected to a common base station using RF antenna cables. In this way, more uniform wireless service coverage within an indoor area can be provided. Considering downlink, DAS usually has similar characteristics with micro base station with single antenna solution. On the other side, connecting remote antennas with RF cables can introduce additional losses in the uplink (depending of the cable length). This can cause that UE transmit with higher powers comparing to the case of single antenna close to the micro BS.

The measurements were carried out in the following manner:

- The transmitted power of the UE (uplink): statistics on cell level, gathered directly from network elements, i.e. Radio Network Controller (RNC)/Base Station Controller (BSC), from L3 messages in which the UEs send the data on transmitter power.
- Electric field strength (downlink):
    - Calibrated Rohde & Schwarz portable measurement system consisting of spectrum analyser R&S FSH6 and antenna R&S TS-EMF in the form of an isotropic radiator. This system is designed for frequency selective measurements of electric field strength in the frequency range from 30 MHz to 3 GHz.
    - Software module White Tigress Baby - Measurements, specially developed for the space measurements in Radio-communications Laboratory, School of Electrical Engineering, University of Belgrade for the purpose of LEXNET project.
    - Measurements were conducted in a number of positions distributed in two buildings (sites): Lola and ETF (building of School of Electrical

Engineering, University of Belgrade) and for the two cases: with micro cell base station turned ON and OFF.

3.2.4.1 Uplink: the power of user equipment for GSM900 voice service

For GSM, the uplink transmitter powers on a cell level may be measured for voice service only. This, on the other hand, represents an advantage as all the measured power samples can be correlated to a single service.

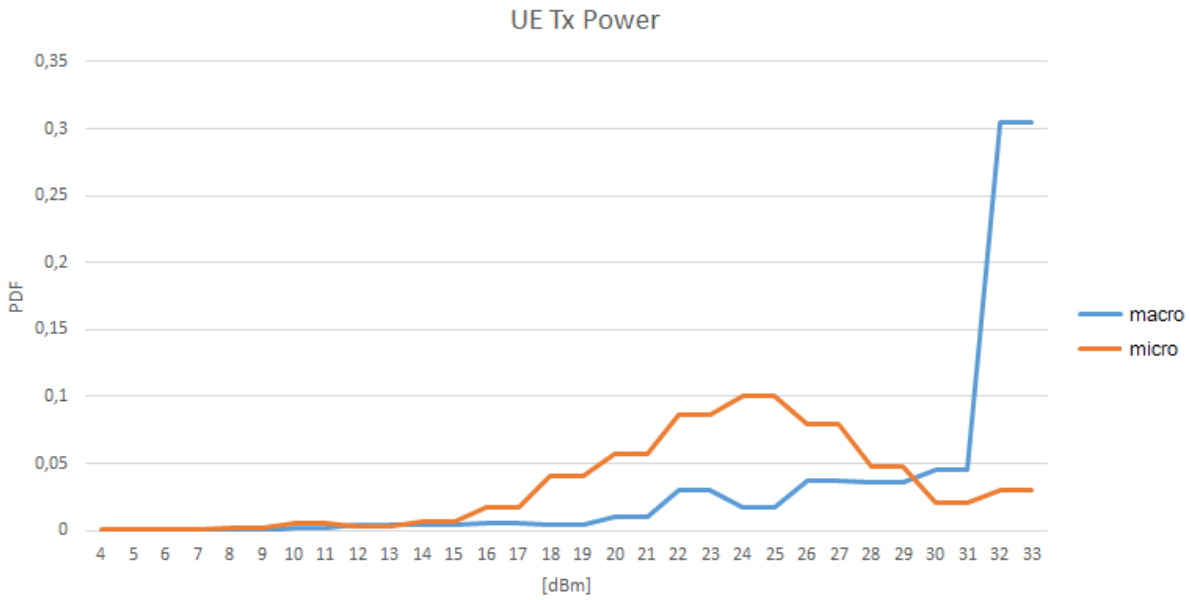

Figure 18: UE Tx power on cell-basis for voice GSM900 service, for a macro and underlaid (indoor) micro cell, site ETF

Figure 18 shows the results for UE Tx power for voice service taken from per-cell network reports, for the macro cell and the underlaid (indoor) micro cell, at the ETF site.

In **Table 29** the average values of the recorded power levels are given. It is from these results that the UEs connected to the micro site transmit on average with lower power than those connected to the macro cell.

Table 29: Average UE Tx power for the GSM900 macro and micro site ETF, voice service

UE Tx POWER	MACRO	MICRO
Average UE Tx Power [dBm]*	29.76	23.84

* Transmitter's power while emitting

Figure 19 shows the results for UE Tx power for voice service taken from per-cell network reports, for the macro cell and the underlaid (indoor) micro cell (DAS solution), at site LOLA.

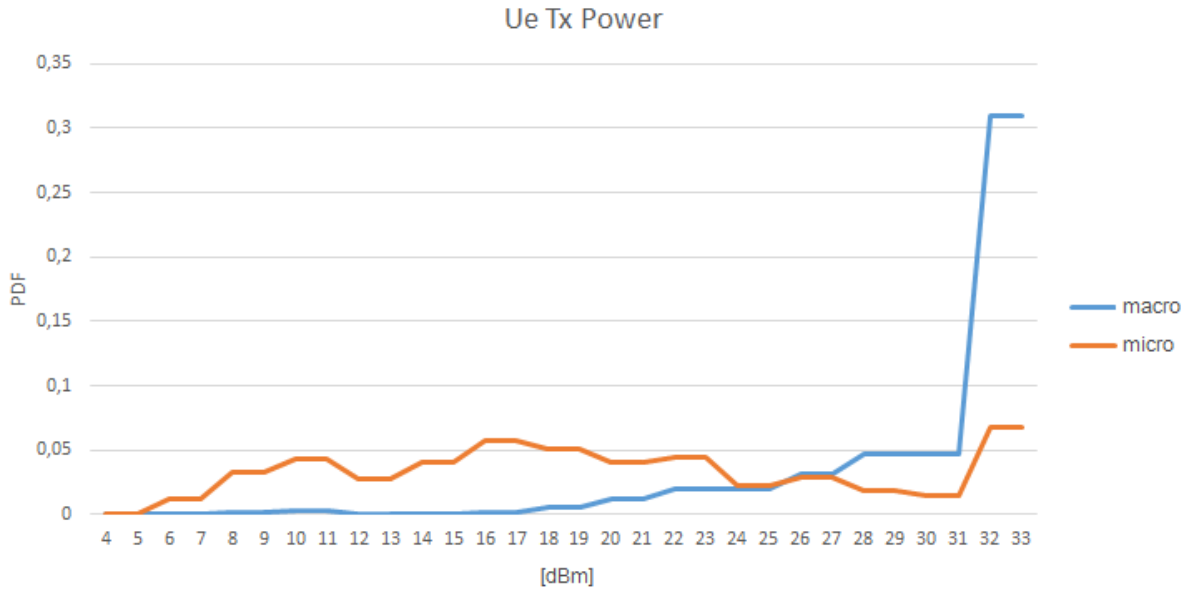

Figure 19: UE Tx power on cell-basis for voice GSM900 service, for a macro and underlaid (indoor) micro cell, site LOLA

In **Table 30** the average values of the recorded power levels are given. Here, the difference between average power levels for customers connected to the macro and those connected to the micro cell is even more visible. This is probably the consequence of the fact that DAS solutions usually provide more uniform coverage of the area than classical micro base stations.

Table 30: Average UE Tx power for the GSM900 macro and micro site LOLA, voice service

UE Tx POWER	MACRO	MICRO
Average UE Tx Power [dBm]*	30.07	19.83

* Transmitter's power while emitting

3.2.4.2 Downlink: electrical field, GSM and UMTS

Measurements were conducted in a number of uniformly distributed positions distributed in two buildings (sites): Lola and ETF (building of School of Electrical Engineering, University of Belgrade) and for the two cases: with micro cell base station turned ON and OFF. In Lola building measurements were conducted in 102 positions and in ETF building measurements were conducted in 108 positions

Band selective measurements were conducted for the following frequency bands and mobile networks:

- GSM 900 (whole band),
- GSM 900 operator TELEKOM,
- GSM 900 operator TELENOR,
- GSM 900 operator VIP mobile,
- GSM 1800 (whole band),
- GSM 1800 operator TELEKOM,
- GSM 1800 operator TELENOR,

- GSM 1800 operator VIP mobile,
- UMTS (whole band),
- UMTS operator TELEKOM,
- UMTS operator TELENOR,
- UMTS operator VIP mobile.

For the sake of brevity, only measurement results obtained for GSM 900 operator TELEKOM and UMTS operator TELEKOM will be considered in this document. It should be stressed that similar results were obtained for the other aforementioned systems operated by TELEKOM and other two mobile operators.

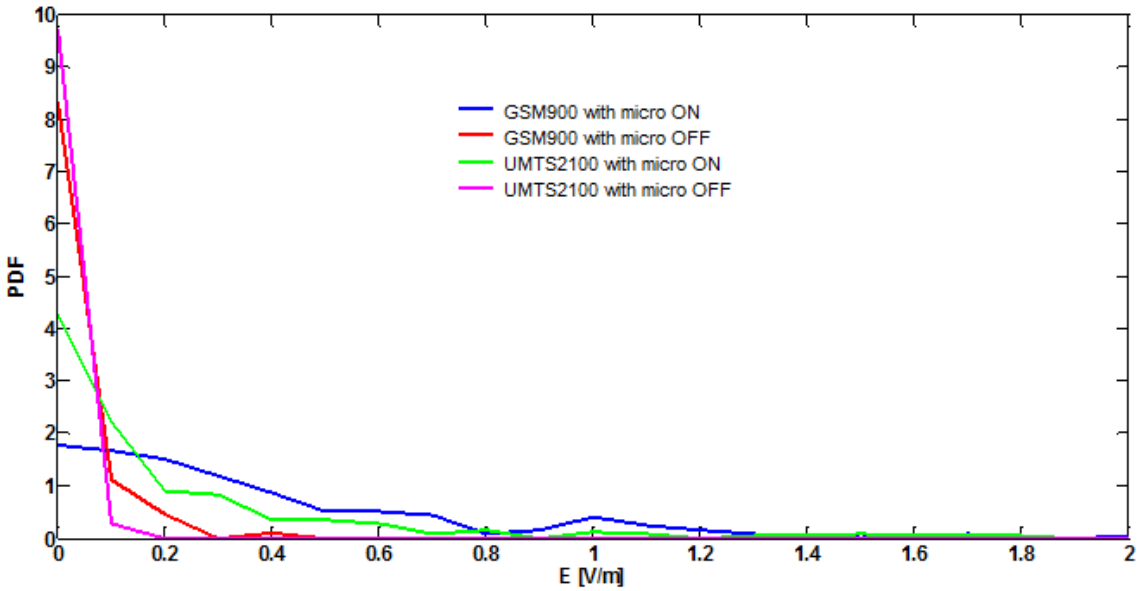

Figure 20: PDF of electrical field strength for GSM and UMTS, for site ETF with micro cells turned ON and OFF

Based on the values obtained in a number of uniformly distributed measurement positions statistical analysis were performed. **Figure 20** shows the PDF of measurements results of the electrical field strength values for GSM900 and UMTS, for the cases when the respective micro cell layer is turned ON and OFF. Additionally, average values of electrical field strength obtained at sites ETF and LOLA with respective micro cell layer turned ON and OFF are presented in **Table 31**.

Table 31: Average values of electrical field strengths at sites ETF and LOLA with respective micro cells turned ON and OFF

	E_average [V/m] (ETF)	E_average [V/m] (LOLA)
GSM 900 with micro ON	0.464	1.119
GSM 900 with micro OFF	0.061	0.235
UMTS with micro ON	0.262	0.355
UMTS with micro ON	0.036	0.129

As expected, from the results presented in **Table 31** it is evident that the addition of the micro cell layer causes the significant growth of electrical field strength level and consequently the downlink EMF exposure.

3.2.4.3 The analysis of EMF exposure (uplink and downlink) for GSM900 voice

EMF exposure was considered for the cases when microcell base stations are deployed or not. In order to compare these two cases a *δEI* is defined, as a part of EI. Starting from the EI equation [LEXNET D2.6], the *δEI* is calculated for:

- one time period (8 hours),
- one population category (adult),
- one environment (indoor for two different buildings),
- one radio access technology (GSM 900),
- two cell types (micro and macro),
- one user profile (heavy user),
- one posture (sitting) and
- one type of usages (voice).

The analysis was performed for the two aforementioned sites (ETF and LOLA) assuming GSM 900 technology for voice service. The parameters taken for calculation of the *δEI* for working hours, site ETF, adults and heavy users are presented in **Table 33**.

Table 32: The *δEI* for working hours, site ETF, adults, heavy users

	MACRO	MICRO
Average Tx Power UL [dBm]	29.76	23.84
Duty factor UL [%]	6.7	5
Normalised SAR (UL)	0.012	0.012
Average usage time in seconds (UL) - 22.87min	1372	1372
Average E DL(V/m)	0.061	0.464
Duty factor DL [%]	100	100
Normalised SAR (DL)	0.0056	0.0056
Average usage time in hours (DL) – working hours	8	8
***δEI* *10^{6} [W/kg]**	36.24	6.92

The values for Average Tx Power in UL were obtained from network, using cell statistics. Duty factor in UL for voice service was obtained experimentally using procedure described in the previous sections. The average values of electrical field strength at sites ETF and LOLA with respective micro cells turned ON and OFF were obtained by measurements in a number of measurement positions statistically. On the other side, the duty factor in DL was assumed to be 100% and the average usage time in hours (DL) was taken to be 8 hours. Values for Normalised SAR (UL), Average usage time in seconds (UL) and Normalised SAR (DL) are taken from [LEXNET D2.6].

From the obtained results it is obvious that the deployment of the additional GSM900 micro layer leads to a *δEI* reduction of about 81% for using voice service over GSM technology.

It should be noted that the reduction in EMF exposure depends heavily on user habits, i.e., usage duration. Hypothetically, if all people would stop using the phone, on addition of the micro layer, the *δEI* would increase due to the increase of downlink exposure. However, since the users do not change their habits and in fact tend to use the mobile phones more extensively, the introduction of the micro layer leads to actual reduction of the *δEI*.

Table 33 shows similar results for site LOLA. Here, the deployment of the additional GSM900 micro layer leads to *δEI* reduction of about 93% for using voice service over GSM technology.

Table 33: The *δEI* for working hours, site LOLA, adults, heavy users

	MACRO	MICRO
Average Tx Power UL [dBm]	30.07	19.83
Duty factor UL [%]	6.7	5
Normalised SAR (UL)	0.012	0.012
Average usage time in seconds (UL) - 22.87min	1372	1372
Average E DL(V/m)	0.235	1.119
Duty factor DL [%]	100	100
Normalised SAR (DL)	0.0056	0.0056
Average usage time in hours (DL) – working hours	8	8
***δEI* *10^{6} [W/kg]**	38.92	2.76

In conclusion, by introducing the micro layer, i.e., by bringing the base stations closer to the user, a significant reduction of the *δEI* for GSM voice service usage can be achieved. Here, one should have in mind that, in the previously analysed scenario, the macro cell was turned on all the time (as usual in mobile networks), i.e., the comparison was done for the *δEI* with micro layer turned on and off, but with active macro layer in both cases.

3.2.4.4 Uplink: The power of user equipment for UMTS CS voice and PS data services

For UMTS, the power levels obtained from network reports on cell level cannot be separated by services. High power levels might mean that the user was close to the base station using a demanding data service, but also that he was far away from the base station. Thus, no correlation between power levels and individual services may be drawn. As a consequence, all calculations may be done only based on statistical, average values.

Figure 21 shows the PDF of UE Tx power levels on a cell-basis for CS voice and PS data UMTS services, when considering a macro and underlaid (indoor) micro cell, at site ETF, and Table 34 summarises the obtained average values. Whereas Figure 22 shows the corresponding data for site LOLA, and **Erreur ! Source du renvoi introuvable.** summarises the obtained average values. From the obtained results it is evident that the micro cell solutions provide significantly lower uplink EMF exposure; specifically, 3.8 dB and 5.9 dB for ETF and LOLA sites, respectively.

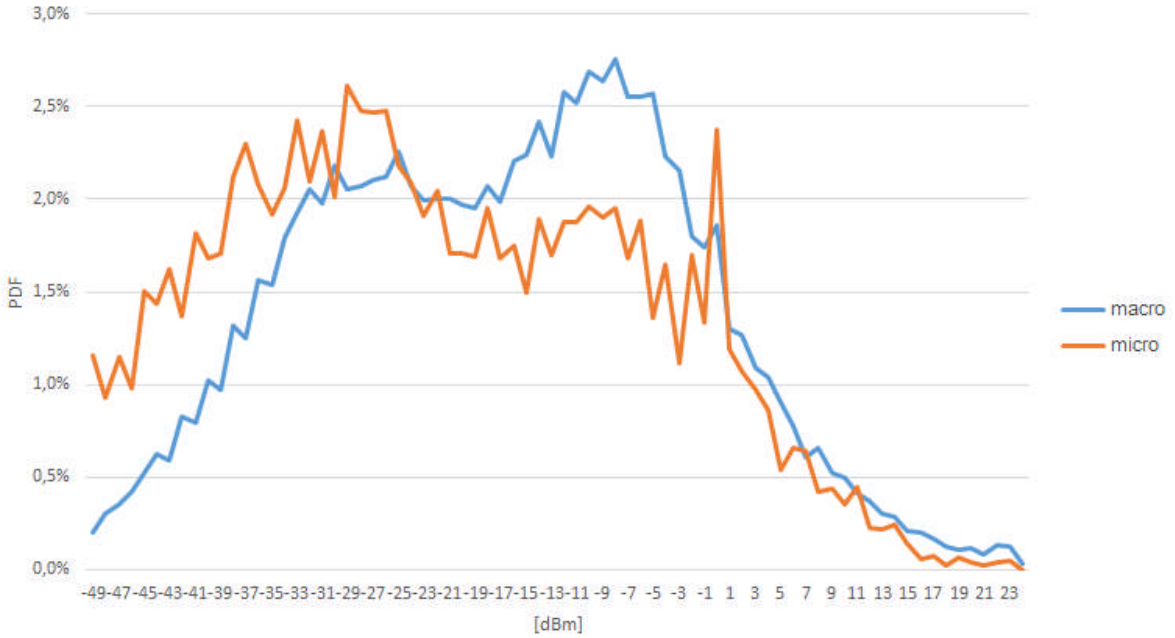

Figure 21: UE Tx power on cell-basis for CS voice and PS data UMTS services, for a macro and underlaid (indoor) micro cells, site ETF

Table 34: Average UE Tx power for the UMTS macro and micro cells, site ETF, CS voice and PS data services

UE Tx POWER	MACRO	MICRO
Average UE Tx Power [dBm]*	-16.57	-20.35

* Transmitter's power while emitting

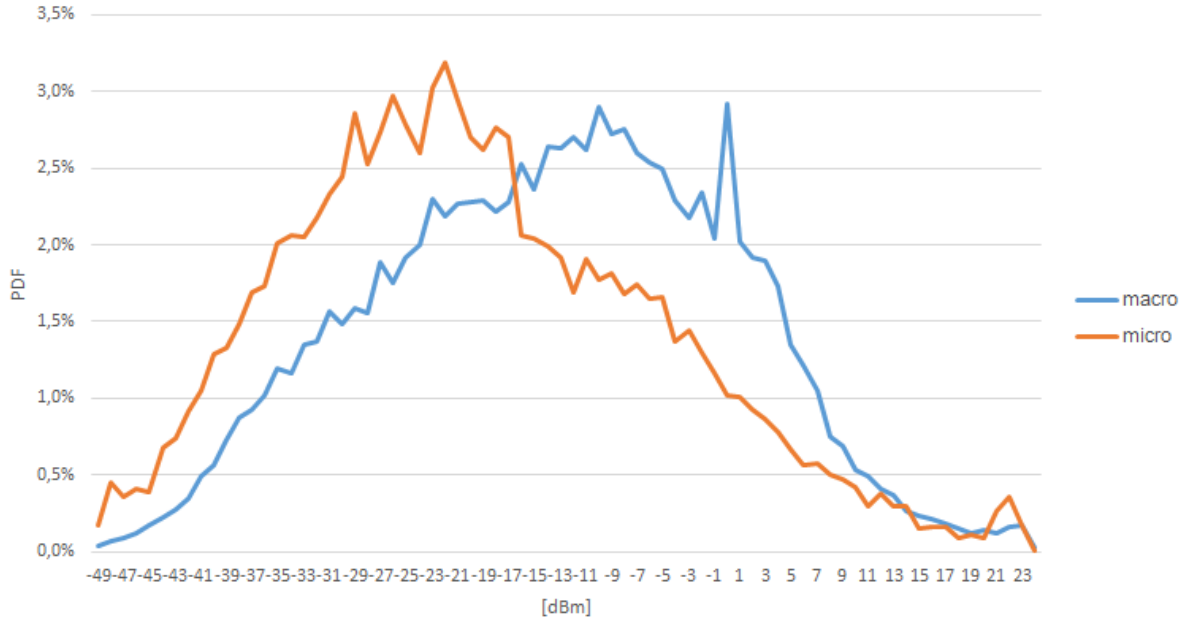

Figure 22: UE Tx power on cell-basis for CS voice and PS data UMTS services, for a macro and underlaid (indoor) micro cells, site LOLA

Table 35: Average UE Tx power for the UMTS macro and micro cells, site LOLA, CS voice and PS data services

UE Tx POWER	MACRO	MICRO
Average UE Tx Power [dBm]*	-13.35	-19.25

* Transmitter's power while emitting

4 EMF-AWARE RADIO RESOURCE MANAGEMENT

In the following, Section 4.1 presents a long-term RRM and connection control scheme that reduces the end-user perceived EMF due to both uplink and downlink communications. Our analysis shows that there is room to limit the EMF in current cellular network and that the proposed solutions can result in notable energy saving with respect to the classic RRM and connection control functionalities without affecting the system performance. Meanwhile, Section 4.2 complements the aforementioned study by analysing the impact of short term RRM on the exposure. Two novel EMF-aware scheduling schemes are proposed for reducing the EMF exposure both in uplink and downlink.

4.1 Enhanced User association in dense Heterogeneous Networks

4.1.1 Introduction

In this section, we finalise the study presented in D5.1 [LEXNET D5.1], and we present a cell association framework for HetNets, which aims to balance the load amongst heterogeneous cells so as to improve the resource usage and to increase the user satisfaction in terms of both data rate and EMF exposure.

In particular, we analyse the optimum cell association by jointly considering DL and UL communications, and we study the relationship between the EMF exposure and the users' QoS. In addition, we present two user centric mechanisms that jointly reduce the EMF exposure induced by the UL and improve the user satisfaction in terms of the DL throughput goal. Finally, considering the system perspective, the proposed solutions distribute the load in the HetNet to enhance the (access/backhaul) network utilisation efficiency. The interested reader can find details on the used system model and notations in Section 3.1 of D5.1 [LEXNET D5.1].

4.1.2 Proposed Solutions

In this section, we propose two centralised algorithms, named as Max User Satisfaction (Max Sat.) and EMF-Aware to deal with the EMF-Aware cell selection problem discussed in D5.1 [LEXNET D5.1]. The proposed algorithms start from a given solution of the cell selection problem, e.g., based on the Reference Signal Received Power (RSRP), and iteratively evolve towards a more beneficial association in terms of user satisfaction and/or user exposure. In particular, although Max Sat. only attempts to increase the user satisfaction in terms of capacity requirements, the EMF-Aware tries to reduce the EMF exposure while jointly improving the user QoS. Specifically, at each iteration, the algorithms evaluate every possible single change in the current association (first step) and then select the most beneficial change (second step). The algorithms stop after a limited number of iterations (the exact number depends on the size of the network), when the achievable gain becomes lower than a small non-negative value of ε.

Let define $\mathcal{U}$ as the set of UEs and $\mathcal{B}$ as the set of eNBs,

- $\mathbf{X}_n$ be the user assignment that maximises $RSRP_{i,j}$ $\forall$ *(i,j)* $\in$ U x B,
- $S(\mathbf{X}_n)$ be the user satisfaction ratio, which measures the fraction of UEs for which the DL capacity requirement (C_{min}) is met
- $EI(\mathbf{X}_n)$ be the aggregated EMF due to UL communications
- $a_{i,j}$ equals 1 if a user *i* is in the coverage area of eNodeB (eNB) *j* (i.e., $RSRP_{i,j}$ is larger than a given threshold) and 0 otherwise

- First Step: Initialisation
  - Calculate $EI(\mathbf{X}_n)$ and $S(\mathbf{X}_n)$
  - $\forall$ *(i,j) s.t.* $a_{i,j} = 1$, compute $EI(\mathbf{X})$ and $S(\mathbf{X})$ whether we change $\mathbf{X}_n$ by associating (respectively, de-associating) the user *I* to (respectively, from) *j*; then, compute the gain(s) Δ_S and Δ_{EI} with respect to the reference association, due to the possible reassignments.
- Second Step: One-user reassignment step
  - IF Max Sat., Find the set $\mathbf{X}^*$ which maximises Δ_S;
  - ELSE IF EMF-Aware, Find the assignment set for which $\Delta_{EI} > 0$; THEN find its subset $\mathbf{X}^*$ that maximises Δ_S;
  - IF $\Delta_S \leq \varepsilon$ exit (the algorithm outputs the current user assignment);
  - ELSE, find $\mathbf{X}_k \in \mathbf{X}^*$ that minimises Δ_{EI} and update the user assignment, accordingly.
  - Set $\mathbf{X}_n = \mathbf{X}_k$, then go to First Step.

4.1.3 Numerical results

In this section, we assess the effectiveness of the proposed solutions, which attempts to limit the EI while considering the side constraint of maximising the user satisfaction. We compare their performance with respect to the approach where each UE is served by the eNB associated with the strongest RSRP and the scheme where each UE is associated with the closest eNB (Min Path Loss). We also consider a Cell Range Extension (CRE) bias of 6 dB to increase the macro cell offloading.

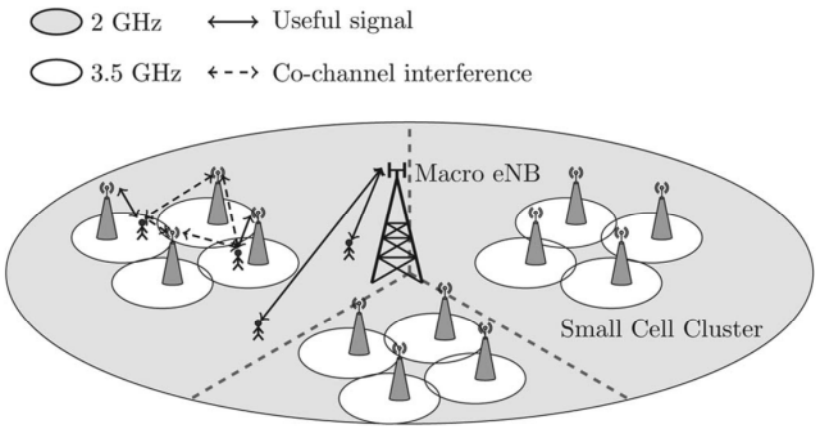

Figure 23: The heterogeneous network deployment under investigation

Our evaluation scenario is composed by a tri-sectorial macro cell and 60 UEs. Moreover, a cluster composed of four neighbouring small cells operating on a

dedicated channel (see **Figure 23**) is deployed in each macro cell sector. The small cell eNBs are characterised by a backhaul capacity (C^{BH}) of 40 Mbps, i.e., the backhaul poses strong constraints to the radio access network capacity. 80% of the UEs are indoors, 2/3 of them are located in the small cell hotspots, and remaining UEs are uniformly distributed in the macro cell. Other relevant parameters follow 3GPP TR 36.872 [3GPP TR 36.872]. The results are averaged over 10^3 independent runs. At the beginning of each run, the clusters of small cells and the UEs are randomly deployed in the macrocell area. Finally, in the simulations presented here $\varepsilon = 10^{-6}$.

Figure 24 shows the user satisfaction ratio with respect to the DL data rate requirement. By implementing the classic RSRP scheme, most of the UEs are associated to the macro eNBs, which limits the resources allotted to the UEs with poor Signal-to-Interference-plus-Noise Ratio (SINR) and achieves the worst performance. CRE enhances the user satisfaction by offloading UEs from overloaded macro eNBs to lightly loaded small cell eNBs. In particular, implementing CRE is particularly beneficial in the region with higher rate requirements, where it achieves 2.8X the user satisfaction of the RSRP scheme. By associating the UEs to the closest eNBs, the system does not suffer from the power unbalance between small cell eNBs and macro eNBs, which enables to effectively share the network load and to achieve up to 6.5X the performance of the RSRP solution. However, the proposed schemes further enhance the user satisfaction through an optimised load balancing that associates UEs characterised by poor SINR to eNBs with large resource availability and UEs with high SINR to loaded eNBs. Accordingly, UEs at the cell edge may meet the data rate requirements at the cost of lower throughput experienced by UEs located nearby the eNBs. As expected, the Max Sat. outperforms the EMF-Aware approach since the latter avoids those associations leading to high EI. The Max Sat. and the EMF-Aware yield up to 8.8X and 7.4X the user satisfaction of the reference scheme.

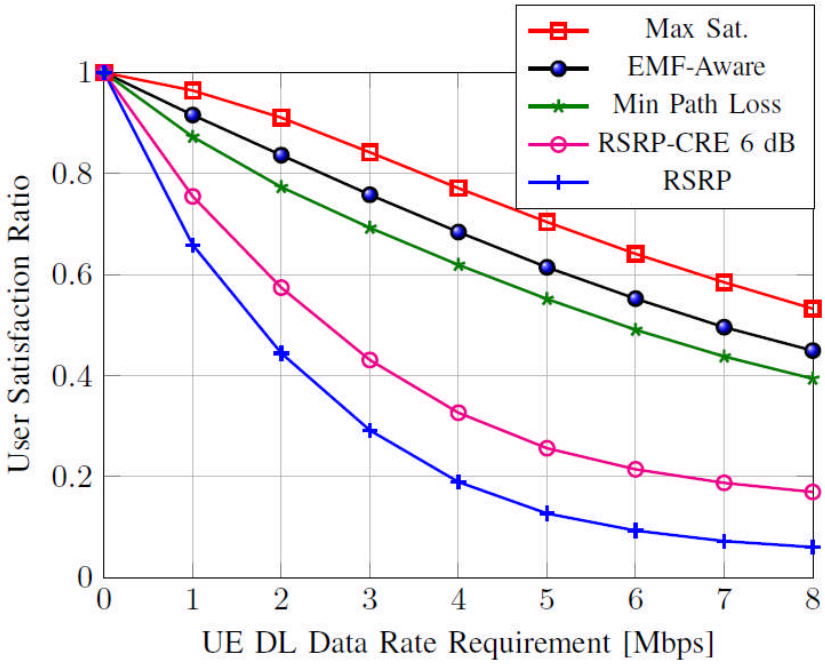

Figure 24: User satisfaction ratio Vs. DL data rate requirement

Figure 25 shows the network utilisation efficiency (i.e., the ratio between the overall cell capacity and the aggregate backhaul capacity) achieved by the different approaches. When using the RSRP scheme, most of the UEs are served by the macro eNB, a high number of small cells are idle, leading to the worst performance. CRE enables to increase the usage of small cell eNB resources through the macrocell offloading, which greatly enhances the network performance. However, Max Sat., EMF-Aware, and the Min Path Loss achieve up to 2.6X the resource utilisation of the RSRP solution. Although these three algorithms are all characterised by high resource utilisations, the proposed solutions fairly distribute resources to increase the user satisfaction, as can be seen in Figure 24.

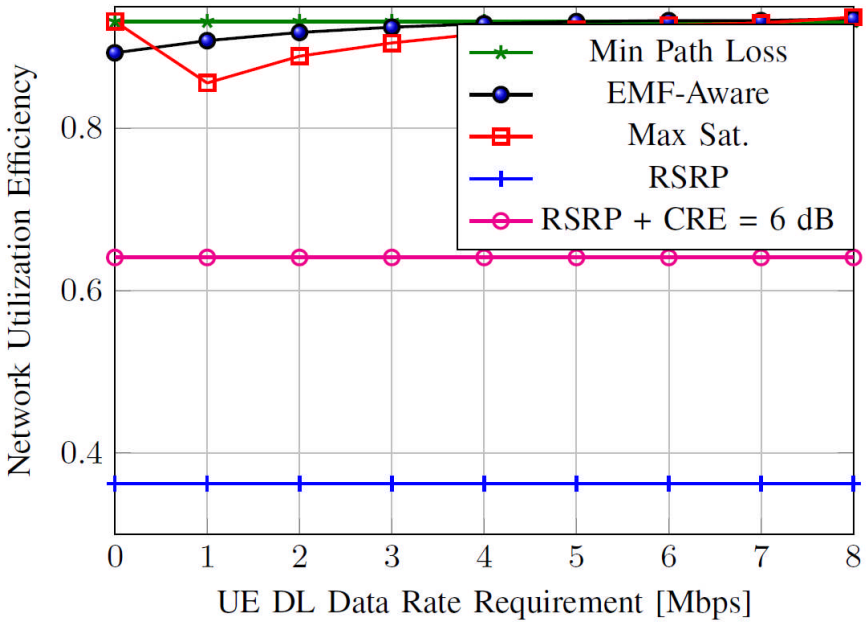

Figure 25: Cell Resource Utilisation vs. DL data rate requirement

Finally, Figure 26 shows the daily EI due to UL with respect to the DL rate requirement. In these simulations, the number of per user allotted frequency resources N^{UL} is computed such that each UE achieves 1 Mbit/s in the UL. The higher the value of N^{UL}, the higher the associated EI is. As expected, CRE is beneficial in terms of exposure with respect to the reference solution based on the RSRP. Moreover, the Min Path Loss scheme strongly reduces the EI by limiting the required UL power per resource block; however, better performance can be achieved through the EMF-Aware solution, where the load balancing reduces N^{UL} resource block (i.e., by offloading to the macro eNB the small cell UEs characterised by high uplink interference). On the other hand, by closely looking at Figure 24 and Figure 25, we can note that to further increase the user satisfaction, it is necessary to implement cell selection patterns that yield to higher EI. In fact, the Max Sat. scheme results in the highest EI in the range of low-medium data rate requirements, where it is possible to satisfy most of the UEs. On the contrary, in the high rate requirements region, only few UEs can meet the rate target and the average EI can be strongly reduced.

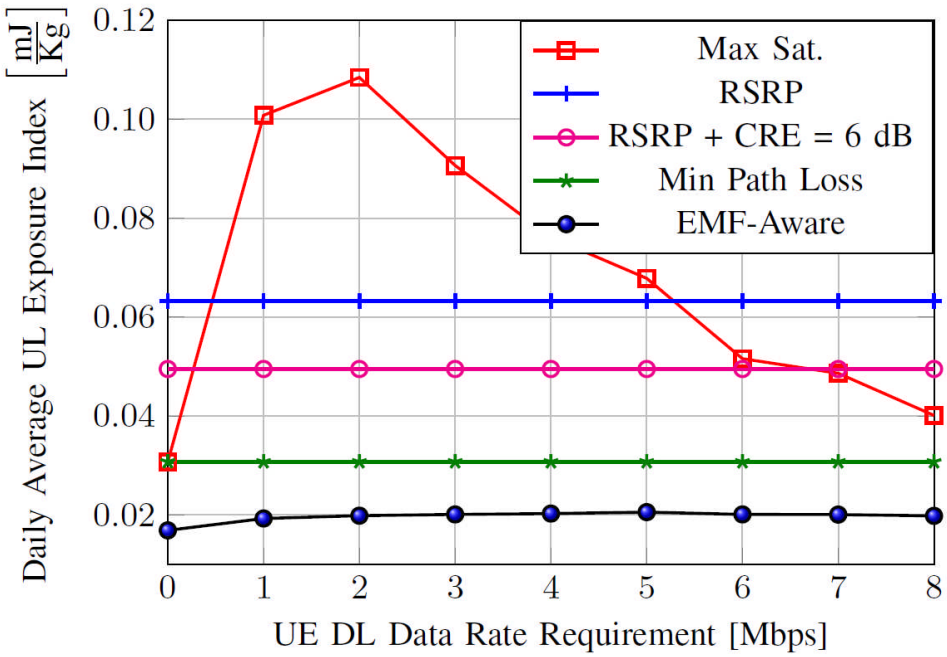

Figure 26: UL Exposure Index vs. DL data rate requirement

4.2 EMF-emission Aware Scheduling algorithms

4.2.1 EMF-emission aware Uplink Scheduling for cellular networks

4.2.1.1 Introduction

In the uplink of mobile communication system, EMF emission can be reduced for instance by using metamaterials between the mobile phone and the human head [Islam 2009], [Ragha 2010], [Gomez 2010] or beamforming [Qiang 2007], [Mahmoud 2008]. However, focusing only on reducing EMF, or equivalently SAR, without considering the spectral efficiency performance would most certainly degrade QoS, as in the works previously cited. Given that electromagnetic emission reduction in the uplink boils down to reducing the amount of energy (power over time) dissipated towards the user [LEXNET D2.4], scheduling is intuitively the right kind of technique for doing so. It is especially the case for reducing the EMF exposure of each individual user within a given transmission duration, while ensuring QoS.

In this regard, we have recently proposed in [Sambo 2014] and [Sambo 2015] novel user scheduling/power allocation schemes for minimising the EMF exposure of each individual user subject to a QoS target, i.e. transmitting a target number of bits. In terms of system model, both these works consider the uplink of a single cell multiuser mobile system with K single antenna users transmitting to a BS equipped with a single antenna. The uplink transmission is assumed to happen over several frames, where each frame contains T equally sized Time slots (TSs) of length l. At each TS, the BS computes the transmit power of each user and performs scheduling to minimise the EMF emission of individual users subject to transmitting a target number of bits.

In [Sambo 2014], a single carrier time division multiple access setting is assumed, where each TS is allocated to a single user such that it occupies the whole bandwidth. In addition, the scheduling is performed based on a priority level mechanism; priority levels are assigned to each user based on its current and past transmit powers. The user with the lowest priority level in TS is scheduled for transmission. Whereas the power allocation is based on the water filling approach over time, where the past channel gains of a user are used to compute its water level. Results, which have also been reported in [Sambo 2014], have shown that our proposed scheme can reduce the uplink emission by around 40% compared to a classic Spectral-Efficiency (SE)-based scheme while keeping QoS. Meanwhile in [Sambo 2015], a multi-carrier Orthogonal Frequency Division Multiple Access (OFDMA) setting is assumed, where the total bandwidth W is divided into N equal subcarriers, and any subcarrier can be allocated to at most one user in a TS but a user can have more than one subcarrier in a TS. The BS is assumed to have perfect Channel State Information (CSI) of all the links between itself and its served users in the network (without delays), which it uses to allocate subcarriers to the users and also perform power allocation. In the following, we highlight the findings of [Sambo 2015], where two novel EMF-aware scheduling schemes are proposed, namely the offline and online EMF emission reduction schemes.

4.2.1.1.1 Offline EMF emission reduction scheme

Our offline EMF reduction scheme is based on the assumption that the BS can perfectly predict the CSI of all the users up to T TSs in advance by using the uplink pilot signals, which are transmitted by each user in the system. Knowing the CSI of each user, the BS performs subcarrier and power allocation across the whole T TSs to minimise the transmission energy and, hence, EMF emission. It is worth noting that this scheme is more theoretical, however, it is well-suited for quasi-static channels over T TSs. For more time varying channel, schemes proposed in [Schafhuber 2002] and [Wong 2004] can be used for CSI prediction. In our optimisation framework, the emitted energy by the user equipment (proxy for EMF emission) is the objective function to be minimised, while total power constraint and target number of transmitted bits are the constraints. Note that both the energy for transmitting data and signalling is taken into account.

4.2.1.1.2 Online EMF emission reduction scheme

Our online EMF emission reduction scheme follows the same optimisation framework as the offline one, but subcarrier and power allocations are performed for each TS while the target number of bits constraint is met over several TSs. Due to the combinatorial nature of subcarrier allocation in the uplink of OFDMA systems, as it is further explained in [Sambo 2015], this scheme performs instantaneous subcarrier and power allocation for all the users in a TS before moving to the next TS based on the CSI of the users on all the subcarriers in that TS. Each user continuously transmits signalling information to the BS in each TS until its target number of bits is met, then the user is removed from the scheduling list. Our online scheme relies on SE-based subcarrier allocation.

4.2.1.2 Performance evaluation and discussion

In the following, the performance of our proposed EMF-aware scheduling schemes is compared against the classic greedy SE-based scheme and the green scheduling

scheme of [Miao 2012]. In the greedy SE-based scheme, the subcarriers are allocated to the user with the best channel gain on that subcarrier in the current TS and the user performs water-filling over its allocated subcarriers. The allocated subcarriers of the user are then sorted in descending order and transmission starts from the best subcarrier. Due to signalling and data transmissions taking place separately in the offline EMF emission reduction scheme, each user can use all its transmit power for data transmission during each TS. Meanwhile, the online EMF emission reduction scheme assumes instantaneous subcarrier and power allocation during each TS as well as simultaneous signalling and data transmission. All users transmit signalling information as long as the user's target number of bits is not met. A Monte Carlo simulation of 10,000 iterations was done to achieve the results. The simulation parameters used are summarised in Table 1 of [Sambo 2015].

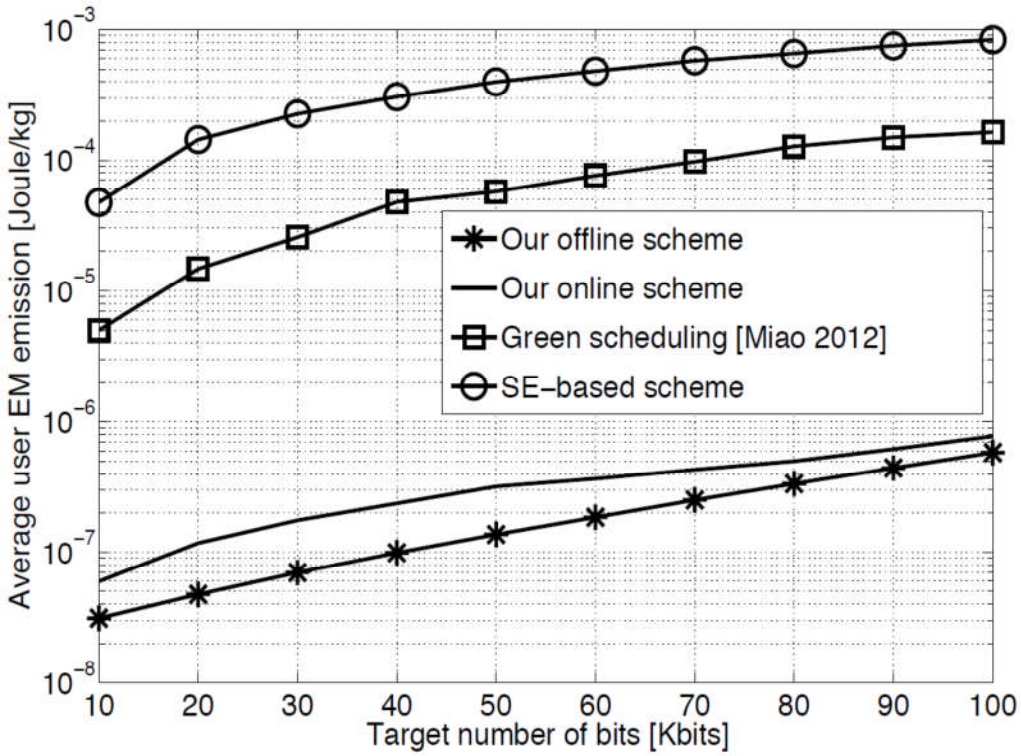

Figure 27: Average user EMF emission comparison of our proposed EMF emission reduction schemes versus the target number of bits for K= 15 users and T= 20 time slots

Figure 27 compares the average EMF emission per user of our proposed schemes versus the target number of bits, against existing schemes, for a bandwidth of W= 20MHz, N= 128 subcarriers, K= 15 users, T= 20 TSs and the duration of a TS, l, is 1ms. Firstly, it can be remarked that our online schemes provide reductions in EMF emission of up to 2 and 3 orders of magnitude compared to the scheme of [Miao 2012] and the greedy SE-based schemes, respectively. Secondly, when comparing our offline and online schemes, the former can further reduce the EMF emission by up to 50%. Except in the offline scheme, all the users have to transmit signalling information during each TS, irrespective of them transmitting data or not, until their bits target is met and they are removed from the subcarrier allocation list; in other words, the offline scheme exhibits the lowest EMF emission because it requires less signalling. On the other hand, the greedy SE-based scheme has the highest EMF emission because it tries to maximise the number of bits transmitted on each

subcarrier by making use of all the available power. It can also be remarked that the average user EMF emission of all the schemes increases as the target number of bits increases. For the offline scheme, given that the number of subcarriers allocated to each user is fixed, more power is needed to achieve the target number of bits when it increases; while more TSs are required to transmit higher number of bits in the online and the greedy SE-based schemes, and the EE scheme of [Miao 2012].

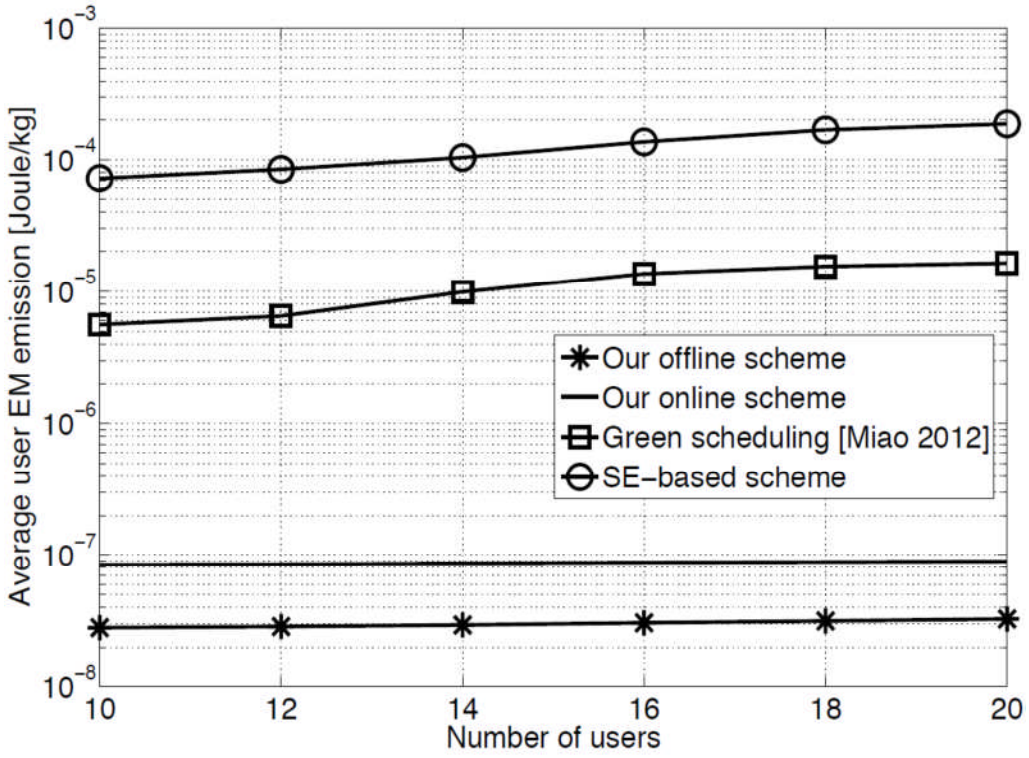

Figure 28: Average user EMF emission comparison of our proposed EMF emission reduction schemes versus the number of users for B= 10 kbits and T= 10 time slots

Figure 28 depicts the average EMF emission per user of our proposed schemes versus the number of users in the network for a bandwidth of W= 10MHz, N= 128 subcarriers, a bit target of B= 10 kbits and T= 10 TSs. The results confirm that our schemes provide an EMF reduction between 2 to 3 orders of magnitude compared with existing schemes. It can also be observed that the average EMF emission per user increases with the number of users in the network. In the offline EMF emission reduction scheme, within the transmission window T, the number of each user allocated subcarriers reduces as the number of users in the network increases, because they have to share the available subcarriers. It implies that the users would have to transmit with more power to achieve the target number of bits. Whereas in our online and the greedy SE-based schemes as well as the scheme of [Miao 2012], given that the number of subcarriers in a TS is fixed, more TSs would be needed to achieve the target number of bits of all the users in the network as the number of users increases.

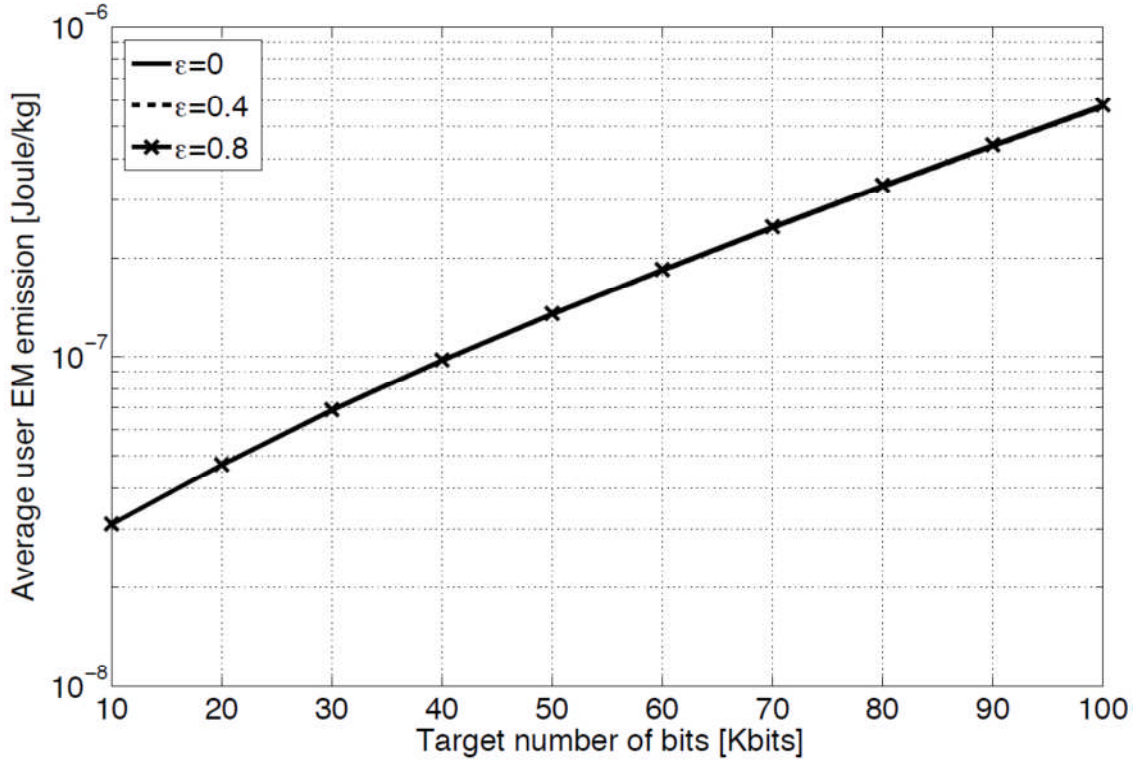

Figure 29: Effect of imperfect channel prediction on the average user EMF emission of our proposed offline EMF emission reduction scheme for K= 15 users

Figure 29 shows the effect of imperfect channel prediction on our offline EMF emission reduction scheme for K= 15 users. The figure is based on the channel estimation model in [Medard 2000] and [Nostrat 2011], with the estimation variance parameter ε= 0, 0:4 and 0.8, with ε= 0 denoting a perfect channel prediction. It can be observed that our proposed scheme is very robust even when the CSI prediction error is very high, as the difference in average EMF emission between a perfect CSI prediction and a very high prediction error (ε= 0.8) is hardly noticeable in **Figure 29**.

Figure 30 depicts the effect of the transmission window size, T, on the offline EMF emission scheme for K= 15 users and B= 10 Kbits. It can be observed that EMF emission reduces as the transmission window increases. When the transmission window increases, more subcarriers become available to the users and, hence, they require lower power transmission to achieve the target number of bits of all the users. Since the transmission window affects the performance of the offline EMF emission reduction scheme, the network operator could vary the length of the transmission window depending on the EMF emission threshold set by the network. Delay sensitive transmissions could have a shorter transmission window, while delay tolerant applications could have a longer transmission window to further reduce the EMF emission towards the users in the network.

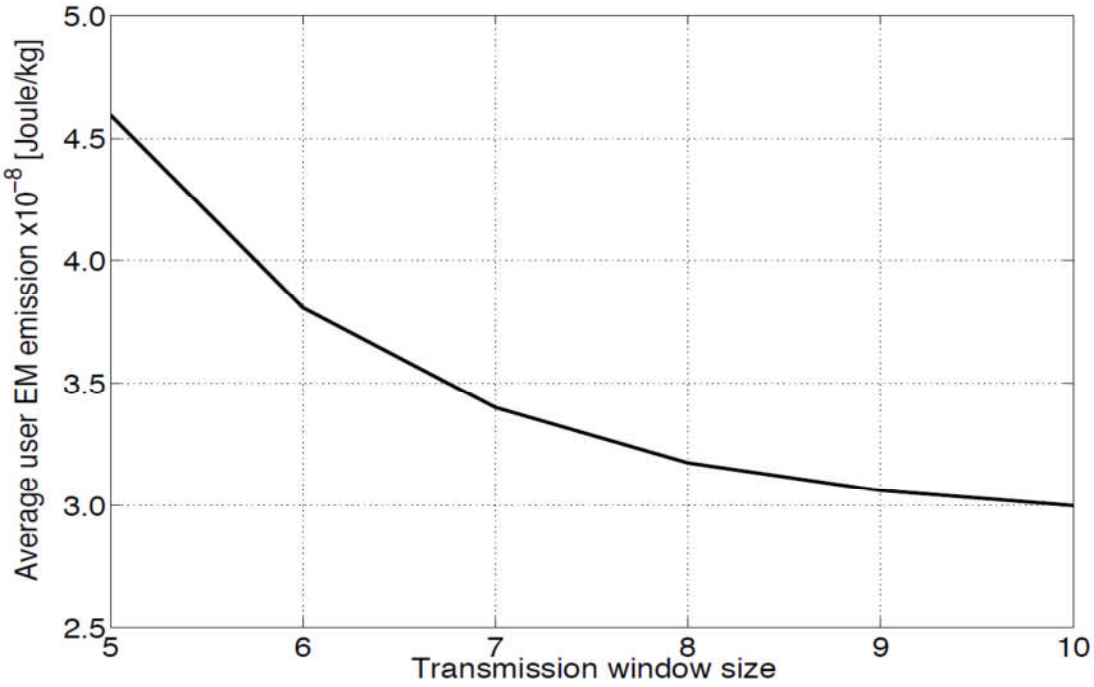

Figure 30: Average user EMF emission of our proposed offline EMF emission reduction scheme versus transmission window size for *K*= 15 users and *B*= 10 Kbits

4.2.1.3 Concluding remarks

4.2.1.3.1 Exposure index gain

From [LEXNET D2.4], the contribution of any user to the EI can be expressed as

$$EI_k = \frac{\mathrm{SAR}_k}{P^{\mathrm{ref}}} \sum_t \left(\hat{p}_k(t) + \sum_n p_{k,n}(t) \right) l, \text{ [J/Kg]} \qquad (4)$$

where n is a subcarrier index, SAR_k is the whole body averaged SAR of the k- th user mobile device, P^{ref} represents the incident reference power, $\hat{p}_k$ denotes the signaling power of user k, $p_{k,n}(t)$ is the transmit power per subcarrier of user k and l is the duration of a TS. It can be remarked **(4)** that if $\mathrm{SAR}_k/P^{\mathrm{ref}}$ is similar for all the users, then reducing the per-user EMF exposure, EI_k, boils down to reducing the per-user transmit energy i.e., the product of the transmit power and time.

Consequently, the gain achieved by our scheme, which is obtained for a heavily loaded system, can be directly plugged into the EI formula. For instance, given uplink users transmitting at 5Mbit/s of information (100 kbits/ (20TS * 1ms)), according to **Figure 27** and **Figure 29**, their EMF emission can be reduced by a factor of **1000** when using our offline EMF-aware scheme instead of a state of the art green scheduler, which is also designed to reduce energy transmission/ consumption.

4.2.1.3.2 Future work

The next step for this work is to extend our uplink EMF-aware scheduling concept to the small cell/Heterogeneous network (HetNet) scenario, where coordination amongst BSs can be used to reduce EMF exposure, as it is further explained in the following section for the downlink scenario.

4.2.2 Downlink Coordinated EMF-emission aware Scheduling for heterogeneous networks

4.2.2.1 Introduction

In the downlink of multi-cell system, it has been shown in [Venturino 2009], [Ng 2012] and [Heliot 2013] that cooperation and coordination can be beneficial to mitigate interference and, in turns, reduce both the transmit power and energy consumption. For instance, in [Venturino 2009], a coordinated scheduling scheme has been proposed for improving the spectral efficiency of multi-cell systems. Then, in [Ng 2012], BS cooperation has been utilised along with beamforming for scheduling resources in an energy-efficient way over the downlink of an orthogonal frequency division multiplexing/OFDMA system; whereas, [Heliot 2013] considered coordinated resource allocation in the downlink of cellular system for reducing the energy consumption. As can be noticed in the definition of the exposure metric in equation (1) of [LEXNET D2.4], the downlink exposure is directly linked to the BS transmit/radiated power such that reducing the transmit power will inevitably reduce the EMF exposure.

In this regard, we have designed novel low-complexity coordinated scheduling algorithm for reducing the downlink EMF exposure (via transmit power reduction) in the downlink of OFDMA cellular and HetNet systems, which are described in more detail in [Heliot 2015a] and [Heliot 2015b], respectively. In these works, we consider the energy consumption as a proxy metric since this approach has proven useful in [Heliot 2013] for reducing the transmit power in a coordinated setting while keeping SE/QoS performance. Both these works consider the downlink of a classic planar cellular system (without small cells in [Heliot 2015a]), as in **Figure 31**, where sectorised BSs with one antenna per sector communicate via an OFDMA air interface over a frequency selective and block faded channel with UEs having a single antenna. Moreover, we assume as in [Karakayali 2006] that BSs can coordinate their transmission, by exchanging information about their respective users' channel gain. Given that most of the downlink interference suffered by any user within the orange-dodecagonal pattern is generated by its closest non-serving BSs of the same and/or other tiers, without loss of generality, we focus on reducing the energy consumption of one of this cluster by using coordinated scheduling.

In [Heliot 2015a], a classic multi-cell single tier scenario is assumed (without small cells) and results have shown that our proposed scheme can reduce the passive exposure by up to 95% in comparison with a classic non-coordinated approach and between 30 to 60% in comparison with an existing coordinated approach, while keeping similar sum-rate performance. Meanwhile in [Heliot 2015b], a multi-cell multi-tier setting is considered, where small cells, which use the same frequency band as the macro cells, are deployed within the coverage area of the macro cell, as depicted in **Figure 31**. In the following, we highlight the findings of [Heliot 2015b] regarding downlink exposure reduction through coordinated scheduling in a HetNet context.

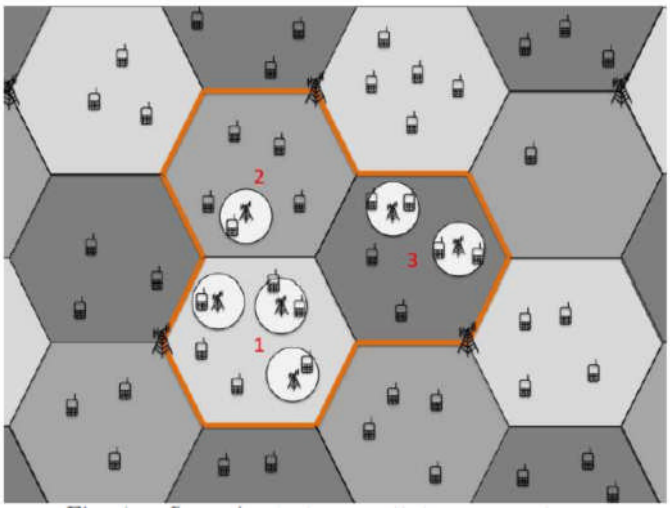

Figure 31: Sectorised planar cellular system layout with small cells

4.2.2.2 Performance evaluation and discussion

In the following, the performance of our proposed coordinated scheduling method, denoted "our scheme", is compared against non-coordinated, no-reuse and SE-based coordinated scheduling approaches. The non-coordinated, denoted "NC-SE" and no-reuse, denoted "NR-SE", scheduling approaches are single cell/sector based approaches, where both power and subcarrier allocations are performed per cell without being aware of the other sectors' interference. Moreover, Greedy subcarrier allocation and SE-based power allocation (water-filling) are utilised in these two schemes. Furthermore, all the subcarriers are shared, i.e. full reuse, in the "NC-SE" scheme, whereas subcarriers are split between the sectors to avoid interference, i.e. each sector has N/3 subcarriers, in the "NR-SE" scheme. The SE-based coordinated approach is the one designed in [Venturino 2009] (Algorithm 3), denoted "Co-SE". Note that this approach has been designed for the classic cellular, however its generalised formulation made it readily usable for the multi-tier scenario. The results depicted thereafter have been obtained via Monte Carlo simulation based on the simulation parameters that are summarised in Section IV of [Heliot 2015b]. In terms of system layout, we have considered the one depicted in **Figure 31**, where small cells are randomly deployed within the coverage area of the macro cell and users are randomly dropped within the orange decagonal area of **Figure 31**. In addition, in order to get a better picture of the effects of coordination (contrary to the results in [Heliot 2015a]), we have also considered the other cell interference coming from the 9 closest macro BSs surrounding the 3 macro BSs depicted in **Figure 31**.

Figure 32 compares the performance of our scheme against the "NC-SE", "NR-SE", and "Co-SE" scheduling schemes vs. the Inter-Site Distance (ISD), for a bandwidth of W= 10MHz, N= 600 subcarriers and K= 20 users, when no small cells are deployed. The results show that our scheme can reduce the transmit power and, hence the downlink exposure, by more than 80% in comparison with the other schemes while keeping similar sum-rate (Σ-rate) performance as the "NC-SE" (roughly equivalent rate) and "Co-SE" (≈3% loss). It can be noticed that the decagonal pattern in **Figure 31**, bounding the area in which coordination is applied, can be repeated all over the classic hexagonal layout. Then, the benefit of coordination is to create a virtuous

chain reaction, where by reducing the transmit power of a cluster of 3 sectors, it will do so for the other clusters, given that the other cell interference experienced by each user cluster will be reduced, as it is been observed in our simulations. This is precisely what our scheme is designed to do and it explains why it can reduce the transmit power and, hence, downlink exposure. Coordination is not the only important factor here for achieving exposure reduction, indeed, using the energy efficiency as an objective function is another one. For instance, it can be remarked that the "Co-SE" scheme does not manage to reduce the transmit power, even though it is also a coordinated scheme; this is due to the fact that this scheme targets spectral efficiency improvement and it uses full transmit power to do so.

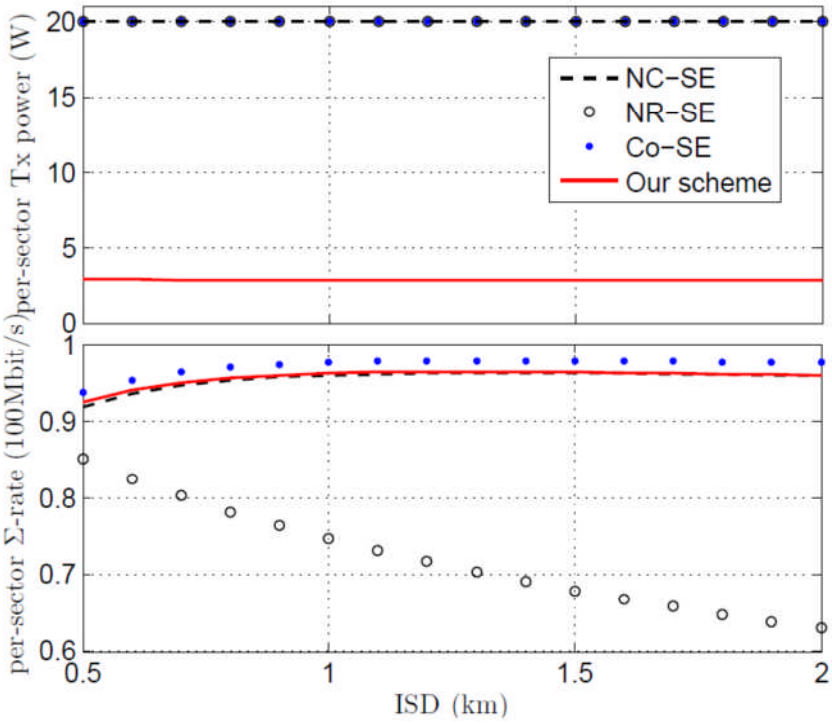

Figure 32: Performance comparison of various scheduling methods in terms of per-sector transmit power and rate vs. the inter-site distance without small cells

Figure 33 compares the performance of the same schemes for the same setting as previously, but when 3 small cells are deployed per sector. The results indicate an even more sharp reduction of power for our scheme. It can reduce the transmit power and, hence the downlink exposure, by more than 99% in comparison with non-coordinated scheme and at the same time provides the best sum-rate (Σ-rate). When adding small cells, the load of the macro decreases and rate can be increased without using too much transmit power, since users served by small cells are usually very close to it. The rate will only be increased if the interference from the macro BS is low; energy efficiency being a trade-off between rate and power, small cells will thus be favoured in comparison with macro BSs, since the former can deliver high rates with low power. As a result, the small cells are driving down the emitted power such that the transmit power of the macro BS is also reduced to the level of the small cells (≈0.1W), in order to not to degrade the overall energy efficiency of the system (by reducing interference). Conversely, the coverage of the macro BS is likely to be reduced as is the rate of the users served by the macro BS, but the overall rate is

improved (see **Figure 34**). It can also be remarked that "Co-SE", which has been designed for multi-cell single tier system, is not well-suited for multi-tier systems since it cannot achieve the best rate as in **Figure 32**, without small cells.

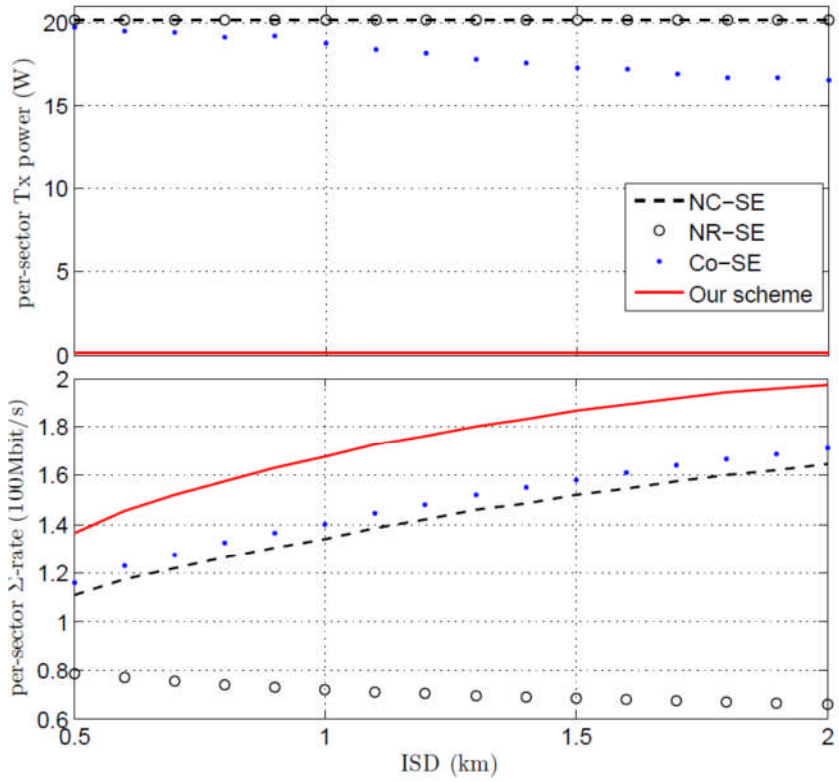

Figure 33: Performance comparison of various scheduling methods in terms of per-sector transmit power and rate vs. the inter-site distance with 3 small cells per sector

Figure 34 compares the performance of the same schemes for the same setting as previously, but as the function of the number of small cells deployed per sector for an ISD of 500m. These results confirm that our scheme can drastically reduce the downlink exposure by up to two order of magnitude in comparison with non-coordinated schemes while maintaining (without small cells) or even improving (as the number of small cells increases) the sum-rate (Σ-rate) of the system.

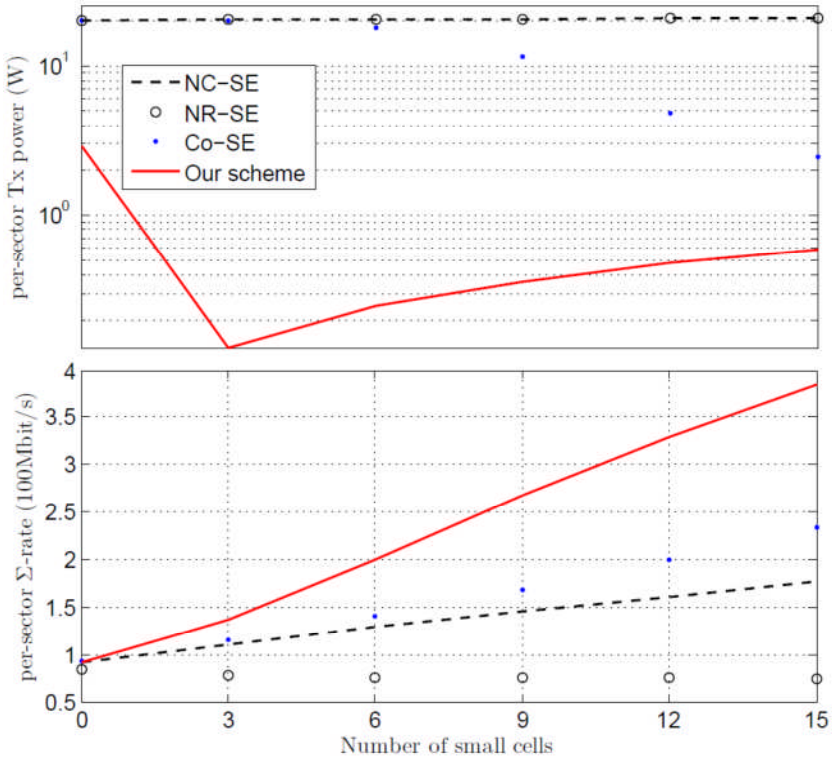

Figure 34: Performance comparison of various scheduling methods in terms of per-sector transmit power and rate vs. the number of small cells per sector

4.2.2.3 Concluding remarks

4.2.2.3.1 Exposure index gain

As already mentioned, according to the definition of the downlink exposure in equation (1) of [LEXNET D2.4], the downlink (passive) exposure is directly proportional to the access points transmit/radiated power such that reducing the latter reduces the former. According to the same formula, reducing the distance between the access point and the user also reduces the exposure index, which vindicates the use of small cells. However, small cell technology is disruptive (adding interference) with regards to a classic cellular system and we have shown that EE-based coordination can mitigate its disruptive effect and be effectively used for reducing exposure.

The gain achieved by our scheme, which is obtained for a heavily loaded system, can be directly plugged into the EI formula. For instance, given a downlink transmission with 3 small cells per sector for an ISD of 500 m, according to **Figure 33** and **Figure 34**, downlink EMF emission can be reduced by a factor **100** when using our coordinated scheduling scheme instead of a non-coordinated or state-of the-art coordinated scheme.

4.2.2.3.2 Future work

The next step for this work is to look at the load balancing between small cells and macro BSs and ensure fairness between the users of both tiers.

5 EMF-QUALITY OF EXPERIENCE/QUALITY OF SERVICE TRADE-OFFS

In this section, the trade-off between EMF and QoE/QoS is studied. Section 5.1 argues that it is possible to reduce the electromagnetic exposure by tuning the QoE perceived by people when they use an application such as a video application. When reasoning on QoE instead of QoS, it becomes possible to study new parameters that can have an impact on the electromagnetic exposure. Indeed, unlike QoS, QoE encompasses not only the networks characteristics, but also the users' characteristics. Whereas section 5.2 studies the EMF-QoS trade-off in indoor Wi-Fi; an extension of the work in Chapter 6 of [LEXNET D5.1] regarding the optimisation Surrogate MOdeling (SUMO) toolbox is undertaken. The SUMO toolbox is here utilised for decreasing EMF exposure while increasing the audio quality in various advanced scenarios.

5.1 EMF and Quality of Experience Trade-off in cellular systems: selection of a transport protocol for video streaming

Since video streaming will represent, approximately, 79% of the Internet traffic in 2018 [Cisco 2014], studying the impact of existing video streaming protocols on the electromagnetic exposure becomes an essential aspect. Dynamic Adaptive Streaming over HTTP (DASH) [Sodagar 2011] is one of the most popular protocols to stream videos over the Internet. For example, it is used by the Netflix platform [Adhikari 2012] and it is implemented as well on the YouTube platform. DASH has been developed to optimise the QoE perceived by the users, adapting the delivery of audio-visual contents to the particular constraints of both networks and terminals. It has been shown to appropriately adapt the delivery of contents to networks whose bandwidth fluctuates, as it is usually the case in wireless networks. Consequently, DASH has been standardised by 3GPP, as reported in both [3GPP TS 26.234] and [3GPP TS 26.244].

The encoding process of an audio-visual content produces multiple formats, the so-called representations, which correspond to various flow rates. Every representation is chopped into segments, which are stored on an HTTP server. Segments are requested independently from each other, by means of either the HTTP GET or the HTTP partial GET method, by a HTTP/1.1 client. All the information about an audio-visual content, i.e., its availability, its network location, its various representations, the structure of their cutting, the segments characteristics, etc. are specified in an extensible markup language file, called Media Presentation Description (MPD). DASH specifies the MPD file and the structure of the segments, whereas the encoding formats of the audio-visual contents, the segment delivery strategies, as well as the specific player, are not within the scope of the standard.

There are different strategies for adapting the delivery of audio-visual contents to the constraints of networks and terminals. They can be divided into two types of algorithms. In the first type, the adaptation is centred at the terminal [Miller 2012]. For example, a HTTP/1.1 client downloads an audio-visual content stored at a HTTP

server with two different representations: one at 1000 Kbps and the other one at 500 Kbps. Having obtained and read the MPD file of the audio-visual content, the client initiates the download by requesting a segment of the 1000 Kbps representation. Then it estimates the available network bandwidth, which equals 500 Kbps, and it therefore selects the following segment in the 500 Kbps representation. Hence, by knowing the network available capacity, the client can select the most appropriate representation for each segment, while the content is being downloaded. In the second approach, this adaptation is made by the operator managing the radio access networks [ElEssaili 2013].

The electromagnetic exposure is currently not taken into account by any of the various adaptation strategies, which usually consider the available bandwidth in the networks, the QoE perceived by the users [DeSimone 2013], and the energy consumed by networks and terminals [Khan 2014]. On the other hand, we advocate that it would be indeed possible to reduce the exposure to EMF by decreasing the volume of information that needs to be transmitted, namely by minimising the corresponding data payload for each of the involved protocols. This section focuses on such reduction at the transport layer.

In radio networks, the Transmission Control Protocol (TCP) is frequently used to guarantee the reliability of the transmissions of DASH segments. On the other hand there are a number of characteristics that would probably favour the use of the User Datagram Protocol (UDP), such as its header size (8 bytes), which is smaller than the TCP header (20 bytes) and, secondly, the fact that an UDP client, unlike a TCP client, does not transmit acknowledgements. Hence, it is sensible to think that UDP could be an interesting solution to reduce the volume of data at the transport layer. This is in fact the main contribution of this work, in which we study the improvements that a (TCP/UDP)-based DASH protocol brings about. As far as the EMF exposure is concerned, in some cases, as is the case of this study, the exposure is reduced indirectly; in this case it will be done by assessing the impact on alternative system level procedures on the resources utilisation. In particular, we will use as an exposure metric the throughput perceived by the application for each sending of the Radio Link Control (RLC) protocol of LTE; which in turn implies a physical transmission; at the same time different QoS parameters will be studied to verify the impact of the proposed solution on the service quality.

5.1.1 Context of study

In this work we consider the delivery of video content over cellular networks by means of the DASH protocol. In particular we focus on the LTE technology, since it is emerging to become one of the main cellular access technologies. In the scenario under study, see

Figure 35, a content server encodes a video stream, typically by using the H.264/AVC codec [Wiegand 2003]. When using DASH, a number of different representations of the same content, each of them having different coding parameters, are generated and stored in one or more HTTP servers. Each representation is characterised by a different quality and thus the data rate required to send them is as well different. In the data plane, a HTTP client at the UE retrieves the MPD file, which provides the location of the different representations. Afterwards,

and by means of HTTP methods (i.e., GET and partial GET), the HTTP client is able to obtain the most appropriate segment according to the perceived quality. As can be inferred from the previous description, the protocol stack that is involved in the communication is as follows: Internet Protocol (IP)/TCP/HTTP/DASH.

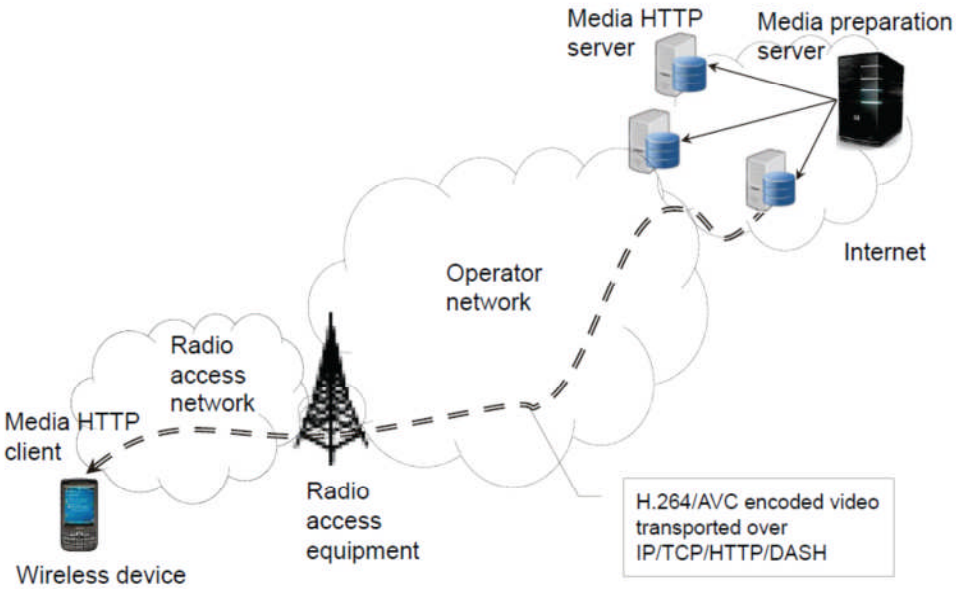

Figure 35: Context of the study

Our initial assumption is that, if the radio access technology itself already provides a certain level of reliability, the use of a reliable transport protocol, like TCP, might be unnecessary, provided that the flow control functionalities can be established in another way; for instance, in a scenario where the content provider is within the same Autonomous System as the network/connectivity provider. In this case, a non-reliable transport protocol, like UDP, may indeed bring in some benefits, as detailed in **Table 36**. The use of UDP avoids, for instance, the transmission of any acknowledgement by the terminal receiving the video segments. In our scenario, the main advantages are related to the uplink resource utilisation, with the consequent reduction of the exposure to the EMF. On the other hand, there are as well some drawbacks that loom when using UDP; these are discussed in the next section. The most relevant one is probably the fact that many firewalls actually block UDP connections.

Table 36: Advantages and drawbacks of using a non-reliable transport protocol

Advantages	Drawbacks
Uplink resource utilisation reduction	Firewall reconfiguration for UDP
Reduction of the exposure to EMF	Modification of servers and clients
Reduction of the radio power consumption	Modification of radio access equipment

5.1.2 Client-Based Representation and Transport Protocol Selection Algorithm

An IP datagram received by the Radio Link Control (RLC) layer of the eNB is segmented before being transmitted over the radio interface. The RLC layers of both

the eNB and the terminal are usually configured to work in the Acknowledged Mode [3GPP TS 25.322]; in other words, the RLC layer of the mobile terminal acknowledges the RLC frames it receives. These acknowledgements are transmitted: 1) at the request of the eNB (poll request); 2) upon expiration of a timer; or 3) when the terminal detects the loss of RLC frames.

In order to ensure a reliable delivery of the audio-visual contents, DASH segments are traditionally transported over TCP connections. On the other hand, we argue that UDP could be usable when the available bandwidth in the radio network is sufficient and considering the fact that the RLC is already ensuring the service reliability. The eNB might be able to estimate the available capacity, by monitoring the corresponding RLC acknowledgements. Whenever an acknowledgement is received (time tk) at the RLC layer of the eNB, this assumes that d_k^{rlc} RLC bits have been successfully received by the mobile terminal and, therefore, the available bandwidth at time t_k can be estimated by

$$b_k^{rlc} = \frac{d_k^{rlc}}{t_k - t_{k-1}}. \quad (5)$$

Afterwards, having applied a low-pass filter with a cut-off frequency of $\frac{1}{\tau}$, the eNB can estimate the available bandwidth, according to Equation (6), which was proposed in [Mascolo 2001].

$$\tilde{b}_k^{rlc} = \left(\frac{\left(\frac{2\tau}{t_k - t_{k-1}}\right) - 1}{\left(\frac{2\tau}{t_k - t_{k-1}}\right) + 1}\right) * \tilde{b}_{k-1}^{rlc} + \left(\frac{b_k^{rlc} + b_{k-1}^{rlc}}{\left(\frac{2\tau}{t_k - t_{k-1}}\right) + 1}\right). \quad (6)$$

The eNB sends the corresponding bandwidth estimations to the HTTP server, allowing it to choose the most suitable segment representation and, then afterwards, the transport protocol will be used. In order to choose a representation for the k^{th} segment to transmit to the HTTP client, the HTTP client implements the S-BR-Q algorithm [DeSimone 2013]. The selection of the representation of the k^{th} segment is made in three steps: first, the algorithm compares the available network bandwidth with the transmission rates of every representation of the k^{th} segment, discarding those of which transmission rates are strictly greater than the available network capacity. Afterwards (second step), the algorithm compares the Peak Signal to Noise Ratio (PSNR) [Hore 2010] of each representation of the k^{th} segment within a certain range $[PSNRmin, PSNRmax]$, discarding those out of such range. In the third and last step, the algorithm selects the representation whose transmission rate is closer to the available network bandwidth.

Regarding the selection of the transport protocol to transmit the k^{th} segment, the HTTP client implements an algorithm that compares the available network bandwidth in the network with the transmission rate of the representation that was selected by the S-BR-Q algorithm. If the difference between the two parameters is greater than a certain Δ_{rate}, the server selects UDP; otherwise, it selects TCP.

The following section will present the main results obtained from a simulation campaign meant to evaluate the performance of the different transport protocols in

LTE networks, in conjunction with the bandwidth estimation algorithm proposed herein. Thus, the results may be afterwards used to estimate the value of the Δ_{rate} parameter.

5.1.3 Experimental evaluation

In order to assess the feasibility and potential benefits of the proposed transport protocol selection algorithm, this section discusses the most relevant results from a simulation campaign that was carried out to study the video delivery performance of various transport protocols and the effect that the rate adaptation algorithm has over them. The simulation has been performed over the ns-3 simulator [NS3] and it is focused on the LTE technology, which is integrated into the simulator by the LENA module [LENA]. The main simulation parameters are summarised in **Table 37**. Furthermore, we use the hybrid-buildings propagation loss model, which provides accurate results in terms of network performance.

Table 37: Simulation parameters

Parameter	Value
UE Tx power	$23\ dBm$
eNB Tx power	$43\ dBm$
UE height	$1.5\ m$
eNB height	$30\ m$
RLC mode	Acknowledge Mode (AM)

The scenario emulates the one illustrated in

Figure 35. The access segment consists on one eNB and one UE; the UE uses a video service that is provided by a server that is in fact connected to the Evolved Packet Core (EPC) of the eNB. Since the simulator does not provide appropriate video service implementations, the corresponding traffic has been modelled as constant bit rate traffic, whose rate is selected from a set of typical values [ITEC], according to the estimated bandwidth. These values range from 46.980 Kbps to 4.726 Mbps (corresponding to the resolutions of 320x240 to 1920x1080), while the service duration has been fixed to 15 seconds and each of the video chunks are 1 second long; this means that the data rate might be updated every second.

We gradually increase the distance between UE and the eNB. At each point, we retrieve the video from the server. In addition, we execute 100 independent simulations per point, so as to ensure the statistical validity of the results. In order to enhance the filtering procedure, we estimate a new sample of $\hat{b}_k^{rlc}$ every 200 ms, by considering the amount of acknowledged data during such interval in the RLC entity of the eNB. Since we are assuming a fixed Acknowledgment (ACK) inter-arrival time, we obtain a filter with constant coefficients. Hence, by selecting the cut-off frequency value, we can better adjust the relative weights of both the last estimated $\hat{b}_{k-1}^{rlc}$ and the last measured b_k samples, so as to estimate a new sample. This filter with constant coefficients can be therefore expressed as

$$\tilde{b}_k^{rlc} = w\,\tilde{b}_{k-1}^{rlc} + \frac{1-w}{2}\,[b_k + b_{k-1}]. \qquad (7)$$

As it can be seen, the new $\hat{b}_k^{rlc}$ sample is calculated by averaging the previous estimated sample $\hat{b}_{k-1}^{rlc}$ and the mean of the two last measures, b_k and b_{k-1}, with weights w and 1-w, respectively.

As mentioned earlier, we have carried out simulations with different settings, moving the UE away from the eNB and studying a number of figures of merit. The distances vary within the interval [150, 810] (with a step of 20 m); for shorter distances, the quality of the link leads to almost ideal conditions, while for distances larger than 810 m the communication suffers from very hostile conditions and it can hardly finish. Furthermore, we have used a τ value that is 10 times greater than the inter-arrival time, $\tau = t_k - t_{k-1}$, thus leading to a weight of w = 0:9 for the last estimated value $\hat{b}_{k-1}^{rlc}$.

5.1.3.1 *Interaction of rate adaptation and transport protocols*

In order to study the impact of the data rate adaptation and its interaction with the transport protocols, **Figure 36** shows the throughput that was observed at the application, as a function of the distance between the UE and the eNB; we compare the results obtained with and without the data rate adaptation functionality. It is important to mention that we measure the throughput by dividing the amount of received data by the time from when the first packet is received until the last one is received. Hence, under certain conditions (for instance if the application had just received one burst of packets), the results may be misleading.

The results yield some interesting outcomes. First, **Figure 36** shows that the bit rate adaptation, as it is configured, has a negative impact over the UDP flow when the channel conditions are good (distances lower than 210 m). On the other hand, under more hostile conditions (distances higher than 400 m) the adaptive technique, applied to UDP traffic, outperforms the other configurations. In fact, the throughput that is observed for the UDP configuration is rather independent of the distance of the wireless link. We can therefore conclude that the rate adaptation mechanisms can favour either TCP or UDP, depending on the conditions of the wireless channel.

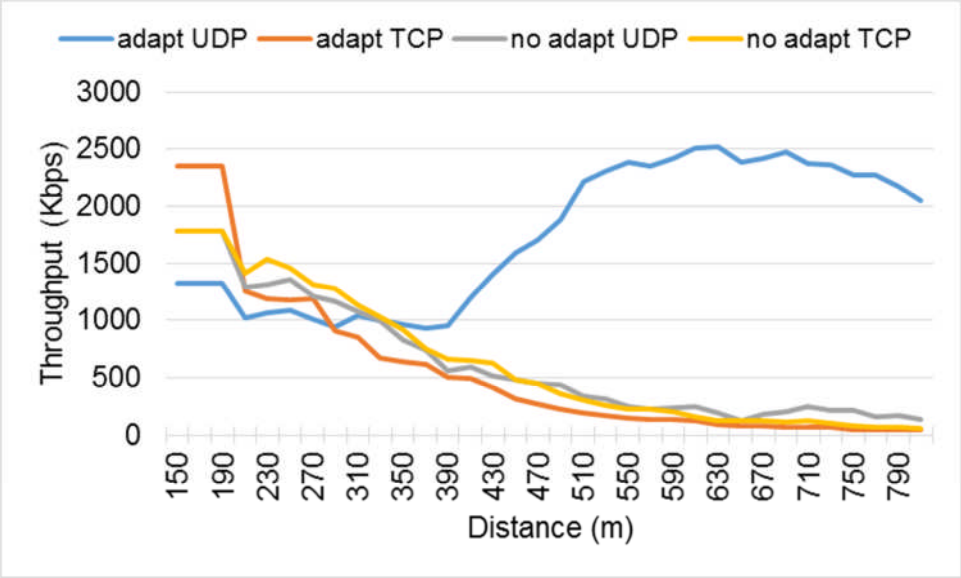

Figure 36: Throughput of the video application with adaptive rate for the different transport protocol configurations

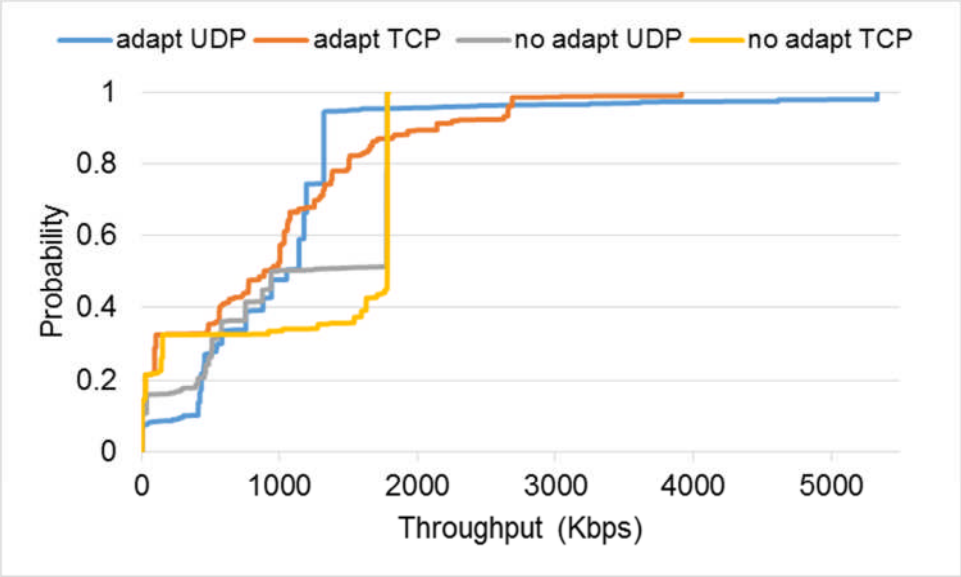

Figure 37: CDF of the throughput measurements. These values are obtained from 1000 simulations with a distance of 300m

Furthermore, and in order to ensure the statistical validity of the average results, **Figure 37** depicts the Cumulative Distribution Function (CDF) of the throughput after carrying out 1000 independent simulation over a distance of 300 m. We can see that the results of the configuration with the rate adaptation technique show a notable variability, which might have been expected, since it is a direct consequence of the rate adaptation.

In order to clarify the fact that under certain conditions (for instance if the application had just received one burst of packets) and complement the results of **Figure 36** and **Figure 37**, **Figure 38** and **Figure 39** provide additional information that sheds light on the amount of data that was actually received by the application. When the rate adaptation is not activated, we assume a constant bit rate of 1663 Kbps; this can be observed on **Figure 39 (a)**, as the value of transmitted data for both no adapt UDP and no adapt TCP is constant.

In addition, **Figure 38** shows the delivery ratio, defined as the percentage of data sent by the server that was correctly received at the UE client. First, as can be seen in **Figure 38(a)**, all configurations exhibit a similar performance when the distance between the eNB and the UE is below 400 m. For higher distances, the adaptive technique, applied to UDP traffic, outperforms the rest of configurations, as was also seen for the throughput. **Figure 38(b)** shows the CDF of this metric, after carrying out 1000 independent simulations at the same point (distance of 300m); we can see that all configurations show a great variability.

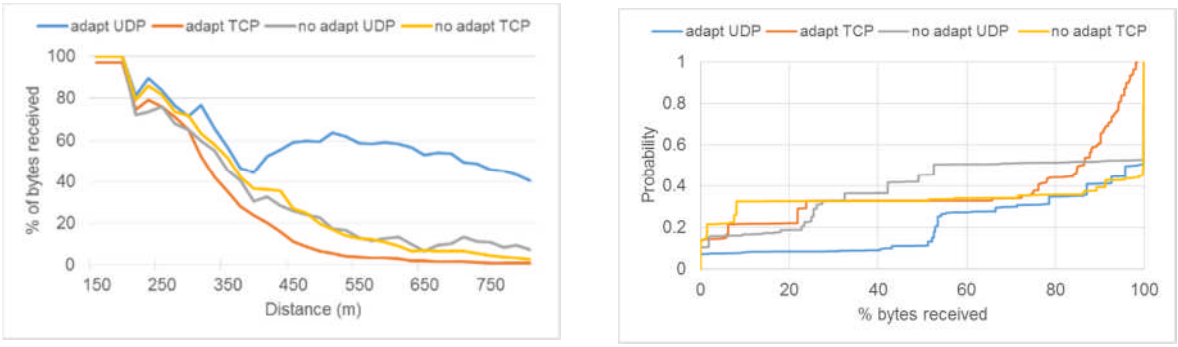

(a) Average values vs. distance (b) CDF at 300m

Figure 38: Average values of data successfully delivered by the application

Finally, **Figure 39** allows us to better understand the performance of the adaptation scheme. We show the amount of bytes that were sent and received by the server and the client application, respectively. Regarding the packets received at the client, **Figure 39(b)** yields a very similar behaviour as the one seen for the other metrics; on the other hand, **Figure 39(a)** illustrates the behaviour of the corresponding filter. For short distances, below 400 m, the filter configuration leads to underestimating the capacity, while for larger distances, the estimation works rather well for UDP, but not for the TCP case. In general, we can conclude that, over the considered scenario, UDP outperforms TCP when the data rate at the application is adapted according to the estimated bandwidth. Besides that, the results suggest that the interaction between TCP and RLC in AM mode has some serious drawbacks, which become rather clear when the data rate changes.

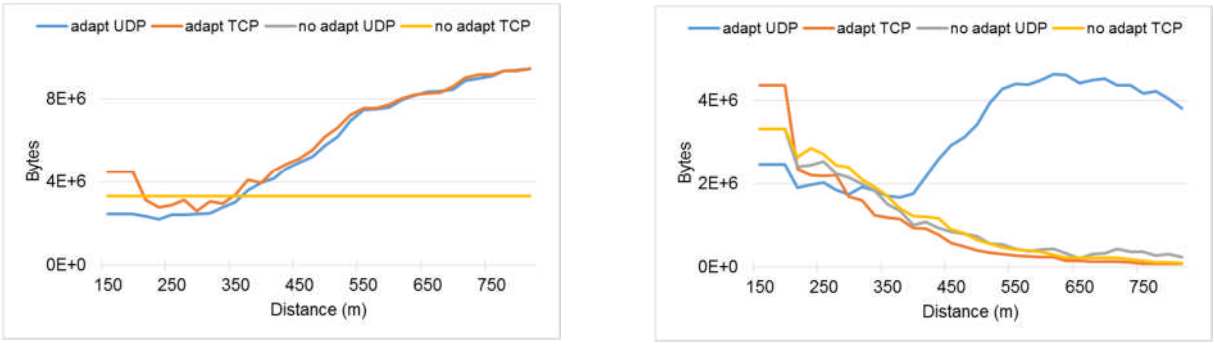

(a) Average transmitted bytes (b) Average received bytes

Figure 39: Application statistics

5.1.3.2 RLC protocol performance

As was discussed previously, one of the main objectives of this work is to assess the feasibility of using UDP as an alternative to TCP as a transport solution for video streaming services, since we advocate that it might reduce the exposure to EMF. This can be achieved by reducing the total number of required transmissions for a given size of content; in our case, we study the transmissions that are performed by the RLC protocol. **Figure 40** shows a measure of their effectiveness, defined as the ratio between the observed throughput and the number of RLC transmissions that

were performed during a session. This metric is therefore a good indication of the trade-off between the observed throughput (QoE) and the overall number of required of RLC transmissions (EMF exposure). **Figure 40** yields that TCP performs worse than UDP when the distance to the base station is low. On the other hand, when the distance increases (up to 400 m), the adaptive version of TCP provides better performance. Finally, as it was also observed for the results of Section **5.1.3.1**, the performance of the adaptive version of UDP outperforms the other configurations when larger distances (> 400 m) are considered.

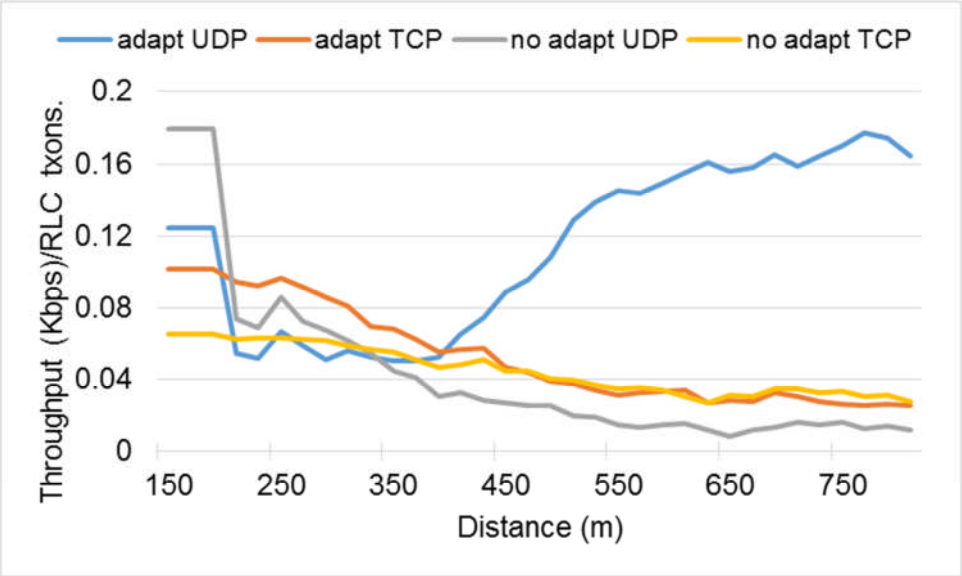

Figure 40: Ratio of the achieved throughput vs. the number of RLC transmissions

In order to assess the statistical validity of the previous results, **Figure 41** shows the corresponding CDF, obtained after carrying out 1000 independent simulations. We shall again observe the notable variability that characterises this metric, especially in the case of UDP with adaptive traffic.

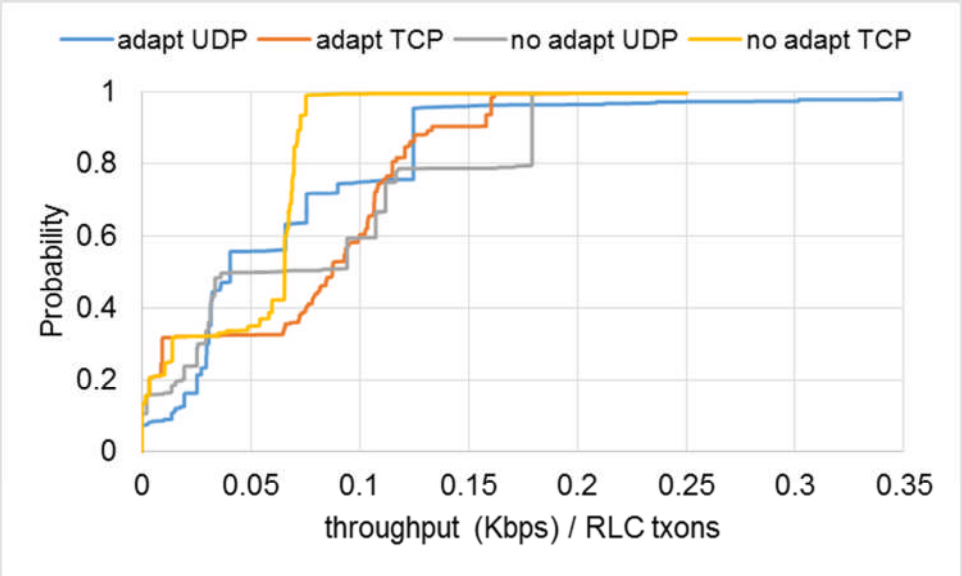

Figure 41: CDF of the ratio of the achieved throughput vs. the number of RLC transmissions at a distance of 300 m

Finally, we have also studied the impact of the rate adaptation over the RLC protocol. We analyse the evolution of the transmission buffer, i.e., a certain amount of data that is waiting to be sent. **Figure 42** represents the CDF of the overall number of bytes at the transmission buffer, for the two transport protocols (with and without the rate adaptation scheme) and at different distances. As can be seen, the adaptive configuration of the traffic flow reduces the size of the buffer both for UDP and TCP. The remarkable difference between the two transport protocols is a consequence of the congestion control algorithms used by TCP. In the particular case of TCP, we see that it is more likely to have an empty buffer when adapting the data rate; this indicates that the cut-off frequency that was selected for the experiments leads to an under-utilisation of the available bandwidth. On the other hand, the rate adaptation applied to UDP heavily reduces the buffer length. Taking into account that the throughput for the adaptive scheme was higher at some distances, we can conclude that the proposed filtering allows taking advantage of those time periods in which the link quality momentarily improves.

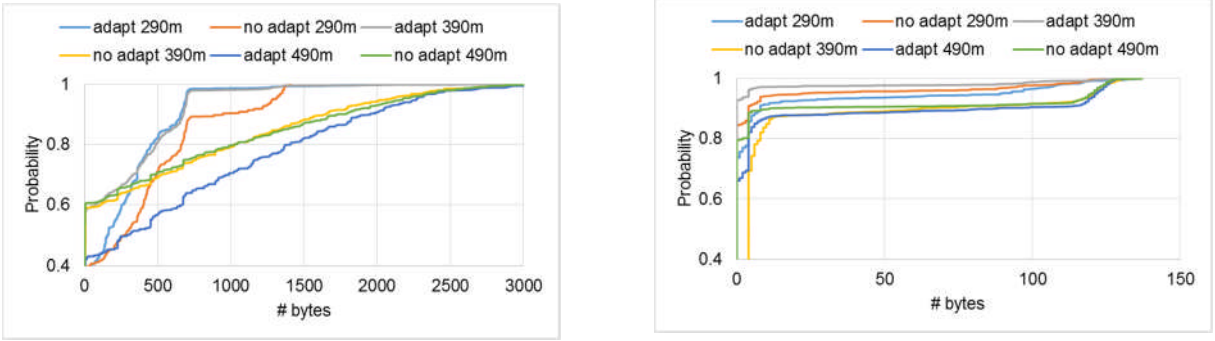

(a) UDP (b) UDP

Figure 42: State of the RLC transmission buffer

5.1.4 Concluding remarks & future work

This contribution presents a novel network-centric algorithm to be used with video streaming services, in particular based on the DASH protocol; its main goal is to reduce the end-users' exposure to EMF. It is based on a cross-layer solution where the video representations as well as the transport protocol are selected according to the bandwidth that is estimated by the network. We have focused on the LTE technology, in particular on the RLC protocol. When it is configured in the acknowledged mode, it provides a reliable communication service. We have proposed a methodology to estimate the available bandwidth at the RLC level, based on a low-pass filter. In order to assess the feasibility of the proposed solution, we carried out an extensive simulation campaign over the ns-3 framework, studying the suitability of different transport protocols.

The obtained results yield that there are certain circumstances, in particular when the wireless channel exhibits poor quality, which would favour the use of UDP instead of TCP for video delivery over LTE networks. We have assessed that the proposed algorithm bring benefits in terms of perceived QoE and the reduction of exposure to EMF.

First, we have studied the impact of the traffic adaptation, in combination with the AM mode of RLC, over the performance of the transport protocols. Despite they correspond to a rather specific adaptation procedure, the results yield that UDP clearly benefits from the traffic variation, and its performance is not jeopardised when increasing the distance between the UE and the eNB. On the other hand, the interaction of TCP flow control and RLC/AM mechanisms has a rather negative impact on the throughput perceived by the user.

Furthermore, we have as well studied the potential impact of the transport protocol selection over the exposure to EMF. UDP has a straightforward gain, since it does not require any traffic in the uplink (as it would be the case of the TCP acknowledgments). Besides, we have also seen that when the conditions of the wireless channel get worse, the RLC frames used to carry UDP traffic are much more effective (in terms of throughput) that those that would carry TCP segments. This might indirectly reduce the exposure to EMF, since the same content could be delivered with fewer transmissions.

In our future work we plan to analyse the interaction between the different network entities: video application, transport protocol and RLC module. Regarding the application, we plan to use the ns-3 emulation capabilities, which would allow us to use real video traffic (for instance, by using the VLC media player/application). In addition, we would like to carry out a similar analysis over different technologies, for instance Wi-Fi, and we would therefore need to establish appropriate bandwidth estimation procedures.

5.2 EMF-QoS Trade-off in indoor Wi-Fi

Wi-Fi systems are often optimised towards (sometimes) conflicting performance objectives (low delay, low exposure, high reliability, etc.) which are difficult to fulfil simultaneously. In such cases, the wireless system will exhibit different optimal operation points (i.e., combinations of settings), corresponding to different requirement trade-offs, which in literature is often referred to as the Pareto front. In chapter 6 of [LEXNET D5.1], an EMF vs. audio quality trade-off scenario was presented in order to show the suitability of the SUMO toolbox for experimentally identifying optimum input parameter combinations (i.e., Tx power and channel) that decrease EMF exposure while increasing the audio quality [Michael 2015]. This section extends our previous work by demonstrating the feasibility of utilising the tool also in (i) scenarios that consist of more devices, (ii) coping with wireless system that has more configurable parameters and (iii) scenarios that use real-time Wi-Fi measurements to calculate the exposure. First, the scenario is enlarged to accommodate more attendees (i.e., 8 => 40 attendees). Second, the LEXNET exposure calculation formula is implemented in Wi-Fi drivers such that they calculate the SAR (uW/Kg) in real-time. Third, the audio quality metric is further extended to accommodate the quality loss due to a raw audio encoding process. Last but not least, we also increased the number of input parameters (i.e., Wi-Fi Tx-Power, Wi-Fi Tx-Rate, Codec Bit-Rate and Codec Frame-Length).

Experiment Scenario

The experiment scenario is composed of a speaker node transmitting an audio signal on Wi-Fi channel 1 (2412 MHz centre frequency), 40 listener nodes listening on the audio signal, a central database collecting the measurement data, a Multi Objective Surrogate-Based Optimisation (MOSBO) optimising the input parameters and an experiment controller orchestrating the experiment. The experiment scenario is presented in **Figure 43**.

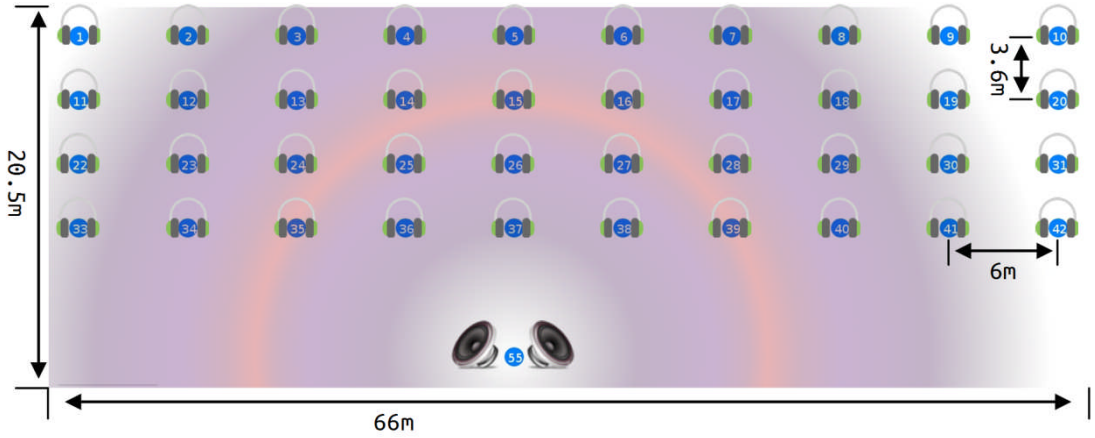

Figure 43: Top level view of the experiment scenario

Input Parameters

While transmitting the audio signal, the speaker node can dynamically adapt four configurable input parameters, namely Wi-Fi Tx-Power, Wi-Fi Tx-Rate, Codec Bit-Rate and Codec Frame-Length. **Table 38** shows the description and ranges of each input parameters. Each of these settings influences both the audio quality and the overall received exposure. Increasing the codec bitrate of an audio signal, for example, will improve the audio quality but increases the exposure. The same follows for Tx-Rate and codec Frame-Length parameters except Tx-Power. Tx-Power only creates a conflicting performance if there is enough background interference to make higher Tx-Power necessary, thereby allowing the stronger signals to be received at the listener end. However, in realistic environments, it is difficult to monitor the overall environment and as such adapting the Tx-Power is important as well. However, an exhaustive search to identify optimal trade-off values would require analysing 7680 configuration combinations, which is not feasible in a reasonable time frame.

Table 38: Input parameters of the Wi-Fi conferencing experiment. The design space is composed of 7680 (32x3x4x20) elements

Input parameters	Description	Range
Codec Bit-Rate	Opus encoder output bit rate	[6400, 7200, 8000,…, 31200] bps
Codec Frame-Length	Opus encoder output frame length	[20, 40, 60] msec
WiFi Tx-Rate	WiFi packet transmission rate	[6, 12, 18, 24] Mbps
WiFi Tx-Power	WiFi packet transmission power	[1, 2, 3, 4, , 20] dBm

The audio transmission flowchart, indicating all input parameters, is shown in **Figure 44**. A raw audio file is given to an encoder unit which outputs compressed audio frames of a given bit rate and frame length using an Opus compression format [Opus]. Afterwards, the Opus encoded frame is encapsulated, rate and power adjusted before sent over the air.

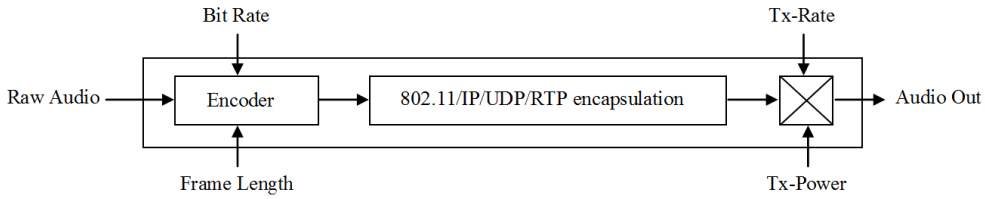

Figure 44: Audio transmit path of the Wi-Fi conferencing experiment

Performance objectives

The wireless system has the following opposed objectives: increase the audio quality while reducing the EMF exposure.

- EMF Exposure

  Current RF exposure metrics, such as incident electric, magnetic field, incident power density, SAR, etc., mainly deal with assessing compliance with exposure limits. Most of these metrics are either uplink-only or downlink-only focused. Recent studies also looked at the combined exposure of uplink and downlink, but on an individual user basis [Aerts 2013], [Lauer 2013]. Varsier et al [Varsier 2015], however, defined the EI which aggregates both DL and UL exposure data and quantifies the total exposure over a population in an area. Assuming that we neglect the uplink exposure by mobile devices from other users, then the EI becomes:

$$EI^{\mathrm{SAR}} = \frac{1}{\mathrm{T}} \sum_{t,p,e,r,c,l,pos}^{N_T,N_p,N_E,N_R,N_C,N_L,N_{pos}} f_{t,p,e,r,l,c,pos} \left[\sum_{u}^{N_U} \left(d^{UL}\, \bar{P}_{\mathrm{TX}} \right) + d^{DL}\, \bar{S}_{\mathrm{inc}} \right] \left[\frac{W}{kg} \right] \qquad (8)$$

  with N denoting a quantity, t a period within the considered time frame T, p population category, e environment, r RATs, c cell type, l user load profile, *pos* posture, u usage of the device, $\overline{P}_{\mathrm{TX}}$ average transmitted power by the mobile device, $\overline{S}_{\mathrm{inc}}$ average incident power density, d^{UL} the uplink dose and d^{DL} the downlink dose, and f is the fraction of the population *p* with user load profile *l* in posture pos connected to RAT r for a cell type c in environment e during the time period t. The fraction f can be obtained from life segmentation data and ICT usage data.

- Audio Quality

The audio quality objective is measured using the Mean Opinion Score (MOS). **Figure 45** shows the aggregate MOS score calculation for the Wi-Fi conferencing scenario.

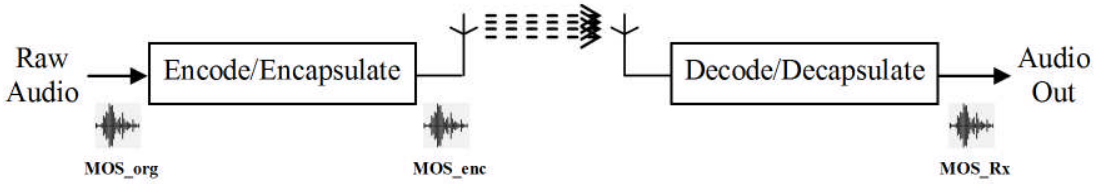

Figure 45: Aggregate MOS calculation layout

As it is seen in **Figure 45**, the aggregate MOS is calculated twice in the audio transmit path first after the encoder unit and later after the Wi-Fi transmission. The encoder, having a reduced output bit rate, introduces a quality loss which is a function of the encoder bit rate.

$$MOS\ enc\ =\ \mathrm{f}(MOS\ org;\ encoder\ bitrate)$$

After the raw audio is encoded, it is transmitted over the wireless medium which also introduces a quality loss due to transmission latency, jitter and packet loss [Base 2015].

$$MOS\ Rx\ =\ \mathrm{f}(MOS\ enc;\ latency;\ jitter;\ packet\ loss)$$

Exhaustive search model

The exhaustive search model is a plot of the objective performances at every input parameter combination. After evaluating all performance objectives, the Optimal Pareto Front (OPF) is generated which is used to make performance comparison. **Figure 46** shows the exhaustive search model and OPF of the Wi-Fi conferencing experiment.

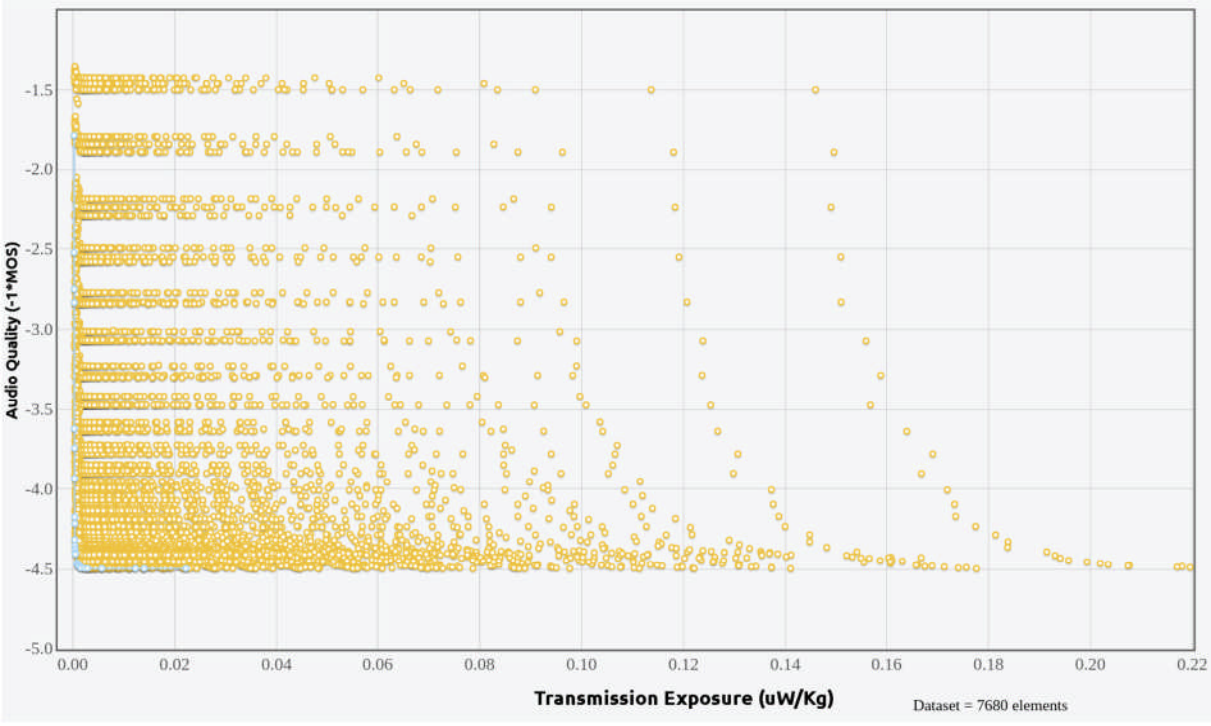

Figure 46: State of the RLC transmission buffer

From **Figure 46**, we observe the followings. There is an exponential pattern between exposure and audio quality objectives when the codec bitrate parameter only varies. As exposure objective linearly depends on the number of packets sent over the air or show linear dependence with the codec Bit-Rate parameter, this also proves the exponential relationship that the audio-quality objective has with the codec Bit-Rate parameter [VQCIETF 2011]. Moreover, these exponential patterns are also logarithmically spaced as we move along the exposure axis due to a variation only on Tx-Power. This also proves the logarithmic relationship between the exposure objective and Tx-Power input parameter. Seeing such patterns with higher visibility, an exponential increase of audio quality as a function of codec bitrate combined with a logarithmic increase of exposure as a function of Tx-Power, is a good indication that Tx-power and codec Bit-Rate are the most dominant parameters affecting exposure and audio quality objectives receptively. To a lesser extent, codec Frame-Length parameter also affects the audio quality objective and zooming into the first three rows on **Figure 46** explains this finding. The codec Frame-Length parameter linearly affects the latency between consecutive audio packets arriving at the listener end and thus a reduced audio quality for an increase in the Frame-Length parameter. On the other hand, the audio quality objective is not improved as we increase the Tx-Power while keeping the other parameters fixed. This is due to the fact that the experiment was performed in a shielded environment in which no interference was present.

Finally, identifying optimal operation points is the main goal of a Pareto optimisation problem. Looking the OPF curve on **Figure 46**, the end points represent the best values of the respective objectives. In our case, we get an exposure limit of 262 fW/Kg and a highest MOS score of 4.494517. These values are the objective limits and cannot be improved any further. On the other hand when considering the best performance trade off pair, we select the point from the OPF set that is closest to the intersection point between the best audio quality line and the best exposure line. In our case, the intersecting point is at MOS = 4.494517 and exposure = 262 fW/Kg and the best performance trade off pair has MOS = 4.493343 and exposure = 2.287 nW/Kg.

Experiment output

Finally, the goal of our solution is to identify the Pareto front without performing an exhaustive search which is not feasible in realistic conditions due to the time-consuming nature of wireless experimentation. To this end, the Wi-Fi conferencing scenario is optimised by using the MOSBO toolbox. The MOSBO toolbox generates surrogate models (see [LEXNET D5.1]) to predict the OPFs. After only 49 iterations an almost OPF was identified (blue line of **Figure 47**). This corresponds to a speed up gain of 7680/49=156.73 (instead of requiring 7680 experiments with exhaustive search, the MOSBO toolbox identifies the new Pareto front with only 49 experiments), thereby experimentally demonstrating the feasibility of quickly identifying optimal operation point that trade-off audio quality with EMF exposure.

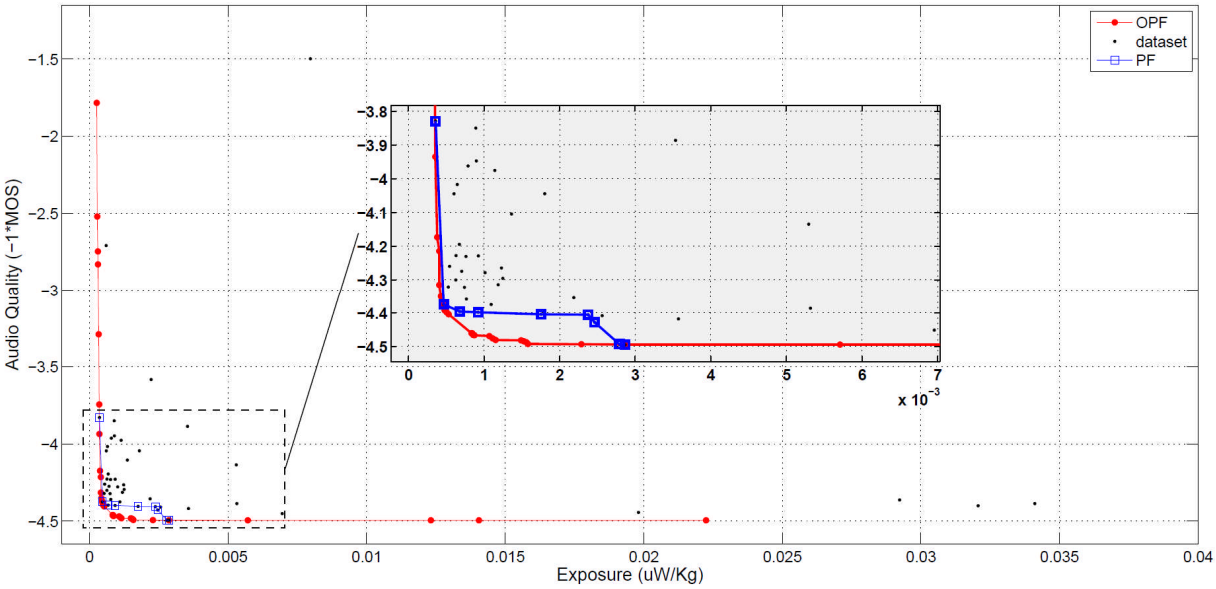

Figure 47: MOSBO Pareto optimisation plot after the stopping criteria is met

Conclusion

The EMF-Audio Quality Trade-off scenario presented showcases the benefit of using MOSBO multi-optimisation toolbox to locate the OPF in a very short time as compared to an exhaustive searching experiment. The OPF is composed of the best EMF and audio quality pairs that are possible and their associated input parameters. From the Wi-Fi conferencing scenario, we conclude that the MOSBO optimisation toolbox retrieved the OPF (least EMF exposure and best audio quality pair) in a very short time with a speed up factor of 156.73.

6 ROUTING PROTOCOL FOR EMF REDUCTION

This chapter is about a practical means to compute the EMF node exposure based on the number and types of packets received by nodes, rather than based on the electromagnetic radiation, which has been the subject of LEXNET WP2. Using the packets as a proxy for exposure measurement is valid in networks where electromagnetic waves are generated by nodes every time a new packet is sent. Such network includes mesh networks, but it could also include cellular or Wi-Fi networks. Since the LEXNET WP2 definition of the exposure index is extensive, but is using the SAR rather than the number of packets, our approach is a simplified version of the accumulated LEXNET WP2 EI, which only keeps the terms and factors of the WP2 EI sum that refer to packets that nodes transmit, receive or forward. In the rest of this chapter, we explain why measuring the exposure based on the number of packets is a relevant for designing new EMF-aware routing protocols. Here we only focus on the packet level, as opposed to general EI definition which considers other communication layers and different type of parameters. For this reason the EI metric in this section will be restricted to packets transmission power instead of the general EI definition.

First, we have designed a packet based theoretical model in order to obtain a valid methodology to study routing solution performance in terms of EMF exposure. This methodology, which is introduced in Section **6.1**, and detailed in **Appendix 2**, may be applied to different algorithms and routing protocols under analysis; in particular it would be used to evaluate RBRP protocol [Iancu, 2014]. Furthermore, an algorithmic solution to the EMF aware routing is proposed, Section **6.2**, in order to have a baseline to which compare routing protocols.

6.1 Theoretical model for assessing network-level EMF exposure

In order to be able to study and evaluate the performance in terms of EMF exposure of the RBRP protocol [Iancu, 2014], we have designed a packet based theoretical model.

Consider the following function, defined for the whole mesh network where N represents the number of nodes:
Exposure: $\mathbb{N} \rightarrow \mathbb{R}_{+}^{N}$
For each node k, $1 \leq k \leq N$ we have the following exposure function components:
$E_n : \mathbb{N} \rightarrow \mathbb{R}_{+}$
such that $Exposure(T) = (e1\,(T), e2\,(T), \ldots, eN\,(T))$, where T represents a discrete time moment within the routing process.

As we describe in detail in **Appendix 2**, the following analytical expression can be used as a proxy for the LEXNET exposure index so as to be used in multi-hop wireless networks:

$$EI(T) = \sum_{k=1}^{N}[e_k(A) + e'_k(A_k)T + \int_0^T \int_0^x e''_k(t)P_k(t)dtdx\ ] \qquad (9)$$

where

$$\int_0^T \int_0^x e_k''(t)P_k(t)dtdx$$
$$= P_k(T-1)e_k(T) - P_k(T-1)e_k(T)$$
$$+ \sum_{U=0}^{T-1}[\sum_{S=0}^{U} P_k(S)e_k'(S-1) - P_k(U)e_k'(U)]$$
$$- \sum_{U=0}^{T-1}\sum_{S=0}^{U} P_k(S)e_k'(S) + \sum_{U=0}^{T-2} P_k(U)[e_k(U+1) - e_k(U)] \quad (10)$$

In these equations *A* is an arbitrary initial time moment, *t* is time, *T* is the moment in time when the last packet is transmitted/forwarded between two nodes, *a* is a fixed initial real value and *x* is a variable, $P_k(U)$ is an extra factor to be added to the formula which is taken to be 1 if the node k transmits/forwards at time moment *U* and 0 otherwise, *U* and *S* are any two integer indexes from 0 to T.
A more practical means of using this extended equation as well as a generalisation that allows for the computation of the EI proxy, when dynamic power management can be applied (i.e. packets can be sent with different power levels), is also presented in detail in **Appendix 2**. As it stands, the formulas were deduced and explained for one power level, including the recurrence functions involving z_n, y_n and w_n, and thus they can be easily adapted to be applied to the case when we consider multiple power levels.

It should also be noted that this methodology may also be applied to different algorithms and routing protocol, not just to the RBRP protocol, and that this methodology can be used in numerical computations of the EI in any type of network.

6.2 Enhanced RBRP algorithm with power management in meshed deployment

With the aim of reducing the EMF exposure in multi-hop networks, it was proposed a RBRP protocol [Iancu, 2014] which, using techniques similar to load balancing, is able to distribute the exposure over an area as well as to reduce its average value. In order to fairly study the goodness of that protocol, this section presents an EMF tailored algorithm to which compares the results of the protocol. For this, an optimisation problem is posed that aims at routing the information packets through those paths with a lower exposure by taking into account both the accumulated exposure and the new one that will be generated as a consequence of the selection.

Furthermore, the algorithm assumes that a dynamic power selection hop-wise is enabled in the nodes, since this transmission power reduction is a key parameter to reduce the global exposure on the scenario.

6.2.1 Network model

The utilised network model is based on graph theory and jointly considers the accumulated exposure and the transmission power. The network is modelled as a graph $G_i = (V, E)$ where V is the set of vertices and E represents the set of edges in

the graph. We consider 2 different types of costs within the graph that, according to the parameter they represents, are given either to a vertex or edge as defined below:

- Accumulated exposure K: this cost is assigned to each node in the network and it indicates the cost associated to the exposure that the node has induced until that moment. The value of this cost is independent of the traffic flow transmitted by the node at a given moment.
- Power P: this is related to the necessary power for the node to transmit a packet to the next hop; thus, it is associated to each edge. This cost is considered to be proportional to the amount of traffic through the edge at that moment.

Due to the different nature of the costs defined above, it is necessary to transform the initial graph so that well known algorithms (e.g. AODV) can be used to find the optimum routes selection. For that, we have defined virtual edges that bear the K cost, so that each node is split into two virtual vertices in order to distinguish between ingoing and outgoing traffic. For that, each initial node W decomposed in W' and W'' which, in turn, are connected by the edge carrying the K cost associated to the induced exposure by the node. This way, the new virtual node W' has the same ingoing edges as the initial W and its only outgoing arc is the one connecting with the vertex W''. In the same way, the vertex W'' has the same outgoing edges as W and the arc connecting with W' as unique entering edge.

In this sense,

Figure 48 shows the graph transformation applied to a simple graph of three nodes at a time moment T. As can be seen, the initial costs of the arcs $X_{xy}P_{xy}$ (where x and y hold for the source and destination of that arc respectively) are regarded to the power necessary to communicate with the neighbour (X_{xy}) multiplied by the amount of traffic through it (P_{xy}). On the other hand, after the transformation, new arcs $K_x(T)$ arise that carry the accumulated exposure cost by each node x until the moment T. Besides, it can be seen that the size of the graphs grows, so that from an initial graph $G = (V, E)$, we obtain a new one $G' = (V', E')$ in which $|V|' = 2|V|$ and $|E'| = |V| + |E|$.

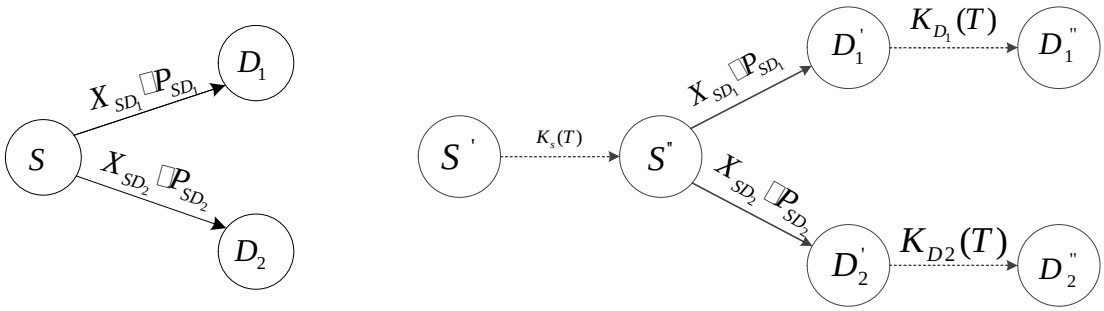

Figure 48: Simple example of graph transformation with 3 nodes. Initial graph G is shown at left and transformed graph G' at right

6.2.2 Problem formulation

Considering the structure of the initial graph, in which the cost related to the transmission power is proportional to the amount of flow in this edge, the problem initially posed is a minimum cost flow problem, which aims at distributing the total flow in the graph so that the global cost is minimised. Analytically the problem can be expressed as

$$\min \sum_{\forall (i,j) \in E} c_{ij} x_{ij}$$

$$\text{s.t.} \quad \forall\, i \in E \sum_{j:(i,j)\in E} x_{ij} - \sum_{j:(j,i)\in E} x_{ij} = b(i) \tag{11}$$

$$\forall\, (i,j) \in E \quad u_{ij} \geq x_{ij} \geq 0 \tag{12}$$

$$\sum_{i \in E} b(i) = 0 \tag{13}$$

where c_{ij} and u_{ij} represent the cost per flow unit and the edge capacity respectively. On the other hand, $b(i)$ holds for the flow originated ($b(i) > 0$) or received ($b(i) < 0$) by each node. Finally, x_{ij} represents the flow present at each edge of the graph. This way, constraint **(11)** ensures that the flow balance of each node corresponds to the generation/consumption of flow at that node; constraint **(12)** ensures that the edge capacity is not exceeded and the global flow balance is forced to be 0 by constraint **(13)**.

There exist in the literature solutions of this problem which focus on the particular properties of it. Since we focus on the network model rather than on the particular algorithm to solve it, we have opted for a classical solution as cycle cancelling algorithm. It is worth highlighting that this algorithm is typically implemented in networks with only one source and one destination (gateway). To overcome this limitation a *virtual* pair origin/destination has been defined so that the capacity of the edges from the virtual origin to each source is one flow unit in order to ensure that each traffic source generates one traffic flow. In the case of the virtual destination, the edges capacity is not limited, since there is no constraint regarding the load balance between the gateways.

It is worth pointing out that, due to the graph transformation presented before, the cost of the new edges is not proportional to the flow, but remains constant; thus the utility function can be represented as follows:

$$\min\left(\sum_{\forall\,(i,j)\in E} c_{ij} x_{ij} + \sum_{\forall\,(i,j)\in E'/E} k_{ij} \right) \tag{14}$$

This practical modification has been considered while implementing the algorithm implementation, and simulation results show that the implemented solution behaves properly. From an implementation point of view, the value of K has been modulated so that, when multiplied by the flow, it presents the same cost.

6.2.3 Results analysis

The proposed network model and algorithm has been assessed from two different angles: first section **6.2.3.1** describes the behaviour of the algorithm over static networks. We compare its performance with other algorithms which consider traditional metrics, in particular an algorithm that minimises the total transmitted power by using a shortest path solution (in which the edge cost corresponds to the power to reach the next hop). On the other hand, section **6.2.3.2** studies the behaviour of the proposed algorithm in more complex scenarios in which the temporal evolution of the accumulated exposure is more relevant; besides different configuration of the algorithm will be studied.

In both cases, the different algorithms are sequentially applied to the graph so that each execution would correspond to discrete events in which the routes are recalculated. At each execution the graph is updated, in particular the accumulated exposure in the nodes, so that the whole procedure tries to reflect the temporal evolution that a protocol would follow but obtaining global optimum results.

Regarding the accumulated exposure, it is worth highlighting that, while the accumulated exposure is a physical parameter (typically measured in electric field units), the algorithm model considers that accumulated exposure by means of the cost parameter K. In this study, considering that all the flows in the network are alike, we have defined as ε the increment of the accumulated exposure per flow of each node during a temporal step (time between two consecutive algorithm execution).

6.2.3.1 Static configuration

This first analysis aims to study the potential of the algorithm for reducing both the transmission power and accumulated exposure. In particular, we have studied scenarios in which 50 nodes, with coverage range of 15 meters, have been randomly deployed (*Poisson* process) over a square surface whose side has been gradually increased in order to modify the network density, and then the connectivity degree of the graph. **Table 39** summarises the parameters of the scenarios studied in this section. In each topology, the results are obtained for different number of traffic sources, while the number of destinations is set to 4; it is worth highlighting that the destinations are deployed in such a way that cover the maximum area. In this sense, the routes can be established to any of the destination, since they are considered as gateways of the network, while the *virtual* destination described below may represent the target network (e.g. the Internet or operator network).

Table 39: Configuration of static topology

	Topology			
	α	β	γ	δ

Sources	{2,4}	{2,4}	{2,4,6,8}	{2,4,6,8}
Area (m^2)	120 x 120	130 x 130	140 x 140	150 x 150

In order to study the exposure evolution, the algorithm has been executed, for all the configurations, 100 consecutive times (time units) modifying the value of the accumulated exposure according to the routes selection. This way, the nodes belonging to one route during the T time units of the experiment will present a value of accumulated exposure εT. Besides, in order to ensure the statistical validity of the results, 100 independent experiments of each configuration are performed. It is assumed that the cost associated to the transmission power is proportional to the power and this, in turn, to the distance between the nodes, with maximum value of 16 dBm. Thus, with a maximum coverage range of 15m, the cost of an edge (i,j) can be expressed as $P_{ij} = \frac{d_{ij}}{15}$, where d_{ij} corresponds to the distance between the nodes. On the other hand, the exposure induced by each traffic flow during a time unit increments the value of K in 5 units; this value has been arbitrarily selected so that the exposure cost is in the same range as the power cost, a finer value selection will be used in future studies.

First, we have analysed the accumulated exposure of the different nodes during one experiment by comparing the performance of the proposed algorithm with those obtained with the minimum power one. **Figure 49** and **Figure 50** show the probability density function of the exposure of the nodes for both algorithms, using the topology α with 2 and 4 traffic sources respectively. The value εT corresponds to the exposure accumulated in a node that would belong to one route during the experiment duration T (in our case 100 steps), while multiples of that value reflects situations in which a node took part of more than one route. As can be observed, the algorithm of minimum power, which has a temporal static behaviour, only presents probability greater to 0 in the multiples of εT. On the other hand, the proposed algorithm is able to balance the exposure; the highest improvement is the probability that a node belongs to one route continuously. In the case with 2 traffic sources, the reduction of this probability is around 30%; while in the scenario with 4 sources, more nodes are generating exposure, so the gain is slightly lower, around 20%.

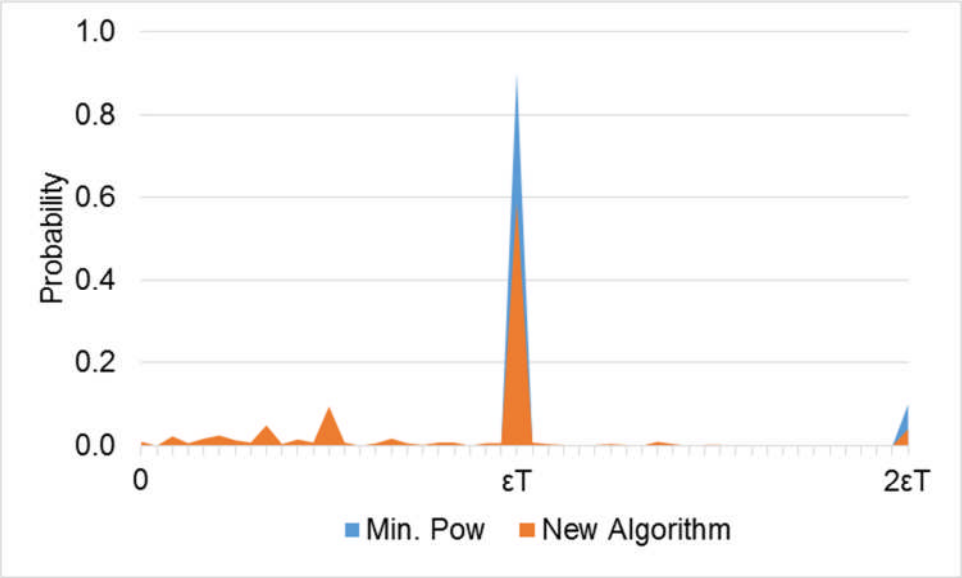

Figure 49: PDF of the exposure of each node in topology α with 2 traffic sources

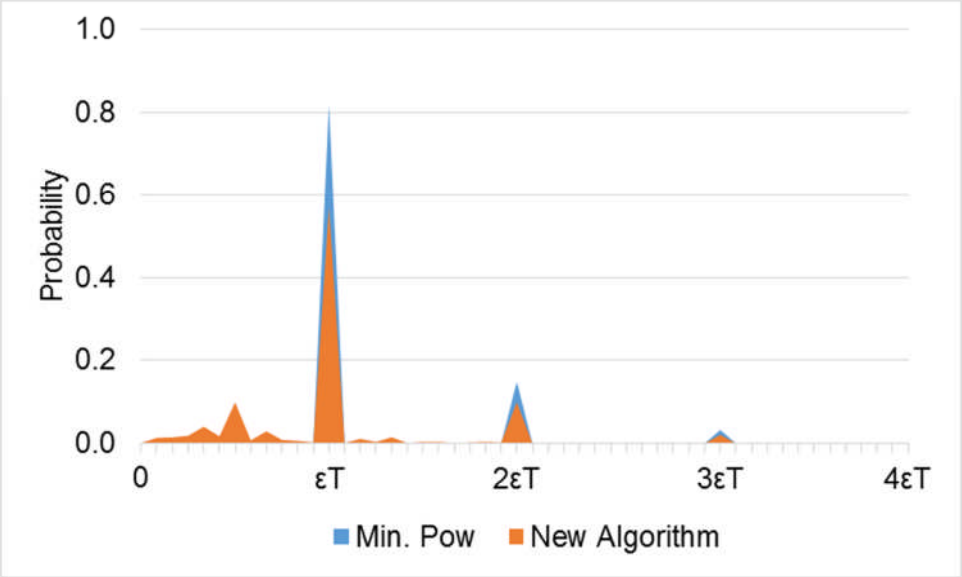

Figure 50: PDF of the exposure of each node in topology α with 4 traffic sources

Once the effect of the algorithm over the exposure is studied, the analysis has been extended in order to consider different topologies and traffic loads. In this sense, **Figure 51** shows the average value of the exposure after 100 independent experiments. According to the results, the benefit of the proposed algorithm, when compared with one that minimises the transmit power, decreases as the network density is reduced. It is due to the fact that the algorithm requires alternative routes in order to hand the traffic flow over a different destination, what is achieved when the network density is higher. Hence, when the network density decreases, it is less likely to find an alternate route. The figure shows that the gain with the less dense topology (δ) is notably lower to the one obtained with the most dense scenario (α). However, the influence of the number of traffic sources does not seem to be as relevant, since its impact on the value may be considered negligible.

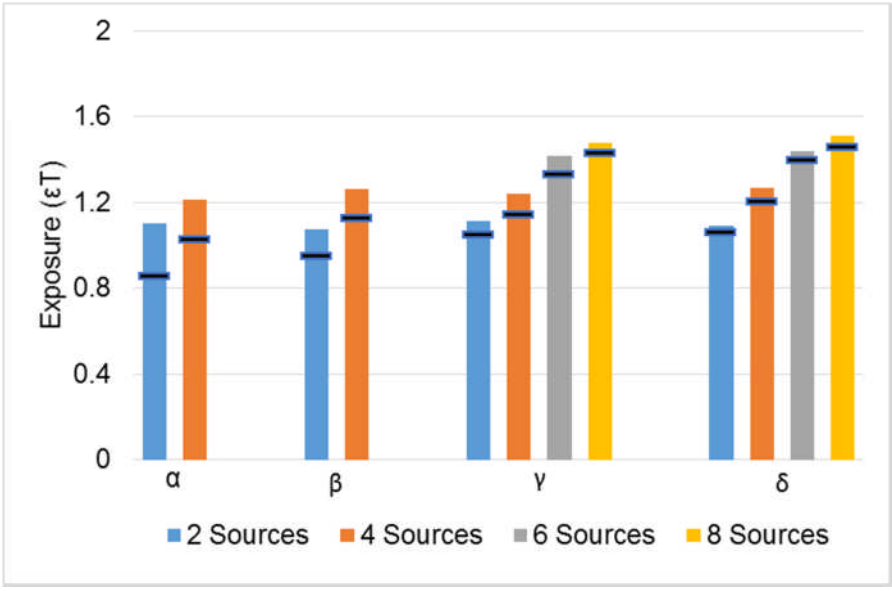

Figure 51: Average exposure per experiment. The markers indicate the value of the proposed algorithm, while the bars show the value of the minimum power algorithm

Taking into account that the exposure generated by the whole network is directly related to the total transmitted power, the algorithm characterisation also includes the study of the transmitted power and its comparison with the optimum one. In this case, we have calculated the transmitted power in the same way as the P parameter, so proportional to the distance as described above.

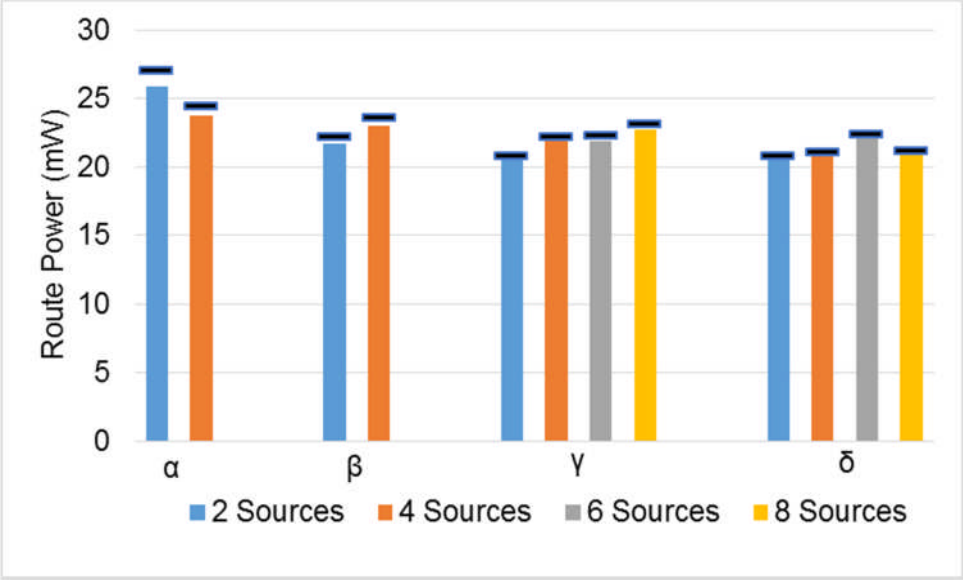

Figure 52: Average power per route. The markers indicate the value of the proposed algorithm, while bars show the value of the minimum power algorithm

The behaviour of both algorithms in terms of transmitted power is shown in **Figure 52**, which represents the average value of the necessary transmission power of all the routes created. It is worth highlighting that, while the minimum power algorithm does not change the routes along the experiment, the proposed solution might do it, so that it is necessary to consider the time a route remain active. In general, it is

shown that a small penalty, in terms of power, exists when using the proposed algorithm. This penalty becomes more irrelevant as the network density increases.

Considering both results, we reach the conclusion that, for this type of static networks, the higher the accumulated exposure gain, the higher the penalty in terms of transmission power.

6.2.3.2 Dynamic configuration

This section studies the behaviour of the algorithm in more complex scenarios where the set of sources is modified during the same experiment. In particular, we now focus on a scenario of size $140\text{x}140\ m^2$ with 9 gateways forming a grid. Besides, 50 nodes, with 15m of coverage range, are randomly deployed from which 4 traffic sources are randomly selected.

In the same way as in the previous study, experiments of $T = 100$ temporal steps are executed, in which the set of sources is modified every 35 steps. Again, the accumulated exposure due to one traffic flow during one time unit is ε. Unlike the previous study, in this case we study the relation between the costs given to the transmitted power and the accumulated exposure. The results brought about by this study may be, afterwards, used to tweak both parameters in a real routing protocol. In this sense, assuming that the cost related to the accumulated exposure is always growing, at some point the criterion of minimising the power would be negligible compared to the accumulated exposure one, hence the former would not have any effect in the routes selection.

The influence of the costs, K (exposure) and P (power) relation, has been analysed in two different ways: first, the power cost P remains constant while the value of K has been modified; secondly, we have studied the algorithm behaviour when an *aging* function is applied to the K value, so that this value decreases when the node is not taking part in any active route. The second approach aims at studying the influence on the overall behaviour of the growing of the K parameter; in this sense the *aging* will foster the use of those routes that have not been selected recently.

Table 40: Costs description of dynamic configuration

Cost parameter	Value
P	distance (m)
ΔK	$\{3,6,9,12,15\}$
∇K	$\{0, \dots, \Delta K\}$

Table 40 summarises the different configuration that have been studied, where the value of P corresponds is computed in the same way as in the previous section. Regarding the K exposure parameter, it is calculated as the value in the previous step plus an increment ΔK for each active route the node belongs to; if a node does not participate in any route, this cost is decremented an amount ∇K. As can be seen in **Table 40**, the values utilised for ∇K are always lower than the ΔK values, besides it is ensured that the K cost is never below 0. Again, 100 independent experiments of each configuration are performed.

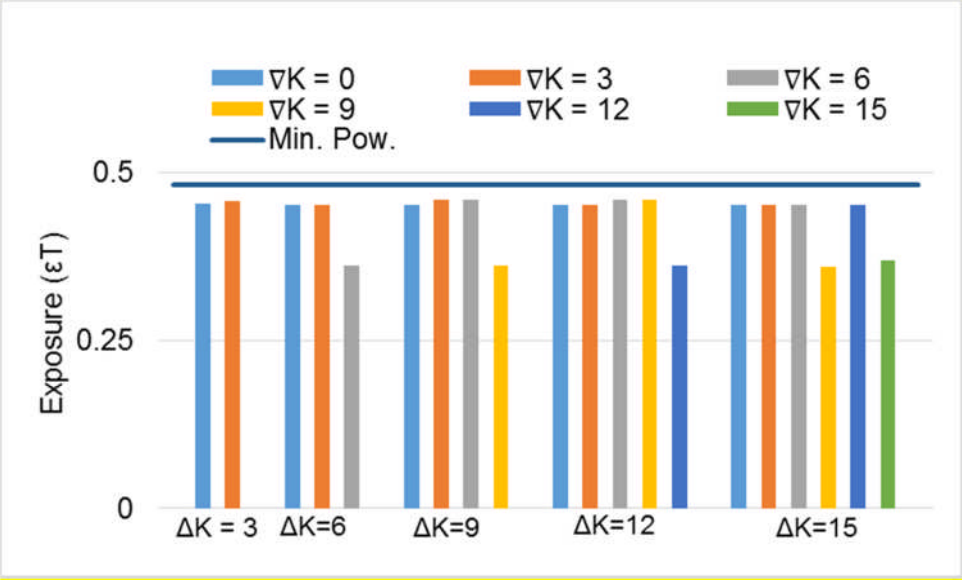

Figure 53: Average accumulated exposure at each node after the experiment. The line indicates the result of the minimum power algorithm, while bars show the result obtained with the proposed algorithm

Firstly, we have studied the exposure by following the same procedure as in the previous section. **Figure 53** shows the average value of this power metric for each configuration. In this case, if a node takes part in the 4 active routes during all the experiment, its exposure would reach a value of $4\varepsilon T$. As it can be observed in **Figure 53**, the fact of varying the sources along the experiment reduces the gain in terms of exposure, compared with the performance seen in the previous study. Nevertheless, the results reflect that the *aging* function has a positive effect, since it makes it possible to re-select routes with fewer hops, which in turn reduce the exposure. Furthermore, according to the results, it seems that the cost related to the exposure had a value relatively high compared with the one related to the power. In particular, for a maximum value of $P = 16$, the value of ΔK should be no lower than 6.

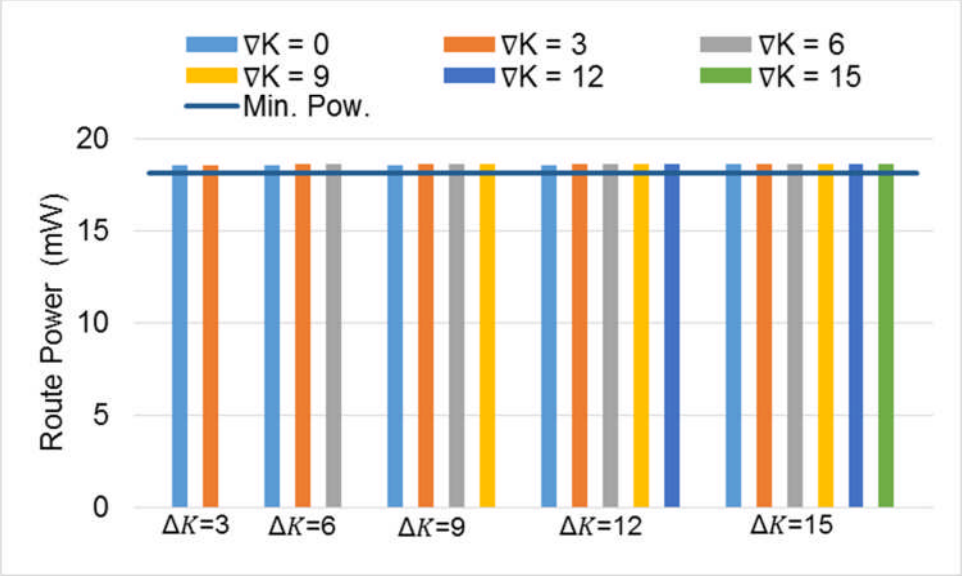

Figure 54: Average power per route. The line indicates the result of the minimum power algorithm, while bars show the value obtained with the proposed algorithm

On the other hand, the influence of the algorithm on the transmission power has been analysed again. **Figure 54** illustrates the average value of the transmission power per route and time unit, for both the proposed solution and the minimum power algorithm. It can be observed that, with more dynamic scenarios, the different configurations present almost the same performance and the average penalty in terms of power is very low.

7 OFFLOADING TECHNIQUES FOR REDUCING THE EMF: THE IMPACT OF WI-FI OFFLOADING ON EMF EXPOSURE

Wi-Fi offloading is evaluated by the LEXNET partners with three complementary simulation tools running on a common dense urban scenario:

1. Coverage-based predictions, from which preliminary results are reported here below;
2. Access network discovery selection function simulation for decision on offloading strategy and core network traffic optimisation;
3. Dynamic system-level simulations.

The first approach tackles the offloading issue from the operator angle, so that realistic decision strategies, in terms of real decision parameters, are implemented. Along with it, the second approach brings the possibility of using a higher abstraction level to study the overall behaviour of the network when using different access policies; this abstraction also allows posing optimisation problems to which the results of a particular policy can be compared to. The simulations in the third tool are performed following radio-planning techniques yielding accurate SINR calculation, as well as the 3D static maps that are used to estimate the received field, UL transmit power and throughput, which allows an accurate estimation of both DL and UL EMF statistics.

The main idea is to complement the results of one tool with the others in order to analyse the same problem from different perspectives. In this section, some preliminary results of the second and third tools are shown so as to illustrate the type of results each tool can bring about and how they can complement each other.

The results concerning the coverage-based predictions are presented in Section 7.1, in which both the overall methodology and some results are depicted. Next, Section 7.2 introduces the analytical tool that carries out dynamic system-level simulation, paying special attention to the network technology models and showing some initial results obtained so far.

7.1 Coverage-based predictions

The simulations in the first tool are performed following radio-planning techniques; they rely on a real urban environment (a district of Paris) and deterministic propagation loss predictions. The simulation process is an extension of the femto-cell and small-cell evaluation methodologies that were respectively reported in [Letourneux 2013][Letourneux 2013] [Letourneux 2013] and [Stephan 2014], tackling the impact of offloading on EMF exposure and user QoS. Different offloading strategies are introduced to predict the traffic distribution into both LTE and Wi-Fi layouts. The final evaluation results will be reported (later this year) in [LEXNET D6.2] (WP6 deliverable), but some intermediate conclusions are presented here and give a first interesting insight into the expected cellular network EMF reduction.

7.1.1 Scenario and methodology

Initial scenario relies on a realistic macro layer composed of 19 sites with tri-sector base stations. Locations of these sites in the high-resolution geographical map data in Paris downtown reflect real dominant configurations with an ISD of 450 m in the 0.98 square km study area. Macro eNBs are deployed over a larger area, on two rings around a central three-sector site in order to take into account realistic interference patterns. Wi-Fi AP's are dropped randomly inside the buildings. The network selection and resource allocation mechanisms are predicted with simple abstraction models.

The coverage tool makes use of deterministic propagation prediction from ray-based Volcano propagation model to obtain in-street and 3D in-building path losses. The framework integrates a static Inter-Cell Interference Coordination (ICIC) Fractional Frequency Reuse (FFR) scheme to mitigate DL interferences in macro network. The ICIC scheme is defined by a re-use factor of 3; and 5% of total radio resources are being allocated to each FFR sub-band.

The user traffic is modelled by a single profile and a 3D heterogeneous spatial distribution with the following rules:

- 600 active users/square km.
- 20% outdoor users, uniformly distributed over the area.
- 80% indoor users, uniformly distributed in the building floors (meaning that the number of users in a building is proportional to its height).

Initial user traffic conditions lead to an interference limited macro network without considering small-cell or Wi-Fi APs densification as studied in [LEXNET D5.1]. In this study the indoor layer will be mainly constituted of Home Wi-Fi APs, which are now often deployed with an open access (depending on the operator policy) and are listed in cellular operator's database. Public Wi-Fi APs may also be included although they are quite outnumbered by Home APs. At the present stage, the Wi-Fi layer is modelled in a very simple way, by considering that an access is always available for any user in terms of coverage and radio resources. Main outputs are SINR calculations and 3D static result maps (for DL received field, and throughput) that lead to the calculation of statistics, and thus to the joint QoS and EMF characterisation of a given offloading strategy.

7.1.2 Evaluation of different offloading strategies

In the following we evaluate the impact of two different offloading policies:

1. The first policy consists in offloading a proportion of the traffic to the Wi-Fi layer without taking into account the user QoS. This policy may be considered close to what ANDSF offers when the network selection only relies on the type of service that is requested by a user.
2. The second policy offloads the users depending on their experienced cellular QoS, i.e., users with the poorest LTE SINR are requested to switch to Wi-Fi, regardless of their running application.

The completed evaluation study will make a comparison of mixed policies considering both the application and radio conditions. Therefore, the simulated policies reported here may be viewed as two extreme cases.

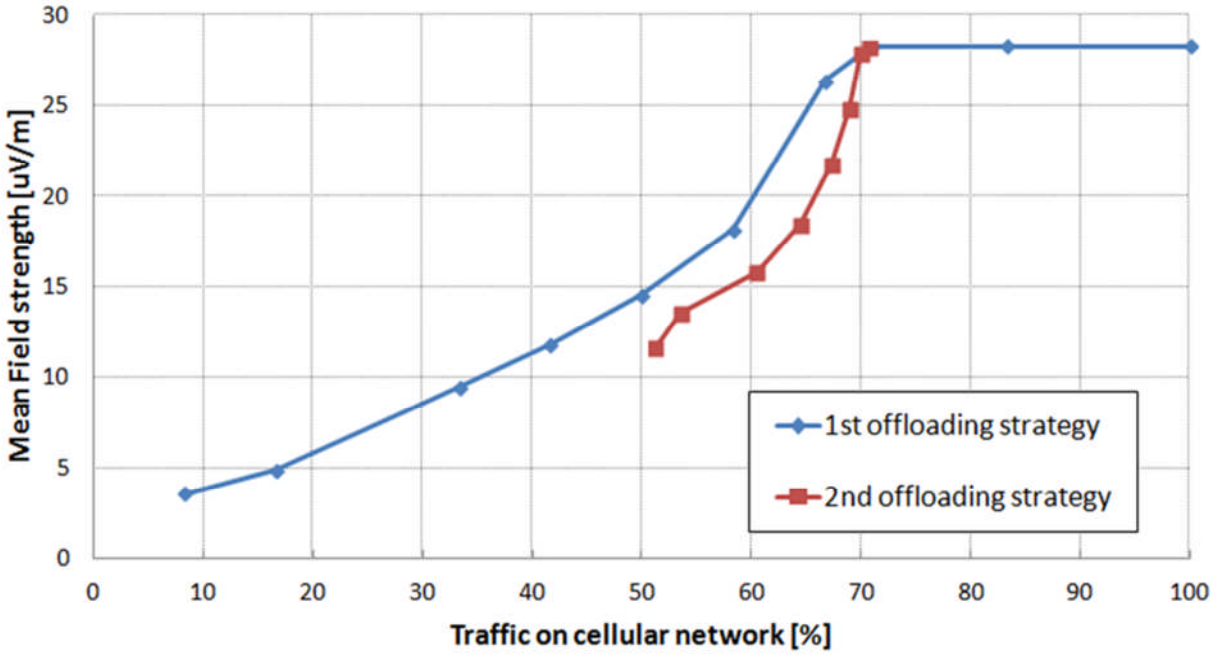

Figure 55: Mean Field Strength with percentage of traffic on cellular network

In **Figure 55** the relationship between EMF exposure and traffic offloading happens not to be linear. The x-axis represents the percentage of traffic that remains in the LTE layout (the offloading ratio is 1 – x). **Figure 56** shows on the secondary y-axis the percentage of users served with success; for instance, 95% of users are served when 70% of total user traffic is absorbed by the cellular network. When decreasing the cellular traffic ratio from 100% to 70% (i.e. low offloading) we observe an almost constant EMF exposure on **Figure 55** but with a higher success rate on **Figure 56**. This is a consequence of the initial traffic condition that was selected for the study, as the cellular network cannot serve more than 70% of the total traffic amount. Then the EMF exposure rapidly decreases when the cellular traffic ratio is going from 70% to 50%, as the traffic decrease both reduces the requested cellular resources and the interference levels. Finally, the EMF exposure becomes proportional to the cellular traffic at lower levels.

The second strategy in which users having the worse SINR are offloaded in priority shows that for the same proportion of traffic on cellular network, EMF exposure is lower. This can be seen as an ideal case from the radio point of view, the reality probably being in the middle of both first and second strategies regarding all metrics of interest in the Wi-Fi offloading context (guaranteed QoS, pricing, etc).

We also observe in **Figure 56** that for similar proportion of traffic on cellular network, the cellular remaining users experience better DL throughputs.

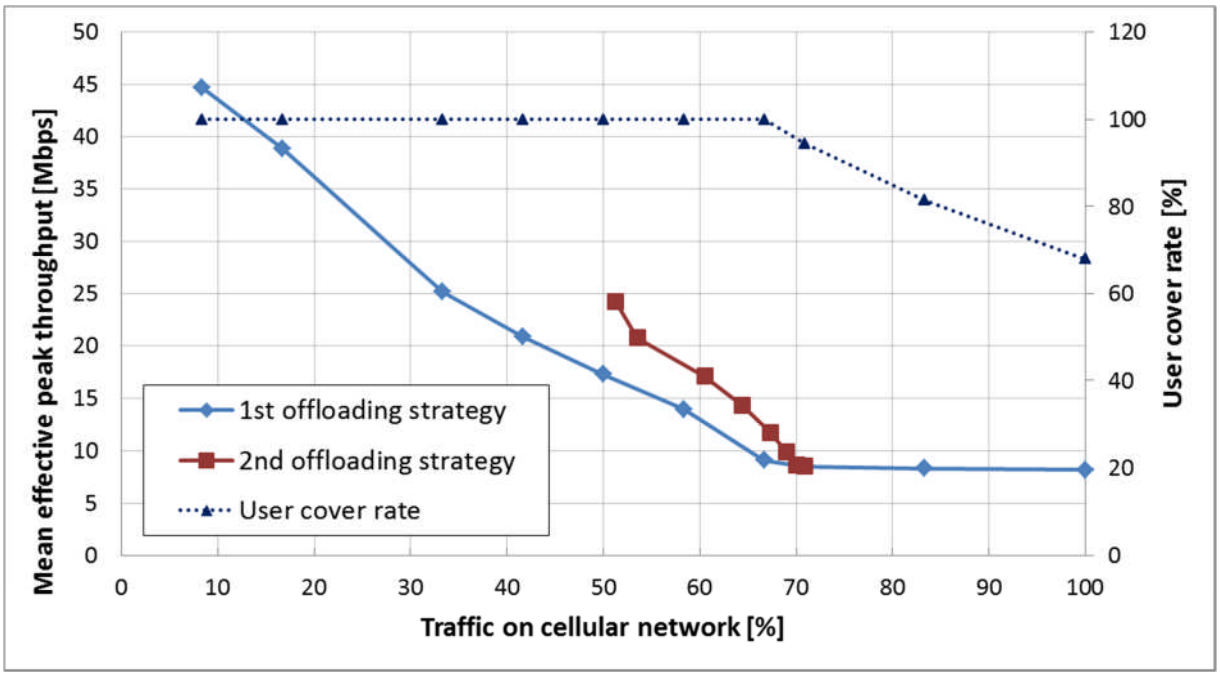

Figure 56: Mean Effective Throughput with percentage of traffic on cellular network

7.2 Dynamic system-level simulations

This section describes the model that has been considered when implementing the analytical tool to perform system-level simulations, for both LTE and Wi-Fi technologies. Before depicting how we have implemented the two technologies, it is worth describing the basics of the framework. Following a discrete time operation, the tool is fed with periodic snapshots of the scenario and, for each of them, it executes an access selection. Those instances contain both the current position of the users and the activity of the services, according to the particular mobility and service patterns. Once the snapshot is loaded, the framework is able to retrieve the connections that are established between users and access elements, following either a particular access selection policy or the outcome of an optimisation problem. In this sense, this approach can be used to compare various access selection policies or to rank them, based on the optimum performance.

This type of analysis requires a relatively high level of abstraction, and some of the results, which the tool is able to offer, are not as accurate as those obtained with radio-planning techniques. The integrated models strongly focus on the power transmitted by different network elements, either LTE eNBs or Wi-Fi APs, to the users; thus, we analyse the downlink component of the EMF exposure. Although the transmit power of different technologies might not have the same impact over the EMF exposure (specially due to the different coverage patterns), the downlink exposure of each technology has a direct relation to its corresponding transmit power, and the exposure induced by an access element can be thus calculated by applying a scale factor to such power. This factor would depend on the particular technology under consideration, as well as on its configuration (for instance, if using sectorisation).

Since there exist clear differences between the two technologies, we have modelled them from different perspectives. In the case of LTE we propose a model that manages the resources on the eNBs, while the statistical Wi-Fi model is based on the distance. In both cases we are able to estimate the transmission power of each network element satisfying the traffic demand of the users, according to the access selection criteria and policies; the traffic demand of user i will be referred to as D_i.

7.2.1 LTE model

The LTE model is based on the management of the resources at the cellular base stations. These are allocated to the users according to their traffic demand and the efficiency of the link between the cell and the user equipment. In this sense, one of the most relevant aspects is how to derive the SINR. We consider a LTE reuse factor equal to 1 and that there is not any cooperation between them, so that all the base stations in the scenario, but the one providing the service, are considered as interference sources.

We define $\mathcal{U}$ and $\mathcal{B}$ as the sets of users and LTE cells, respectively. We assume that each LTE cell j manages a total number of physical resource blocks tot_{RB_j}, to which the same power PRB_j is allocated. We also assume that the resource blocks of all the cells have the same bandwidth BW_{RB}. In addition, we define the SINR of user i when connected to LTE cell j as

$$SINR_{ij} = \frac{\gamma_{ij} P_{RB\,j} N_{Rb\,ij}}{N_{ij} + I_{ij}} \tag{15}$$

where $N_{RB_{ij}}$ is the number of blocks allocated to user i. The parameter γ_{ij} considers path-loss, shadowing, and fast fading, between user i and eNB j. Finally, N_{ij} and I_{ij} are defined as the noise and interference received powers, respectively. N_{ij} can be considered as proportional to the bandwidth allocated to that user and can be therefore expressed as $N_{ij} = N_0 N_{RB_{ij}} BW_{RB}$, where N_0 corresponds to the noise spectral density.

In order to calculate the interference, we assume random scheduling and the same amount of resources in all cells. Under this assumption, interference appears when the same physical resource block is allocated by the serving and interfering cells. If we denote the total number of resource blocks at cell k as $Ntot_{RB_k}$, the probability that a resource allocated to user i by cell j is interfered by a block allocated by cell k can be expressed as $\frac{1}{Ntot_{RB_k} Ntot_{RB_j}}$. Bearing this in mind, the interference power $I_{RB_{ik}}$ of such block can be expressed as

$$I_{RB_{ik}} = \frac{1}{Ntot_{RB_j}} \cdot \frac{P_{RB_k}\,\gamma_{ik}}{Ntot_{RB_k}} \tag{16}$$

where γ_{ik} accounts for the propagation between user i and the interfering cell k.

All in all, the total interference perceived by user i when connected to cell j, from all the interfering cells in the scenario, is defined as shown below. This expression indicates that the interfering power is proportional to the amount of resources $N_{RB_{ij}}$ allocated to the user (i.e. it considers the bandwith used for the connection) and to the total power transmitted by the interfering cells ($N_{RB_{km}}$).

$$I_{RB_{ij}} = N_{RB_{ij}} \cdot \sum_{k \in \mathcal{B}/j} I_{RB_{ik}} \sum_{m \in \mathcal{U}} N_{RB_{km}} \tag{17}$$

Finally, the SINR of the association between user i and cell j is finally calculated as shown in **(18)**. As can be seen, the SINR does not depend on the number of resource blocks that are allocated to the user, but it does to the power transmitted by the interfering cells.

$$SINR_{ij} = \frac{P_{Rj}\,\gamma_{ij}}{N_0 BW_{RB} + \sum_{k \in \mathcal{B}/j} I_{RB_{ik}} \cdot \sum_{m \in \mathcal{U}} N_{RB_{km}}} \tag{18}$$

Once we know the SINR, we can derive the spectral efficiency of each potential connection using a modified version of the Shannon-Hartley's channel capacity formula [Mogensen 2007], as can be seen below

$$S_{ij} = BW_{eff}\eta \, \log_2\left[1 + \frac{SINR_{ij}}{SINR_{eff}}\right] \tag{19}$$

in which BW_{eff} and $SINR_{eff}$ are correction factors that include the system overhead and the adaptive modulation and coding effect. With this, the number of resource blocks that are allocated to user i by the selected cell j is calculated so that the user demand is satisfied: $D_i = N_{RB_{ij}} \cdot BW_{RB} \cdot S_{ij}$. Finally, the power transmitted by an LTE cell j on its connection with user i is calculated as shown in **(20)**.

$$P_{LTE_{ij}} = N_{RB_{ij}} \cdot P_{RB_{ij}} \tag{20}$$

It is worth highlighting that the proposed model does not directly depend on the specific system parameters, and it might therefore be used for different scenarios and configurations.

7.2.2 Wi-Fi model

Unlike LTE, current Wi-Fi technology does not allocate resources to the different users, who contend to use the shared wireless channel. In this case, we proposed a statistical model, based on the distance between the user and the AP. In particular, we estimate the raw data rate DR that a user might obtain from an AP, according to the particular distance between them and the probability of having a line-of-sight link. According to the study presented in [Coll 2013], the data rate of 802.11g, in outdoor scenarios, can be modelled with the mathematical functions that are shown below

7.3 $DR_{NLOS}(p_1, p_2, d) = A \cdot \left[1 - \frac{1}{1+e^{-p_1(d-p_2)}}\right]$

$$DR_{LOS}(p_1, p_2, d) = \begin{cases} A & d < p_1 \\ k \cdot \left(\frac{1}{d} - \frac{1}{p_2}\right) & p_1 \leq d < p_2 \\ 0 & d \geq p_2 \end{cases} \quad (21)$$

where A is the maximum data rate supported by the AP (54 Mbps for 802.11g), d is the distance between the user and the AP and both p_1 and p_2 are parameters that are fixed according to the scenario.

In this case, we define the time that a user is using the shared channel as the basic resource from a single AP. If DR_{ij} is the maximum data rate at which user i could be connected to AP j (depending on the distance between them), and D_i is the traffic demand of such user, the percentage of time the corresponding connection (when the AP is not available for other users) will be active can be calculated as $\frac{D_i}{DR_{ij}}$. Finally, we can calculate the power transmitted by AP j to user i as defined in **(22)**, where P_{t_j} represents the nominal transmit power of the access point (typically 20dBm).

$$P_{WiFi_{ij}} = P_{t_j} \frac{D_i}{DR_{ij}} \quad (22)$$

7.3.1 Model validation

This section discusses some preliminary results that were obtained with the analytical framework proposed in this work, so as to illustrate how it complements the analysis that we might expect from radio-planning tools. Before we describe the scenario that will be used to carry out the analysis, we introduce the system parameters that have been used.

7.3.1.1 Scenario of interest

For the LTE network deployment, we consider eNBs with 3 sectors and reuse factor 1. Each cell (sector) has a bandwidth of 20MHz, corresponding to 100 physical resource blocks of 180 KHz each. Besides, we consider a maximum transmission power of 43 dBm, a transmission gain of 18 dBi and a noise figure of 6 dB. The antenna pattern and propagation models are those defined by the 3GPP specifications for system based simulations [3GPP TS 36.814]. Furthermore, we consider a lower bound for the SINR of −10 dB; below this value, we assume the signal to be too low and therefore the cell is deleted from the candidate list. Last, the maximum spectral efficiency has been fixed to 5 bps/Hz.

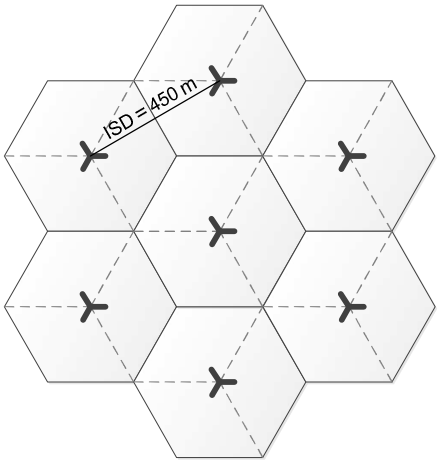

Figure 57: Cellular network deployment, transmission power of each antenna is 43 dBm

The deployment of the base stations follows an hexagonal pattern, as depicted in Figure 57, where the ISD is 450 m, covering an overall surface of $1350 \times 1350\ m^2$.

Concerning the Wi-Fi layout, the maximum data rate DR_{ij} is calculated by a step-wise function according to the distance model previously described (Section 7.2.2); in this sense, and based on the distance between user i and AP_j, we estimate DR_{ij}. Furthermore, we scale it by 0.5, accounting for the overhead of the lower layers. The number of available APs is modified in the different studies.

In order to assess the flexibility of the tool, we consider different types of users and services, as shown in Table 41. Each of the services follows an ON-OFF model, while users move according to a random waypoint model with a speed that is randomly selected within $[1,3]\ m/s$. It is worth highlighting that those services interrupted due to lack of connectivity, are not considered in the following, until the time the original service was scheduled to finish. The framework can establish certain rules; in this particular study, we assume that users of type 3 are not allowed to connect to the Wi-Fi network since the traffic load of the services of this user type is the lowest. On the other hand, the rest of users would first attempt to connect to a Wi-Fi AP, and, only if this is not possible, would connect to a LTE cell.

Table 41: Configuration parameters of users and services

Services	**Type**	**Traffic (Kbps)**	**ON (sec.)**	**OFF (sec)**
	Video (V)	1000	300	1200
	Internet (I)	128	60	80
	Enterprise (E)	128	90	120
Users	**Type**	**Services**	**Amount (%)**	**Access**
	1	V+I	20	All Networks
	2	I+E	10	All networks
	3	E	70	Only cellular

For this scenario, we have analysed 360 snapshots, generated every 10 seconds, according to the aforementioned models; thus the overall analysis lasts for 1 hour.

7.3.1.2 Experimental results

Figure 58 shows the power transmitted by the whole network. As can be seen, the deployment of a different number of APs does not have a strong impact over the total transmission power, at least for the access policy we have considered.

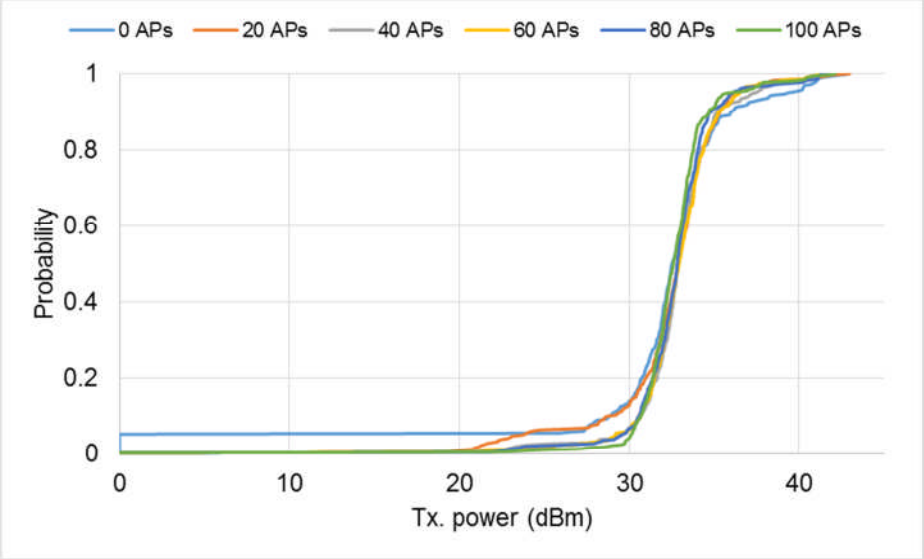

Figure 58: CDF of the total power transmitted by the network

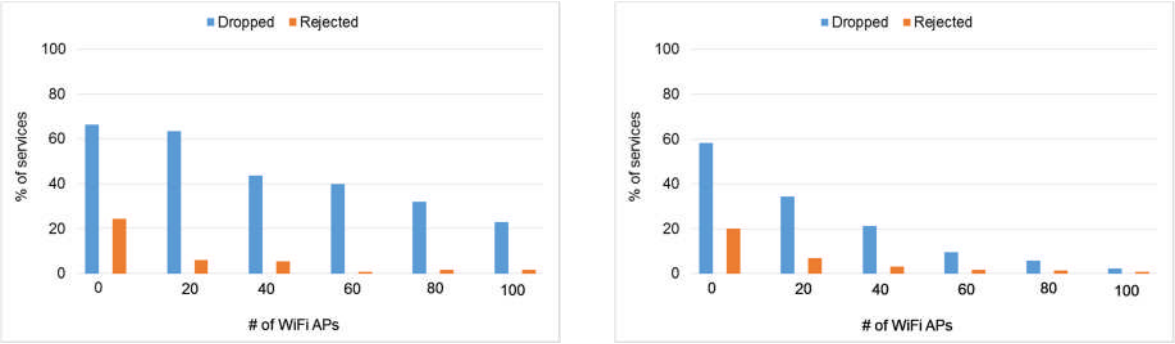

(a) Video

(b) Enterprise

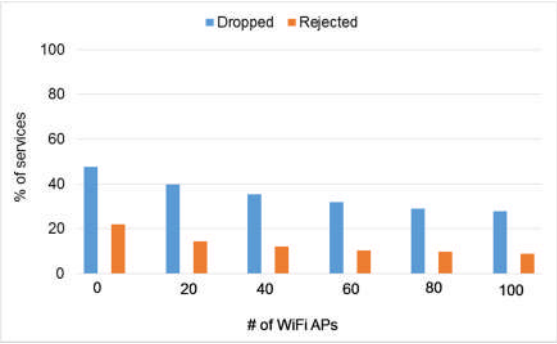

(c) Internet

Figure 59: Services dropped and rejected vs. the number of Wi-Fi APs in the scenario

In order to see the influence over the QoS parameters, **Figure 59** represents the percentage of services that are rejected (not initiated) and dropped for the various configurations. The results show that if the number of Wi-Fi APs is increased, the probability of interrupting services gets lower. It is important to point that the main reason to reject services is the low SINR that users might suffer if they are close to the cell edge. In this case the influence of the larger number of deployed APs is clearly visible in the observed results.

Another aspect worth highlighting is the different behaviour observed for the various services and, in particular, Internet services. A relevant percentage of them (70%) are not allowed (policy) to use the Wi-Fi network and as a consequence, the number of interrupted services is not affected by the number of APs; however, for the other service types, the figure yields a clear benefit of increasing the number of APs.

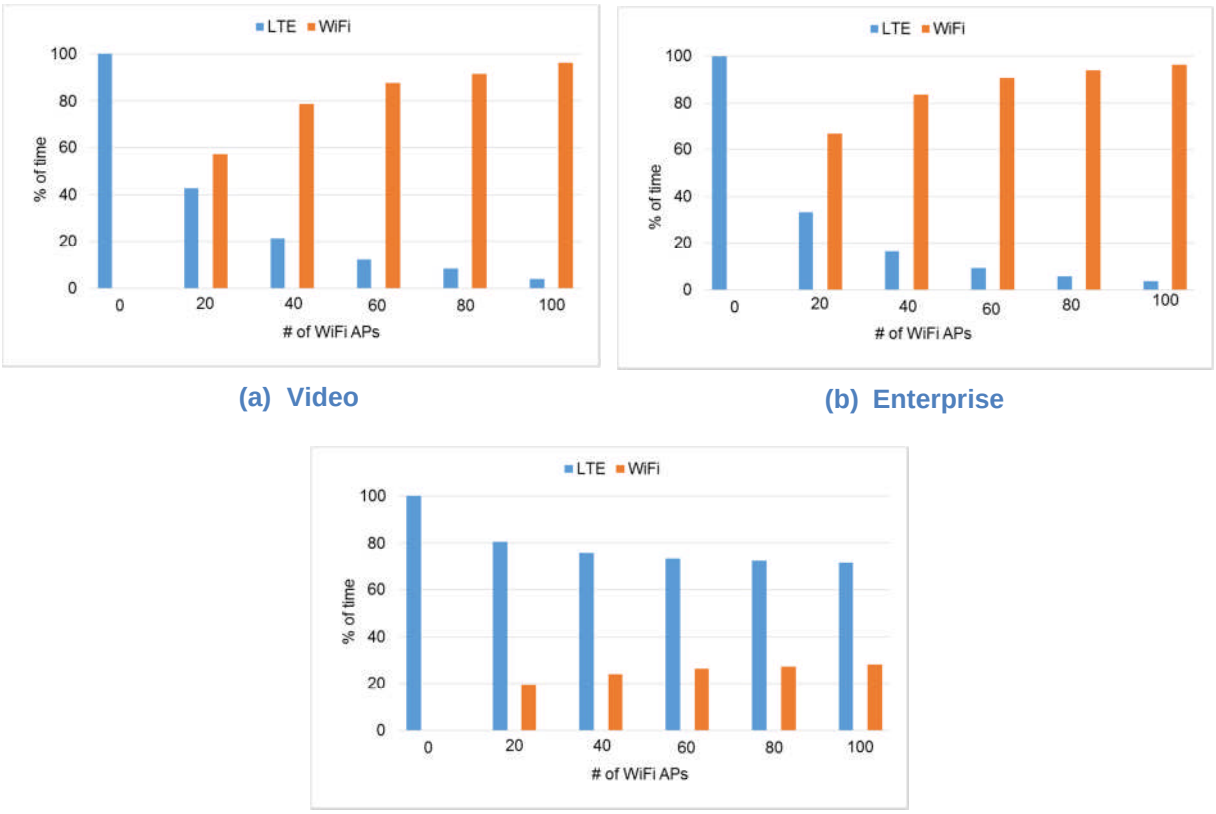

(a) Video

(b) Enterprise

(c) Internet

Figure 60: Percentage of time in each technology vs. the number of Wi-Fi APs in the scenario

Finally, we have also assessed the appropriate operation of the access policy. In this sense, **Figure 60** shows the percentage of time that different services are connected to each of the two available technologies; this metric includes as well the time that the services dropped when connected. For the Video and Enterprise services, the figure yields that they connect to the Wi-Fi network as soon as APs become available. In fact, for the scenario embracing 40 APs, more than 80% of these service types connect to Wi-Fi. On the other hand, we can see that the simple access policy used modulates the behaviour of the Internet services; although they tend to connect

to Wi-Fi networks as soon as they become available, there is still a relevant number of them that keep using the LTE connection, as a consequence of the users not allowed (policy) to use Wi-Fi networks; this leads to a worse QoS of this service type, as was shown in **Figure 59**, since it service suffers from a larger reject probability.

This preliminary analysis shows the potential of the proposed methodology and framework. Although the transmitted power values are not as accurate as those that might be obtained with radio-planning tools, the evolution that was observed for the services provides valuable information to better understand the impact that a particular access policy might have over the overall network behaviour. Furthermore, the framework would allow broadening the study with various access policies, comparing them with the optimum performance (outcome of the optimisation problem).

7.4 Concluding remarks

Those preliminary results will be complemented in the framework of WP6. A joint analysis of three simulator results will be reported later in order to assess several Wi-Fi offloading policies that could be implemented at network level (those strategies differ in terms of target offloading volume and network selection criteria), comparing the impact onto the network performance, user QoS and EMF levels.

The workflow will make it possible to consider different offloading strategies that may be configured through the ANDSF. Analysis of network information will help identifying average user profiles (services, location and RAT) and network maximum throughput for different time slots. User QoE may also be improved thanks to a mobility manager and the improvement of IEEE 802.11u, which prevent users to connect to an AP if radio conditions are not sufficient. The repartition of users on the different networks will then be done depending on channel conditions and interferences on both 3GPP and non-3GPP layers but also on cell loads. The evaluated policies still must be clearly specified. The process would finally provide the policy to be considered by users to manage in real time the different services requests.

The scenario will be enriched in the coverage-based simulator to include three additional contributions that are missing right now but are necessary for a complete evaluation: the prediction of LTE UL characteristics (throughput, and mean transmit power); a more realistic Wi-Fi layout and the prediction of offloaded user QoS; the assessment of EMF increase into the Wi-Fi layout (related to the higher duty cycle).

Regarding the system-level simulator, a model for indoor Wi-Fi layout will be added and optimisation techniques to reduce the EMF exposure will be studied.

8 CONCLUSIONS AND RECOMMENDATIONS

This deliverable has summarised the various achievements of WP5 towards reducing human exposure to EMF without compromising the QoS/QoE. In this regards, innovative network architectures and management procedures have been proposed, spanning from high-level planning and optimisation to low-layer protocols, and including techniques such as EMF-aware cell planning, cell association, routing, offloading, scheduling. The quantification of exposure being another key contribution of the LEXNET project as well as being very important for showcasing the EMF reduction capability of the WP5 schemes, this deliverable has provided guidelines on how to use the EI assessment framework of WP2 in the context of WP5. Indeed, given that the EI metric is a long-term per-area metric and that network management metrics are usually short-term per-user metrics, some interfacing is required to effectively assess the EMF exposure of network management techniques via the EI metric, as it has been reported in Section 2. In this regard, Section 2 has provided an EI evaluation methodology for WP5, which is composed of three steps (applicability of life segmentation data, traffic model, and relation between EI and WP5 technologies) corresponding to the EI generalised scenario of WP2.

By relying on this EI evaluation methodology, Section 3 has also showcased EI performance of Hetnet (GSM, UTMS, or LTE with Wi-Fi systems) systems when considering different scenarios, varying usage, mobility, number of users, etc., in order to better comprehend the impact of exposure on different systems configurations and users' behaviours. In a single macro-cellular scenario, results have shown that UMTS has a much lower exposure value, compared to the other systems. Moreover, given that UMTS is based on CDMA technology, its exposure performance is more sensitive to variation in the number of users. The results also indicated that the type of service does not have a large influence on the system performance. Interestingly, it was also demonstrated that power control has a major impact on the EI values. More interestingly, simulations have also shown that the uplink from the users' terminal is responsible for over 90% of the EI, when the user is either making a call or using a data connection. In order to complement these simulations results, real-network measurements assessing the impact of the services used, technologies and radio conditions for legacy systems and cell offloading have been conducted. Results have indicated that addition of the micro cell layer causes a significant increase in downlink EMF exposure. Whereas in the uplink, introducing a micro layer, i.e. by bringing the base stations closer to the users, can reduce the exposure of GSM voice service usage by more than 40%.

In Section 4, novel short and long-term EMF-aware radio resource management techniques have been developed for both uplink as well as downlink setups. Firstly, an optimum EMF and QoS- aware cell association scheme that jointly considers DL and UL exposure has been proposed for a HetNet scenario. Results have indicated that the proposed scheme achieves high resource utilisation while enhancing the user satisfaction through an optimised load balancing. This improved load balancing reduces the number of per user allotted frequency resources, which in turn reduces the EI. It has also been remarked that further increase in the user satisfaction is linked with cell selection patterns that yield higher EI. Secondly, two novel EMF-aware scheduling schemes have been designed for the uplink of cellular systems and

downlink of HetNet systems, respectively. The former minimises the EMF exposure of each individual user subject to a QoS target, whereas the latter uses coordination between tiers to reduce the downlink EMF exposure. Results have shown that the uplink and downlink scheduling schemes can drastically reduce the uplink and downlink EMF emission (by a factor 1000 and 100 respectively), when compared to SotA schemes.

The trade-off between EMF exposure reduction and user QoS/QoE has been studied in Section 5 for both cellular and Wi-Fi systems. Firstly, a novel transport selection algorithm has been proposed for video streaming services (in particular based on the DASH protocol) while achieving a trade-off between EMF exposure reduction and QoE. It is based on a cross-layer solution where the video representations as well as the transport protocol are selected according to the bandwidth that is estimated by the network. The results have demonstrated that the use of UDP instead of TCP can reduce the EMF exposure, ensuring a more efficient usage of network resources in hostile conditions. Indeed, UDP has a straightforward gain, since it does not require any traffic in the uplink (as it would be the case of the TCP acknowledgments). Secondly, an optimisation framework including realistic audio metric as well as real time exposure measurement capability has been developed for achieving the best EMF vs. audio quality trade-off with low-complexity in a Wi-Fi conferencing scenario. Results have indicated that the proposed MOSBO multi-optimisation toolbox provides the best possible EMF, audio quality and their associated input parameters, as compared to an exhaustive searching experiment. However, it does so by reducing the computational complexity (execution time) by a factor of at least 150 in comparison with exhaustive search.

As far as routing is concerned, Section 6 has first provided a theoretical framework for assessing network-level EMF exposure and providing guidelines for implementing a more practical EMF-aware routing protocol, the RBRP. This framework, being protocol agnostic, can be used to evaluate the performance of different routing techniques in terms of EMF exposure. Furthermore, this evaluation can be applied to solutions able to dynamically change the transmission power. In addition, a formulation of an optimisation problem has been posed, that jointly considers the accumulated exposure and the transmission power, and an algorithm has been proposed to solve it. It can be used as a reference to assess the performance of routing protocols, and the obtained results provide valuable information to fine-tune the RBRP protocol. Due to its design, RBRP can be easily adapted to include power management, thus mimicking the algorithm behaviour. The results of this algorithm, both over static and dynamic scenarios, indicate that it is indeed able to balance the exposure. In addition, we have also seen that the exposure reduction is higher over dense static networks.

A methodology to evaluate the impact of Wi-Fi offloading on EMF exposure has been proposed in Section 7, through three complementary simulation tools. Preliminary results show that the analyses that can be carried out with the three tools are complementary between each other; the final evaluation of offloading techniques under a common scenario will be evaluated in WP6 of LEXNET. Two offloading strategies have been proposed: the first one tackles the offloading issue from the operator angle, whereas the second one brings the possibility of using a higher

abstraction level to study the overall behaviour of the network when using different access policies. Results have shown that for both strategies the EMF exposure is proportional to the cellular traffic when the load is low, whereas when the offered traffic is high, the EMF exposure reaches a maximum value and then saturates. In addition, the second strategy exhibits a lower EMF exposure than the first one. The impact of offloading has also been assessed through dynamic system level simulation. The results of these simulations have indicated that increasing the numbers of Wi-Fi APs do not have a strong influence on the total Tx power of the networks. For the various services that have been considered (video, internet, enterprise), it has also been shown that increasing the number of Wi-Fi APs decreases the probability of interrupting these services. This is however less true for internet services that are mostly not allowed (policy) to use the Wi-Fi network according to our particular scenario where moving user equipment using internet services are not allowed to manage handover between Wi-Fi and LTE in order to avoid service disruption. Finally, regarding access policy, video and enterprise services tend to connect to Wi-Fi as soon as APs become available, while this is not the case for internet services.

Based on the numerous conclusions drawn from the different works undertaken in WP5, we have come up with a set of recommendations for reducing EMF exposure without compromising QoS in future network architectures and management technique design:

- The Global EI developed in WP2 provides a strong basis for assessing the exposure for a population over a period of time nominally 24 hours. However, in order to validate the individual studies on networking technologies and their impact it was essential to break this down into sub-scenarios based on technology availability during different times during that period. A methodology was developed that enabled most of the technologies to be assessed in terms of its contribution towards the overall EI. Different network reference scenarios were developed to validate the different network technologies which made comparison difficult. However many of the EI components provided useful guidance on population, usage and other factors.
- Future communication systems need to minimize the uplink power of user devices as it is a major component of exposure of people to EMF. More dense networks can lead to a decrease in EI, because user's mobile devices will need to transmit less as base stations or access points are closer to the user.
- For voice service, from the standpoint of the UL direction (the main component of user exposure), the following recommendations can be drawn:
    - when GSM, UMTS and WLAN services are simultaneously available, UMTS should be used for lowest exposure. The only exception is for WLAN in bad propagation conditions. After WLAN, in bad propagation conditions UMTS CS (circuit service) is better choice than UMTS Skype VoIP service.
    - GSM service is by far the worst, especially in noisy environments.
    - Higher density of base stations / access points provides a lower exposure.

    - Adding micro-cells in the network significantly reduces the EI for GSM voice services.

- In current wireless technologies, the connection between the user and the serving base station /access point is generally based on the strength of the received downlink signal. This may notably reduce the user experienced performance in the uplink communication and increase the co-channel interference. Additionally, when power control can be used at the user device, this classic approach also augments the EMF exposure. Accordingly, our recommendation is to take into account jointly the downlink and the uplink communications to manage the connection control in future wireless systems.
- In the uplink, for low to medium traffic demand, EMF-aware scheduling can be used to drastically reduce active exposure given its effectiveness at balancing the exposure between users. Whereas, in the downlink, it is recommended to use coordination mechanism in conjunction with scheduling to smartly manage the interference and in turn significantly decrease the downlink EMF exposure.
- In the case that the wireless channel exhibits hostile conditions, UDP should be favoured over TCP for video delivery over LTE networks for reducing EMF while maintaining QoE.
- Many realistic systems exhibit unpredictable behaviour that is difficult to capture in mathematical models and/or simulations. As such, EMF/QoE trade-off analysis in practical deployments typically include a number of parameters that influence multiple performance metrics in unpredictable manners. The use of surrogate models can be used to experimentally or at run-time optimise such unpredictable, "black-box" systems in a minimum amount of iterations. As such, I would recommend combining existing mathematical solutions with alternatives such as discussed in Section **5.2** that can cope with the complexity and unpredictability of real-life deployments.
- The use of EMF-aware routing does not lead to a significant decrease of the EMF exposure, due to its cumulative characteristic. Furthermore, it is not straightforward to include it as a figure of merit in the optimisation process, but we have seen that the number of transmitted packets might be an appropriate proxy to be used in the routing decision procedures. By integrating this metric (either in the algorithm or the protocol itself) we achieve a much fairer distribution of the exposure within a network, at the same time, it brings about a certain degree of load balancing.
- Wi-Fi offloading can be beneficial for reducing EMF, as hinted in Section 7; a deeper analysis will be performed in framework of WP6 and our final recommendations will be then reported in [LEXNET D6.2].

REFERENCES

[3GPP TR 36.872] 3GPP, "3GPP TS 25.322, Small cell enhancements for E-UTRA and E-UTRAN - Physical layer aspects (release 12)," Tech. Rep., 2013.

[3GPP TS 25.322] 3GPP, "3GPP TS 25.322, radio link control (RLC) protocol specification (release 11)," Tech. Rep., 2013.

[3GPP TS 26.234] 3GPP, "3GPP TS 26.234, transparent end-to-end packet-switched streaming service (PSS); protocols and codecs (release 12)," Tech. Rep., 2014.

[3GPP TS 26.244] 3GPP, "3GPP TS 26.244, transparent end-to-end packet switched streaming service (PSS); 3GPP file format (3GPP) (release 13)," Tech. Rep., 2014.

[3GPP TS 36.814] 3GPP, "3GPP TS 36.814, Technical specification group radio access network; further advancements for e-utra physical layer aspects (Release 9)," Tech. Rep., 2010.

[Adhikari 2012] V. Adhikari, Y. Guo, F. Hao, M. Varvello, V. Hilt, M. Steiner, and Z.-L. Zhang, "Unreeling netflix: Understanding and improving multi-cdn movie delivery," in proc. INFOCOM, March 2012, pp. 1620–1628.

[Aerts 2013] S. Aerts, D. Plets, L. Verloock, L. Martens, and W. Joseph, "Assessment and comparison of total RF-EMF exposure in femtocell and macrocell scenarios," Radiation Protection Dosimetry, vol. 162, no. 3, pp. 236-243, Dec. 2014.

[Base 2015] N. K. Base, How is mos calculated in pingplotter pro?, 2005. Last accessed May 9, 2015. [Online]. Available: https://www.pingman.com/kb/article/how-ismos-calculated-in-pingplotter-pro-50.html

[Cisco 2014] CISCO, "Cisco visual networking index: Forecast and methodology, 2013-2018," 2014.

[Coll 2013] B. Coll-Perales, J. Gozalvez, and J. Sanchez-Soriano, "Empirical performance models for p2p and two hops multi-hop cellular networks with mobile relays," in proc. ACM PM2HW2N '13, pp. 21–28, New York, USA, 2013.

[DeSimone 2013] F. De Simone and F. Dufaux, "Comparison of dash adaptation strategies based on bitrate and quality signalling," in proc. IEEE MMSP, pp. 087–092, Sep. 2013.

[ElAbdellaouy 2014] H. El Abdellaouy, A. Pelov, L. Toutain, and D. Bernard, "Mitigation of electromagnetic radiation in heterogeneous home network using routing algorithm", in proc. WiOpt, pp. 326-332, Hammamet, Tunisia, May 2014.

[ElEssaili 2013] A. El Essaili, D. Schroeder, D. Staehle, M. Shehada, W. Kellerer, and E. Steinbach, "Quality-of-experience driven adaptive http media delivery," in proc. ICC, pp. 2480–2485, Jun. 2013.

[Gomez 2010] R. Gómez-Villanueva, H. Jardon-Aguilar, and R. Linares y Miranda, "State of the Art Methods for Low SAR Antenna Implementation," in proc. EuCAP, Barcelona, Spain, Apr. 2010.

[Heliot 2013] F. Héliot, M. A. Imran, and R. Tafazolli, "Low-complexity energyefficient coordinated resource allocation in cellular systems," IEEE Trans. Commun., vol. 61, no. 6, pp. 2271–2281, Jun. 2013.

[Heliot 2015a] F. Héliot, T. Yang, C. H. Foh, "Low-complexity Green Scheduling for the Downlink of Coordinated Cellular System," in proc. IEEE ICC, Jun. 2015.

[Heliot 2015b] F. Héliot, T. Yang, C. H. Foh, “Low-complexity Green Scheduling for the Coordinated Downlink of HetNet System,” in proc. IEEE CAMAD, Sep. 2015.

[Hore 2010] A. Hore and D. Ziou, “Image quality metrics: Psnr vs. ssim,” in proc. ICPR, pp. 2366–2369, Aug 2010.

[Iancu, 2014] V. Iancu, L. Diez, L. Rodríguez de Lope, E. Slusanschi and R. Agüero. "A reward-based routing protocol to reduce the EMF exposure over wireless mesh networks", in proc. IFIP Wireless Days, 2014.

[ICNIRP 1998] International Commission on Non-Ionising Radiation Protection (ICNIRP), “Guidelines for limiting exposure to time-varying electric, magnetic, and electromagnetic fields (up to 300 GHz),” Health Phys., vol. 4, pp. 494– 522, Oct. 1998.

[Islam 2009] M. T. Islam, M. R. I. Faruque, and N. Misran, “Reduction of Specific Absorption Rate (SAR) in the Human Head with Ferrite Material and Metamaterial,” Progress In Electromagnetics Research C, vol. 9, pp. 47–58, 2009.

[ITEC] ITEC - dynamic adaptive streaming over HTTP. DASH VLC plugin. [Online]. Available: www.itec.uni-klu.ac.at/

[Karakayali 2006] M. K. Karakayali, G. J. Foschini, and R. A. Valenzuela, “Network coordination for spectrally efficient communications in cellular systems,” IEEE Wireless Commun., vol. 13, no. 4, pp. 56–61, Aug. 2006.

[Khan 2014] S. Khan, D. Schroeder, A. El Essaili, and E. Steinbach, “Energy-efficient and QOE-driven adaptive HTTP streaming over LTE,” in proc. IEEE WCNC, pp. 2354–2359, April 2014.

[Lauer 2013] O. Lauer, P. Frei, M.-C. Gosselin, W. Joseph, M. Roösli, and J. Fröhlich, “Combining Near- and Far-Field Exposure for an Organ-Specific and Whole-Body RF-EMF Proxy for Epidemiological Research: A Reference Case,” Bioelectromagnetics, vol. 34, pp. 366–74, Jul. 2013.

[LENA] LTE-EPC NEtwork simulAtor. [Online]. Available: http://networks.cttc.es/mobile-networks/software-tools/lena/

[Letourneux 2013] F. Letourneux, Y. Corre, E. Suteau, and Y. Lostanlen, “3d performance analysis of a heterogeneous lte network with indoor small-cells in a real urban environment,” in proc. IEEE ICC, pp. 5209–5213, June 2013.

[LEXNET D2.1] G. Vermeeren et al., “D2.1 Current metrics for EMF exposure evaluation,” INFSO-ICT-318273 LEXNET (Low EMF Exposure Future Networks), Tech. Rep., Apr. 2013, [Online]. Available: http://www.lexnet.fr/scientificoutputs/publicdeliverables.html

[LEXNET D2.3] G. Vermeeren et al., "D2.3 Scenarios,” INFSO-ICT-318273 LEXNET (Low EMF Exposure Future Networks),Tech. Rep., Nov. 2013, [Online]. Available: http://www.lexnet.fr/scientificoutputs/publicdeliverables.html

[LEXNET D2.4] E. Conil et al., “D2.4 Global wireless exposure metric definition v1,” INFSO-ICT-318273 LEXNET (Low EMF Exposure Future Networks), Tech. Rep., Nov. 2013. [Online]. Available: http://www.lexnet.fr/scientificoutputs/publicdeliverables.html

[LEXNET D2.6] Varsier et al, “D2.6: Global Wireless Exposure Metric definition v2,” INFSO-ICT-318273 LEXNET (Low EMF Exposure Future Networks), Tech. Rep.,

Nov. 2014, [Online]. Available: http://www.lexnet.fr/scientificoutputs/publicdeliverables.html

[LEXNET D5.1] M. Popović et al., "D5.1 Smart low-EMF architectures: novel technologies overview," INFSO-ICT-318273 LEXNET (Low EMF Exposure Future Networks), Tech. Rep., Oct. 2014. [Online]. Available: http://www.lexnet.fr/scientificoutputs/publicdeliverables.html

[LEXNET D6.2] J. Stephan et al., "D6.2: Report on validation," INFSO-ICT-318273 LEXNET (Low EMF Exposure Future Networks), Tech. Rep., to appear in Nov. 2015, [Online]. Available: http://www.lexnet.fr/scientificoutputs/publicdeliverables.html

[Mahmoud 2008] K. R. Mahmoud, M. El-Adawy, S. M. Ibrahem, R. Bansal, and S. H. Zainud-Deen, "Investigating the interaction between a human head and a smart handset for 4G mobile communication systems," Progress In Electromagnetics Research C, vol. 2, pp. 169–188, 2008.

[Mascolo 2001] S. Mascolo, C. Casetti, M. Gerla, M. Y. Sanadidi, and R. Wang, "TCP westwood: Bandwidth estimation for enhanced transport over wireless links," in proc. ACM MobiCom '01, pp. 287–297, New York, USA, 2001.

[Medard 2000] M. Medard, "The effect upon channel capacity in wireless communications of perfect and imperfect knowledge of the channel," IEEE Trans. on Inform. Theory, vol. 46, no. 3, pp. 933–946, May 2000.

[Miao 2012] G. Miao, N. Himayat, G. Y. Li, and S. Talwar, "Low-complexity energy-efficient scheduling for uplink OFDMA," IEEE Trans. on Commun., vol. 60, no. 1, pp. 112–120, Jan. 2012.

[Michael 2015] M. T. Mehari, E. De Poorter, I. Couckuyt, D. Deschrijver, J. Vanhie-Van Gerwen, D. Pareit, T. Dhaene, and I. Moerman, " Efficient global optimization of multi-parameter network problems on wireless testbeds", Ad Hoc Networks, Vol 29, pp 15-31, 2015.

[Miller 2012] K. Miller, E. Quacchio, G. Gennari, and A. Wolisz, "Adaptation algorithm for adaptive streaming over http," in proc. Packet Video Workshop, pp. 173–178, May 2012.

[Mogensen 2007] P. Mogensen, W. Na, I. Kovacs, F. Frederiksen, A. Pokhariyal, K. Pedersen, T. Kolding, K. Hugl, and M. Kuusela, "Lte capacity compared to the Shannon bound," in proc. IEEE VTC-Spring, pp. 1234–1238, April 2007.

[Ng 2012] D. W. K. Ng, E. S. Lo, and R. Schober, "Energy-efficient resource allocation in multi-cell OFDMA systems with limited backhaul capacity," IEEE Trans. Wireless Commun., vol. 11, no. 10, pp. 3618–3631, Oct. 2012.

[Nostrat 2011] B. Nosrat-Makouei, J. Andrews, and R. Heath, "MIMO interference alignment over correlated channels with imperfect CSI," IEEE Trans. on Signal Process., vol. 59, no. 6, pp. 2783–2794, Jun. 2011.

[NS3] Network simulator 3. [Online]. Available: http://www.nsnam.org/

[Octave 2015] GNU Octave. [Online]. Available: https://www.gnu.org/software/octave/

[Opus] Opus Codec. [Online]. Available: https://www.opus-codec.org/

[Pedersen 2013] K. I.Pedersen, Y. Wang, S. Strzyz, and F. Frederiksen, "Enhanced inter-cell interference coordination in co-channel multi-layer LTE-advanced networks", IEEE Wireless Commun., vol. 20, issue 3, pp. 120-127, June 2013.

[Plets 2013] D. Plets, J. Wout, K. Vanhecke, and L. Martens, "Exposure Optimisation in Indoor Wireless Networks by Heuristic Network Planning", Progress In Electromagnetics Research, Vol. 139, pp. 445-478, March, 2013.

[Qiang 2007] C. Qiang, Y. Komukai, and K. Sawaya, “SAR investigation of array antennas for mobile handsets,” IEICE Trans. on Commun., vol. 90, no. 6, pp. 1354–1356, 2007.

[Ragha 2010] L. Ragha and M. Bhatia, “Evaluation of SAR Reduction for Mobile Phones Using RF Shields,” International Journal of Computer Applications, vol. 1, no. 13, pp. 80–85, Jan. 2010.

[Riverbed] Riverbed Modeler, Mar. 2015. [Online]. Available: http://www.riverbed.com/

[Sambo 2014] Y. Sambo, F. Héliot, and M. A. Imran, “A User Scheduling Scheme for Reducing Electromagnetic Emission in the Uplink of Mobile Communication Systems,” in proc. IEEE OnlineGreenComm, Nov. 2014.

[Sambo 2015] Y. Sambo, F. Héliot, and M. A. Imran, “Electromagnetic Emission-aware Schedulers for the Uplink of OFDM Wireless Communication Systems,” submitted to IEEE Trans. on Veh. Tech., Aug. 2015.

[Schafhuber 2002] D. Schafhuber, G. Matz, and F. Hlawatsch, “Adaptive prediction of timevarying channels for coded OFDM systems,” in proc. IEEE ICASSP, vol. 3, pp. 2549–2552, Orlando, USA, May 2002.

[Sodagar 2011] I. Sodagar, “The MPEG-DASH standard for multimedia streaming over the internet,” IEEE MultiMedia, vol. 18, no. 4, pp. 62–67, Apr. 2011.

[Stephan 2014] Stephan, J. ; Brau, M. ; Corre, Y. ; Lostanlen, Y, “Joint analysis of small-cell network performance and urban Electromagnetic Field exposure”, in proc. EuCAP, pp. 2623-2627, The Hague, Netherlands, Apr. 2014.

[Varsier 2015] N. Varsier, D. Plets, Y. Corre, G. Vermeeren, W. Joseph, S. Aerts, L. Martens, and J. Wiart, “A novel method to assess the human population exposure induced by a wireless telecommunication network,” Bioelectromagnetics, Jun. 2015.

[Venturino 2009] L. Venturino, N. Prasad, and X. Wang, “Coordinated scheduling and power allocation in downlink multicell OFDMA networks,” IEEE Trans. on Veh. Tech., vol. 58, no. 6, pp. 2835–2848, Jul.2009.

[VQCIETF 2011] Voice Quality Characterization of IETF Opus Codec, Florence, Italy, 2011.

[Wiegand 2003] T. Wiegand, G. Sullivan, G. Bjontegaard, and A. Luthra, “Overview of the H.264/AVC video coding standard,” IEEE Trans. Circuits and Systems for Video Tech., vol. 13, no. 7, pp. 560–576, Jul. 2003.

[Wong 2004] I. Wong, A. Forenza, R. Heath, and B. Evans, “Long range channel prediction for adaptive OFDM systems,” in Proc. Asilomar Conference on Signals, Systems and Computers, pp. 732–736, vol. 1, Nov. 2004.

APPENDIX 1: INTERNAL REVIEW

	Reviewer 1: Massinissa LALAM			Reviewer 2: Günter Vermeeren		
	Answer	**Comments**	**Type***	**Answer**	**Comments**	**Type***
1. Is the deliverable in accordance with						
(i) the Description of Work?	☒ Yes ☐ No		☐ M ☐ m ☐ a	☒ Yes ☐ No		☐ M ☐ m ☐ a
(ii) the international State of the Art?	☒ Yes ☐ No		☐ M ☐ m ☐ a	☒Yes ☐ No		☐ M ☐ m ☐ a
2. Is the quality of the deliverable in a status						
(i) that allows to send it to EC?	☐ Yes ☐ No	I have some questions that I put in my comments through the whole document. If answered, I think that the document is ready for the EC.	☐ M ☐ m ☐ a	☐ Yes ☐ No	A revision of the document is needed before it can be send to the EC.	☐ M ☐ m ☐ a
(ii) that needs improvement of the writing by the editor of the deliverable?	☒ Yes ☐ No	Some polishing is needed in the edition of the whole document.	☐ M ☐ m ☐ a	☒ Yes ☐ No		☐ M ☐ m ☐ a
(iii) that needs further work by the partners responsible for the deliverable?	☐ Yes ☒ No	Minor clarifications are needed in some parts (that I put in comments) but nothing really blocking	☐ M ☐ m ☐ a	☐ Yes ☒ No	Some clarifications and discussions should be added, and some recalculations might be needed but no new work should be preformed	☐ M ☐ m ☐ a

* Type of comments: M = Major comment; m = minor comment; a = advice

APPENDIX 2: A THEORETICAL FRAMEWORK/MODEL/METHOD FOR ASSESSING NETWORK-LEVEL EMF EXPOSURE (WITH IMMEDIATE POSSIBLE APPLICATIONS FOR MESH NETWORKS

A2.1 How to compute the exposure if packets can be sent with only one possible transmit power level

Consider the following function, defined for the whole mesh network where N represents the number of nodes:
Exposure: $\mathbb{N} \rightarrow \mathbb{R}_+^N$
For each node k, $1 \leq k \leq N$ we have the following exposure function components:
$E_n : \mathbb{N} \rightarrow \mathbb{R}_+$
such that $Exposure(T) = (e1\,(T), e2\,(T), \ldots, eN\,(T))$, where T represents a discrete time moment within the routing process.

Actually, we can assume that each next moment when we have a routing action in the network (e.g., packet send, intermediary packet forward), we have a different moment T.

We consider as being of interest each time moment when an event of sending or forwarding a packet in the network, at any node level, occurs. We do not restrain the generality if we say that no such events concerning 2 packets occur simultaneously, so at each new time moment T we only deal with one packet, i.e. only one of the N nodes transmits or forwards a packet, the rest of the nodes being idle. Also, we do not consider the time in seconds, but rather as the index of a send/forward event, i.e. always the first send event will happen at $T = 1$, the second would happen at $T = 2$, etc. This is not incorrect, because there exists a bijection between any pair of continuous intervals in R. As a possible refinement of this observation, in order to be more precise with respect to the exact time moment, when going continuous (from $\mathbb{N}$ to $\mathbb{R}_+$), we could also consider as many intermediary time moments T as needed, during which time moments the network is idle, i.e. no event of send/forward will occur.

We define the Exposure function to be continuous and to have both the first and the second derivative and it is obtained, at each node level, from interpolating between the integer, discrete values for each discrete considered time moment that have been defined at the previous observation.

$Exposure : \mathbb{R} \rightarrow \mathbb{R}_+^N$
Actually, $e_k(T)$ represents the accumulated individual node exposure of node k at moment T over all the transmitted and forwarded packets.
It follows that $\forall\, T \in \mathbb{N} : e_k(T+1) \geq e_k(T)$. In our work we consider that they exist and denote: **(1)** $e_k'(T)$ as being the derivative with respect to T of each e_k function, and **(2)** $e_k''(T)$ as being the second derivative with respect to T of each e_k function. This implies that $e_k'(T) \geq 0$, since e_k is an accumulative function.

Also, we can say some things about e_k'':

$0e_k''(T) > 0 \iff$ the rythm of accumulating exposure on node k has increased, which means that either more and more packets have passed through node k around the time moment T or the transmission power of node k has increased.
$e_k''(T) = 0 \iff$ the rythm of accumulating exposure on node k is constant
$e_k''(T) < 0 \iff$ the rythm of accumulating exposure on node k has decreased, which means that either less and less packets have passed through node k around the time moment T or the transmission power of node k has decreased.

We can see a clear relationship between the second derivative on node k, e_k'', and the virtual price increase and decrease model in the Reward Based Routing Protocol [Iancu, 2014]. Consequently, we can write the accumulated exposure, expressed as the Lexnet defined Exposure Index (EI) as follows:

$$EI(T) = \sum_{k=1}^{N} e_k(T) \quad (23)$$

It follows that we could write e_k as an expression of its first and second derivative, as shown in section III. By integrating over the number of individual events in random moments in time or in discrete determined moments in time (e.g. each second) we do not restrict the generality of this approach. This is ensured by the double integral format of the proposed solution, as is described in the following sections. This implementation assumes that once every second, there is a new event generated in the network, even if not necessary on the current node.

A2.1.1 Expressing the individual node exposure

In order to define the expression of the individual node exposure, $e_k(T)$, we could refer to it as being the area below the graphic of $e_k'(T)$, which is itself the area below the graphic of $e_k''(T)$, respectively. It is well-known that the area between 2 points, a and x, below the graphic of a 1 variable function h that is derivable, can be expressed formally by means of the *Riemann* integral:

$$\int_a^x h'(t)dt = h(x) - h(a) \quad (24)$$

If we consider a to be a fixed initial real value and x to be variable, we get:

$$h(x) = h(a) + \int_a^x h'(t)dt \quad (25)$$

Now if the function h is two times derivable, considering that we know the expression/shape of the function h'', we could similarly express h' as:

$$h'(x) = h'(a) + \int_a^x h''(t)dt \quad (26)$$

If we integrate this once again, between a and b we get:

$$\int_a^x h'(x)dx = \int_a^x h'(a)dx + \int_a^b \int_a^x h''(t)dtdx$$
$$\iff h(b) - h(a) = (b - a)h'(a) + \int_a^b \int_a^x h''(t)dtdx \quad (27)$$

$$\Leftrightarrow\Rightarrow h(b) = h(a) + (b - a)h'(a) + \int_a^b \int_a^x h''(t)dtdx$$

If we return to our functions, i.e., $e_k(T)$, $e'_k(T)$ and $e''_k(T)$, for each node k we could consider every maximal interval $[A, B]$ with $A, B \in N$, during which the node transmits or forwards at each moment $T \in \mathbb{N}, A \leq T \leq B$. It follows that we can safely write the following expression:

$$e_k(T) = e_k(A) + e'_k(A)(T - A) + \int_A^T \int_A^x e''_k(t)dtdx \quad (28)$$

We could consider that $e''_k(A)$ and $e_k(A)$ are known constants. On the other hand, for each interval $[B, C], B, C \in \mathbb{N}$, during which node k does not transmit at all, we assume that the node exposure remains constant:

$$e_k(C) = e_k(B) \quad (29)$$

leading to the following expression for the exposure index:

$$EI(T) = \sum_{k=1}^{N} e_k(A) + e'_k(A)T + \int_0^T \int_0^x e''_k(t)dtdx \quad (30)$$

The expressions above are true provided that, at any step T, any node k transmits/forwards something. In more realistic scenarios, not all nodes k transmit simultaneously. We then have to consider: **1)** an extra factor to be added to the formula, namely $P_k(U)$, which is taken to be 1 if the node k transmits/forwards at time moment U and 0 otherwise; and **2)** an individual initial time moment A when each node k starts transmitting, denoted A_k, each A_k being specific to the corresponding node k. In this realistic case the expression for the EI becomes more complex and is expressed analytically as:

$$EI(T) = \sum_{k=1}^{N} [e_k(A) + e'_k(A_k)T + \int_0^T \int_0^x e''_k(t)P_k(t)dtdx\ ] \quad (31)$$

where

$$\begin{aligned} &\int_0^T \int_0^x e''_k(t)P_k(t)dtdx \\ &\quad = P_k(T-1)e_k(T) - P_k(T-1)e_k(T) \\ &\quad + \sum_{U=0}^{T-1} [\sum_{S=0}^{U} P_k(S)e'_k(S-1) - P_k(U)e'_k(U)] \\ &\quad - \sum_{U=0}^{T-1} \sum_{S=0}^{U} P_k(S)e'_k(S) + \sum_{U=0}^{T-2} P_k(U)[e_k(U+1) - e_k(U)] \end{aligned} \quad (32)$$

The practical means of using this extended equation is described below. In this latest equation *T* is the moment in time when the last packet is transmitted/forwarded between two nodes, $P_k(U)$ is an extra factor to be added to the formula which is taken to be 1 if the node k transmits/forwards at time moment *U* and 0 otherwise, *U* and *S* are any two integer indexes from 0 to T.

A2.1.2 A practical mean to compute the exposure index

The last formula deduced in the previous section is quite hard to read and also impractical to use. We plan to show some more usable formulas in this section, which could ultimately be used in numerical computations of the EI in any type of network. Bearing in mind the formulation presented before, we know that for an interval when a node transmits, we have:

$$e_k(T) = e_k(A_k) + e_k'(A_k)T + \int_{A_k}^{T}\int_{A_k}^{x} e_k''(t)dtdx. \quad (33)$$

Note that it is most likely that each A_k is a different integer number for each individual node k, and we consider $A_1 \leq A_2 \leq \ldots \leq A_N$.
We first want to compute $\int_A^x e_n''(t)dt$, where A is an arbitrary initial time moment, $A \leq A_1$, and we plan to find a recurrence formula for it.

$$\begin{aligned} &\int_A^x e_k''(t)dt = \sum_{S=A}^{[x]-1}\int_S^{S+1} e_k''dt + \int_{[x]}^{x} e_k''(t)dt \\ \Leftrightarrow &\int_A^x e_k''(t)dt = \sum_{S=A}^{[x]-1}\int_S^{S+1} e_k''(t)dt + \int_{[x]}^{x} e_k''(t)dt \end{aligned} \quad (34)$$

But considering that each individual packet generates a fixed amount of exposure, $e_k''(t) = e_k''(S)$ for each unit time interval $[S, S+1)$, we get:

$$\int_A^x e_k''(t)dt = \sum_{S=A}^{[x]-1} e_k''(S) + e_k''([x])\{x\}, \quad (35)$$

where $[x]$ represents the integer part of x and $\{x\}$ represents the fractional part of x, i.e., $x - [x]$. If we integrate this from A to T we get a sum of two integrals:

$$\int_A^x e_k''(t)dt = I_1 + I_2 \quad (36)$$

where

$$I_1 = \int_A^T \sum_{S=A}^{[x]-1} e_k''(S)dx \quad (37)$$

and

$$I_2 = \sum_{x=A}^{T} e_k''([x])\{x\} \quad (38)$$

If we compute I_1 for $T \geq A + 1$ we get:

$$I_1 = \sum_{S=0}^{T-A-1} (T - A - 1 - S)e_k''(a + S) \quad (39)$$

If we compute I_2 for $T \geq A + 1$ we get:

$$I_2 = \frac{1}{2}\sum_{S=A}^{T-1} e_k''(S) \quad (40)$$

This means that the expression of the accumulated exposure, due to the transmit power, between time moments A and T, without considering the event that is going to take place at time moment T and including the event that took place at time moment A is:

$$\begin{aligned}\int_A^x e_k''(t)dt &= \sum_{S=0}^{T-A-1}(T-A-0.5-S)e_k''(A+S) \Rightarrow e_k(T)\\ &= e_k(A)+e_k'(A)(T-A)+\sum_{S=0}^{T-A-1}(T-A-0.5-S)e_k''(A+S)\\ &\Rightarrow EI\\ &= \sum_{k=1}^{N}e_k(A_k)+\sum_{k=1}^{N}e_k'(A_k)\,(T-A_k)+(T\\ &-A_k)\sum_{k=1}^{N}\sum_{S=0}^{T-A-1}(T-A-0.5-S)e_k''(A+S)\end{aligned} \tag{41}$$

where A_k is the initial moment since the node k has started transmitting, supposing that all nodes are transmitting at moment T. Otherwise, some terms of the sum and some parts of the integral would remain constant or zero, respectively.

A usable recurrent formula for practical exposure calculation:

In order to make the EI calculation even simpler, for $T > A + 1$ we assume:

$$e_k(T) = e_k(A_k) + (T - A_k)e_k'(A_k) + z_{k_T}, \tag{42}$$

where

$$z_{k_T} = \sum_{S=0}^{T-A_k-1}(T-A_k-0.5-S)e_k''(A_k+S). \tag{43}$$

It means that we get the following recurrent relation:

$$\begin{aligned}z_{k_{T+T_1}} &= \sum_{S=T-A_k}^{T+T_1-A_k-1}(T+T_1-A_k-0.5-S)e_k''(A_n+S)\\ \Rightarrow z_{k_{T+T_1}} &= z_{k_T}+T_1\sum_{S=T-A_k}^{T+T_1-A_k-1}e_k''(A_k+S)\\ &+\sum_{S=T-A_k}^{T+T_1-A_k-1}(T+T_1-A_k-0.5-S)e_k''(A_k+S)\end{aligned} \tag{44}$$

and denote

$$y_{k_{T_1}} = \sum_{S=T-A\_k}^{T+T_1-A_k-1}e_k''(A_n+S) \Rightarrow y_{k_{T_1+1}} = y_{k_{T_1}} + e_k''(T+T_1) \tag{45}$$

And

$$\begin{aligned}w_{k_{T_1}} &= \sum_{S=T-A_k}^{T+T_1-A_k-1}(T+T_1-A_k-0.5-S)e_k''(A_k+S) \Rightarrow w_{k_{T_1+1}}\\ &= w_{k_{T_1}} + y_{k_{T_1}} + e_k''(T+T_1)\end{aligned} \tag{46}$$

we get

$$z_{k_{T+T_1}} = z_{k_T} + T_1 y_{k_{T_1}} + w_{k_{T_1}} \Leftrightarrow e_k(T+T_1) = e_k(T) + T_1 e'_k(A_k) + T_1 y_{k_{T_1}} + w_{k_{T_1}} \quad (47)$$

Since the node level and the global exposure are accumulative, and it does not change between moments when the node does not transmit, in order to incrementally compute the terms $e_k(T)$ and also the exposures $EI(T)$ at each step, from moment 0 of the network, it would be easiest to always have ready the intermediary arrays: $y_{k_{T_1}}$, z_{k_T} and w_{k_T}.
Note that $z_{k_A} = y_{k_0} = w_{k_0} = 0$.

A2.2 How to compute the exposure if packets can be sent with *more* possible transmit power level

For the same problem as above, we define k discrete transmit power levels for each node ($PL_{k_x}(node_i)$), such that $PL_{k_x}(node_j)$, ∀ possible nodes $i, j (1 \leq i, j \leq n)$:

$$PL_0(i) < PL_1(i) < \cdots < PL_{k-1}(i) \quad (48)$$

Let all $PL_k(node_i)$, with $k_z \in 0,1,\dots,k-1$ and $i \in 1,2,\dots,n$, form the set $\mathcal{PL}$, where $card(\mathcal{PL}) = k$.
Thus, the exposure due to routing function becomes:
$Exposure : \mathcal{PL} \times \mathbb{R}_+ \rightarrow \mathbb{R}_+^n$

Similar to the approach with only one power level, we define the level of exposure for each node, by considering for each node *n* the correspondent group of functions for the previously defined single function $e_n(T)$: $r_n(PL_i, T)$, as being the exposure for node n at time T, considering that at time moment T we will be using PL_i power level at node n. The effective value of the newly generated exposure at the level of node n at moment T is obtained as follows, by using an auxiliary column vector, $V_n(T)$ (which is actually the correspondent of $P_n(T)$):
$e''_n(T) = [r''_n(PL_0, T)\ r''_n(PL_1, T)\ \dots\ r''_n(PL_{k-1}, T)]V_n(T)$, where the column vector $V_n(T) = [00 \dots 1 \dots 0]$ and $V_n(T)[i] = 1$ only for the precise power level i that has been used for transmitting or receiving the packet at node n at time moment T; the rest of the positions of the $V_n(T)$ are 0. In case node n is not transmitting anything at time moment T: $V_n(T) = 0$.
So, similarly and in the same conditions as set before, we have:

$$\begin{aligned} & e_n(T) \\ & = e_n(A) + e'_n(A)(T-A) \\ & + \int_0^T \sum_{S=A}^{[x]-1} \left[\int_S^{S+1} r''_n(PL_0, t)dt \dots \int_S^{S+1} r''_n(PL_{k-1}, t)dt \dots \right] V_n(S)dx \\ & + \int_0^T \left[\int_{[x]}^{x} r''_n(PL_0, t) \dots \int_{[x]}^{x} r''_n(PL_{k-1}, t) \right] V_n([x])dx \end{aligned} \quad (49)$$

Observation 1:

For any individual transmission (i.e., individual packet send or packet forward), the exact single position j where the $V_n(T)[j] = 1$ is established by the signaling protocol, in order to obtain a minimum cost for a given (source, destination) pair.

Observation 2:
If we generalize the $V_n(T)$ vector and consider, instead of $V_n(T) \in \{0,1\}$, that: $\sum_{i=0}^{n} V_n(T)[i] = 1, 0 \leq i \leq k$ and $V_n(T) \in \{0,1\}$, in case node n is transmitting (otherwise $\sum_{i=0}^{n} V_n(T)[i] = 0, 0 \leq i \leq k$, and $V_n(T) \in \{0,1\}$), we could obtain a vector of the probabilities related to each node n, of transmitting or receiving with power level i at time moment T.
Also similar to the reasoning in the previous section, with only one power level, the RBRP implementation cost for multiple discrete power levels can be defined as:

$$Cost_n(T) = \left[F\left(r_n''(PL_0, T)\right)\ F\left(r_n''(PL_1, T)\right)\ \ldots\ \ F\left(r_n''(PL_{k-1}, T)\right)\right]V_n(T)$$

where F is an increasing function, as explained and argued before, in particular even the identity function F(x) = x, also meaning that the inverse function G is identical to F: $G(x) = x$.

All the formulas deduced and explained for one power level, including the recurrence functions involving z_n, y_n and w_n, can be easily adapted to be applied to the multiple power level case.